The identification of ligands of cardiac Connexin 45 (Cx45) and their possible association with the development of the cardiac conduction disorder, Progressive Familial Heart Block Type II (PFHBII)

Nqobile Nxumalo

Thesis presented in partial fulfilment of the requirements for the degree Master of Science (Human Genetics) in the Faculty of Medicine and Health Sciences at Stellenbosch University

Supervisors: Prof. Craig Kinnear and Prof. Valerie Corfield

Faculty of Medicine and Health Sciences

Division of Molecular Biology and Human Genetics

April 2019

DECLARATION

By submitting this thesis/dissertation, I declare that the entirety of the work contained therein is my own, original work, that I am the sole author thereof (save to the extent explicitly otherwise stated), that reproduction and publication thereof by Stellenbosch University will not infringe any third party rights and that I have not previously in its entirety or in part submitted it for obtaining any qualification.

April 2019

Date: ……

Signature: ……

ABSTRACT

Connexins are gap junction proteins which allow selective permeability of small metabolites and ions between cells. Three main cardiac isoforms (Cx40, Cx43 and Cx45) which have been extensively studied are unequally distributed throughout the heart, suggesting specific functional roles. Connexins 40, 43 and 45 null mice have been shown to develop cardiac abnormalities, including conduction disturbances similar to those of known human diseases. Interestingly, features of human myotonic dystrophy (DM) include cardiac conduction disturbances; the DM-causative gene encodes a protein kinase (DMPK) that is a ligand of the COOH-terminus of Cx43. This has lead to the suggestion that other unidentified Cx ligands may be involved in cardiac conduction, and, if defective, may cause conduction disease. It is proposed that such ligands may be involved in the pathophysiology of the conduction disease PFHB II. To date, most studies have focused on Cx43; hence the main aim of this study was to assess functional specificity of cardiac Cx45 to further understand its role in cardiac function and possibly in the development of cardiac conduction diseases. Yeast-2-hybrid technology was applied to identify putative Cx45 ligands; by constructing a bait clone encoding the Cx45 COOH-terminus domain and using it to screen a cardiac cDNA library in *S. cerivisiae*. Successive selection stages reduced the number of putative ligands from 371 to 25. Selected ligands were identified by sequence homology searches in Genbank databases and prioritised for further study based on likely biological relevance and subcellular localisation. The authenticity of putative protein interactions was further assessed by mammalian 2 hybrid analysis. The priortised ligands included three mitochondrial proteins (NADH dehydrogenase subunit IV, thioredoxin 2, and cytochrome C oxidase subunit I), and four cytoplasmic proteins (obscurin, myomegalin, CD63-antigen and SCF-apoptosis response protein 1) which bore biological relevance to cardiac function. In contrast, in another study (R. Keyser, 2007, MSc Thesis – University of Stellenbosch) most Cx40 ligands were cytoplasmic proteins.

In addition to Y2H and M2H, whole exome sequencing (WES) was conducted to identify PFHBII-causing mutations. Numerous filtering and variant prioritization tools were used to identify plausible PFHBII-causing variants in the PFHBII patients based on *in silico* predictions of their potential to cause disease and the function of these genes its situated in. These included two variants associated with obscurin, a Cx 45 ligand. This variant was was also identified in three of the patients which could be predicted to cause disease. Based on chromosome mapping, the Cx 45 ligands identified in the current study could be excluded from involvement in PFHB II.

Obsurin, in spite its chromosomal location, is an exception due to its clinical association with dilated cardiomyopathy, a clinical symptom of PFHBII. The link between obscurin and dilated cardiomyopathy in PFHBII patients needs to be investigated further.

OPSOMMING

Connexins (Cx) is gaping verbindings proteïene wat die selektiewe deurlaatbaarheid van klein metaboliete en ione tussen selle toelaat. Drie goed-bestudeerde hart iso-forme (Cxs40, 43 en 45) is oneweredig deur die hart versprei, wat dui op hul spesifieke funksionele rolle. Daar is aangetoon dat Cx uit-klop muise hartkwale ontwikkel, onder meer geleidingsongeruimdhede soortgelyk aan sekere bekende menssiektes. Dit is interessant om op te merk dat menslike miotoniese distrofie (DM) kenmerke soos hartgeleidingsongeruimdhede insluit; die DM-veroorsakende geen kodeer vir ‘n proteïen-kinase (DMPK) wat ‘n ligand van die karboksielterminus van Cx43 is. Hierdie observasie het gelei tot die voorstel dat ander, ongeïdentifiseerde Cx ligande betrokke kan wees by hartgeleiding en, indien defektief, geleidingsiekte mag veroorsaak. Daar is voorgestel dat sulke ligande betrokke kan wees by die patofisiologie van die geleidingssiekte PFHBII. Tot op hede het meeste studies gefokus op Cx43; derhalwe was die hoofdoel van hierdie studie om die funksionele spesifisiteit van hart Cx45 te bepaal om sodoende ‘n beter begrip van Cx45 se rol in hartfunksie, of moontlik in die ontwikkeling van hartgeleidings siektes, te vorm. Gis-2-hibried-tegnologie is aangewend om moontlike Cx45 ligande te identifiseer; ‘n aas-kloon wat kodeer vir die COOH-terminale domein van Cx45 is gekonstrueer en is gebruik om ‘n hart kDNS-biblioteek te fynkam in *S. cerevisiae*. Opeenvolgende selekteerstadiums het die hoeveelheid moontlike ligande verminder van 371 na 25. Geselekteerde ligande is geïdentifiseer deur sekwensie-homologie soektogte in Genbank databasisse en is geprioritiseer vir verdere studie op grond van hul waarskynlike biologiese relevansie en subsellulêre lokalisering. Die egtheid van moontlike proteïen-interaksies is verder bepaal deur soogdier 2-hibried analise. Die geprioritiseerde ligande sluit in drie mitokondriale proteïene (NADH dehidrogenase sub-eenheid IV, tioredoksien 2 en sitokroom C oksidase sub-eenheid I) en vier sitoplasmiese proteïene (obskurien, miomegalien, CD63-antigeen en SCF-apoptosis respons proteïen 1) wat biologies relevant is tot hartfunksie. Hierteenoor het ‘n studie (R. Keyser, 2007, MSc Thesis – University of Stellenbosch),) bevind dat meeste Cx40 ligande sitoplasmiese proteïene is.

Behalwe vir Y2H en M2H, is wieele exome sequencing (WES) uitgevoer om PFHBII-veroorsakende mutasies te identifiseer. Verskeie filter- en variantprioriteringsinstrumente is gebruik om waarskynlike PFHBII-veroorsakende variante in die PFHBII-pasiënte te identifiseer gebaseer op siliko voorspellings van hul potensiaal om siekte te veroorsaak en die funksie van hierdie gene is geleë in. Dit sluit twee variante in wat verband hou met obscurine, 'n Cx 45 ligand. Hierdie

variant was ook geïdentifiseer in drie van die pasiënte wat voorspel kan word om siekte te veroorsaak. Gebaseer op chromosoom kartering, kan die Cx 45 ligande wat in die huidige studie geïdentifiseer is, uitgesluit word van betrokkenheid by PFHB II. Obsurien, ten spyte van sy chromosomale ligging, is 'n uitsondering as gevolg van sy kliniese assosiasie met verwydde kardiomyopatie, 'n kliniese simptoom van PFHBII. Die verband tussen obskurine en verwydde kardiomyopatie in PFHBII pasiënte moet verder ondersoek word.

TABLE OF CONTENTS

ACKNOWLEDGEMENTS

Jesus my Lord and Saviour – Through it all You've stayed true. Somandla, angazi impilo yami ingayini ngaphandle kwakho. O Umuhle!

Ma – Thanks for being a woman of courage. Imithandazo yakho izwakele. NGIYABONGA!

Thando, Mnotho, Sabu – My amazing blessings! You guys inspire me to be more.

S'fiso "Big brother" – Angiwakhohlwa amazwi owasho 2004, ngiphelelwe ithemba about the development of my career. You are a visionary Mtaka-Ma.

Njabu and Mqhele "Gwegwe" – You guys are wonderful. So proud to have in our clan!

Proph Chris, Ps Noms, my RGO family and Ps Mtho – your prayers, counsel and support I value deeply.

Craig – Thanks for your willingness to bring my dream back to life. Words can't express my gratitude.

Valerie – I knew our meeting at Scifest was going to change my life. Your constructive criticism, advice and training are highly valued… It's been rough I must admit.

Hanlie – Your guidance and kind advice are appreciated. Thank you!

Everyone in the MAGIC lab, particularly Lundi and Amsha – I don't know how I would have coped without your assistance and guidance.

Lastly, I would like to thank the MRC, Harry Crossely foundation for the financial support.

LIST OF FIGURES

LIST OF TABLES

THESIS STRUCTURE

The thesis is structured as four chapters. In Chapter 1 *(Sections 1.1.2 to 1.1.7)* the literature for the connexin structure in gap junction architecture and formation, their role in cell-cell communication, protein-protein interaction, cardiovascular function and diseases associated with connexin mutations is presented. Further literature for connexin deficient animal models, selected inhetited cardiac conduction disorders, methods to study protein-protein interactions as well as whole exome sequencing is presented (*sections 1.1.8 to 1.1.11*). *Section 1.1.12* presents the research focus and study objectives.

Chapter 2 is organized into 2 parts, where part I one focuses on the methodology followed for the identification of Cx 45 ligands while part II entails the approach adopted for whole exome sequencing and analysis of bioinformatics data.

Chapter 3 presents the results obtained from the experiments conducted while Chapter 4 discusses the study outcomes and concludes the thesis.

CHAPTER ONE: LITERATURE REVIEW AND STUDY BACKGROUND

1.1 INTRODUCTION

The cells of multicellular organisms need to communicate with each other for the successful exchange of nutrients and signals. In order to achieve this goal, multicellular organisms have evolved multiple strategies. These include long-range interactions mediated by neural or endocrine mechanisms or short-range interactions mediated by direct physical contact. This is accomplished in a number of ways, mostly by the formation of a series of pores, or communicating channels, which facilitate cell–cell communication. In animal cell systems, gap junctions between the cells form one such communication system (Dbouk *et. al.*, 2009; Hussain, 2014; Vinken, 2016; Aasen *et. al*., 2018).

For the heart, a multicellular organ, to beat efficiently, both physical and electrical factors come into play, which facilitate the synchronised manner in which cardiomyocytes operate. This synchrony is a result of three types of cell junctions known as the **fascia adherens** and **desmosomes**, which both serve as anchors of the desmin cytoskeleton facilitating structural connectivity, and **gap junction proteins**, which facilitate the passage of ions from one cell to another (Severs, 2000; Dbouk *et. al*., 2009; Vinken, 2016; Aasen *et. al.*, 2018). So, because of their role in cell-cell communication and in cardiac impulse propagation, gap junctions will be the focal point of this review.

Gap junction channel communication is one of the most widespread communication mechanisms in animal cells. It was first demonstrated in 1959, by Hama, who ultimately published the first electron micrographs of gap junctions in earthworm giant axons (Hama, 1959). In the same year, studies were performed in nerve cells of crayfish where it was noted that, by inserting an electrode in each of the interacting cells and applying some voltage, a large amount of current flowed between them (Furshpan *et al*, 1959). Subsequent studies also showed that small fluorescent dye molecules injected into a cell could pass to a second cell without leaking into the extracellular space (Simpson et al, 1977, Brink and Dewey, 1980). These findings were collectively significant in shedding light on the cell-cell communication phenomenon, making gap junctions the pillar of cell-cell communication studies.

Gap junction channels are mainly constituted of a conglomerate of proteins known as connexins (Cxs) which gives the channels the ability to selectively allow the passage of ions and small particles, from one cell to another. Six of these Cx units make up half a channel, which is also known as a connexon (Bruzzone, 2001, Evans and Martin, 2002, Dbouk et al, 2009; Hussain, 2014, Vinken, 2016; Aasen *et. al.*, 2018).

To date, 21 Cx isoforms have been identified in humans, some of which have been linked to known human diseases. They extend from isoforms of 21 to those of 70 kilo daltons (kDa) in size (Martin and Evans, 2004, Hussain, 2014; Vinken, 2016; Aasen *et. al.*, 2018). This variation in molecular weight is useful in distinguishing the various isoforms, for instance, a 45kDa Cx is referred to as Cx45. In another system, different Cxs are abbr eviated with GJ, for gap junction, and serially numbered according to the order of their discovery. Additionally, the three α, β and γ Cx gene homology groupings are considered. These groupings are determined by comparing DNA sequences and length of the cytoplasmic domains, particularly that cytoplasmic loop and the carboxyl (COOH)-terminal domain by ClustalW alignments (Sohl and Willecke, 2003). Connexin 43, for instance, was the first of the α-group to be discovered, and was designated GJA1. Connexin 45, although now known to be in the γ-group, is still known as GJA7, because it was initially perceived to be an α–group member (Sohl and Willecke, 2003). So, due to discrepancies such as these, the former system, based on molecular weight, is the most favoured in distinguishing the various Cxs.

Work by Fernandez et al., 2005 identified the PFBH II causative gene locus to be in the 2.85 Mb regions in Chromosome 1q13.2 – q13.3. Subsequent to this, no studies have been conducted to explore the causative genes of this condition using next-generation sequencing (NGS). Recent advances in next generation sequencing have evolved our understanding of many cardiovascular diseases which provides insights to other types of heart diseases and the management of these disorders.

Whole-exome sequencing (WES) is application of the next-generation technology to determine the variations of all coding regions, or exons, of known genes. WES provides coverage of more than 95% of the exons, which contains 85% of disease-causing mutations in Mendelian disorders and many disease-predisposing SNPs throughout the genome. For this reason, sequencing of the complete coding regions

(exome) has the potential to uncover the causes of large number of rare, mostly monogenic, genetic disorders as well as predisposing variants in a number of diseases(Rabbani *et al*., 2014) including PFBH II under study.

1.2 CONNEXIN STRUCTURE IN GAP JUNCTION ARCHITECTURE

All Cx isoforms present a common topology, composed of four transmembrane segments; three (TM1, TM2 and TM4) of which are hydrophobic, while the third segment (TM3) is amphipathic; three loops - one intracellular (IL) and two extracellular (EL1 and EL2) - and a cytoplasmic amino (NH_2-) terminus and a carboxyl (COOH-) terminus (Bruzzone, 2001; Pfenniger *et. al*., 2011; Solan and Lampe, 2017) (Figure 1.1). The four transmembrane domains possess α-helical conformations and, as shown in Figure 1.1, the two extracellular loops, which facilitate docking by recognising compatible Cxs, are held together by di-sulphide bonds through three cystein residues (Martin and Evans, 2004). The amino acid sequences of EL1 and EL2 and the NH_2-terminus are highly conserved (van Veen *et al.,* 2001) among the various isoforms, while major differences are observed in the amino acid sequence and length of the COOH-terminus (Goodenough *et al*., 1996; Evans and Martin, 2002) and the IL (Saez *et al*., 2003). In the present study, it was based on these differences and on its involvement in protein-protein interactions that the COOH-terminal domain of Cx45 was used as bait in the yeast-2-hybrid (Y2H) “fishing expedition”. The rationale was that the COOH-terminal domain would allow selection of the specific Cx45 ligands, which would ultimately give an indication of specific and possibly overlapping functions of various isoforms.

Cxs present a common topology, and they have also been shown to generally present a common and simple gene structure, which constitutes two exons, one of which contains part of the 5’ untranslated region (5’UTR), separated by an intron of variable length, while the other exon constitutes the remaining 5’UTR segment, a full coding region and the 3’ untranslated region (3’UTR) (Figure 1.2) (Sohl and Willecke, 2004). The *Cx43* gene, one of the major cardiac isoforms, presents this gene structure (Figure 1.2).

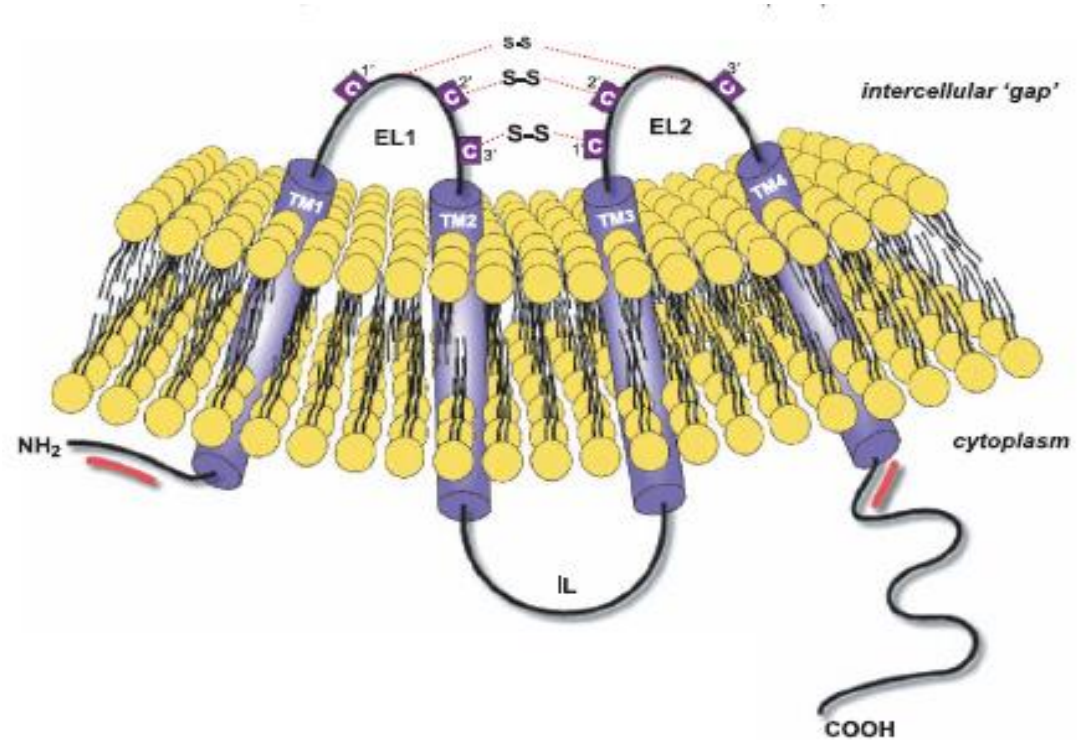

Figure 1.1 Generic connexin topology and arrangement on cell membrane.

Connexins span the membrane four times with two highly conserved extracellular loops (EL1 and EL2). The amino (NH_2) terminus, intracellular loop (IL) and carboxyl terminus (COOH) lie within the cytoplasm (Martin and Evans, 2004).

Figure 1.2 Common gene structure of a connexin with splicing of 5'UTR.

The part in orange represents the coding region (adapted from Sohl and Willecke, 2004).

Connexin genes 40 and 45, on the other hand, present a rather more complex structure which is thought to be due to the usage of alternate promoters, with multiple transcription factors (to be discussed in section 1.1.4.3), and alternative

splicing which then produce different 5' UTRs of the Cx mRNA (Oyamada *et al*., 2005, 2013). The *Cx40* gene in humans has only two exons, similar to the structure presented in figure 1.2, while in mice it consists of three exons as shown in Figure 1.3 A. On the other hand, *Cx45* in humans consists of three exons (exons 1 and 2 containing the 5' UTR and exon 3, part of the 5'UTR, the full coding region as well as the 3'UTR) (Figure 1.3C) while in mice, it has five exons (exon 1A, exon 1B, exon 1C, exon 2 containing the 5'UTR and exon 3, which contains the rest of the 5'UTR, the coding region, as well as the 3'UTR) (Sohl and Willecke, 2003; Teunissen and Bierhuizen, 2004; Anderson *et al*., 2005). As can be seen in *Cx40* and *Cx45*, Cxs may also present varying transcripts between species as well as among different tissues of a species. In *Cx40* for instance, the transcript containing exon AS (Figure 1.3A) is scarce in hearts of mice embryos but abundant in the oesophogus (Oyamada *et al*., 2005, 2013).

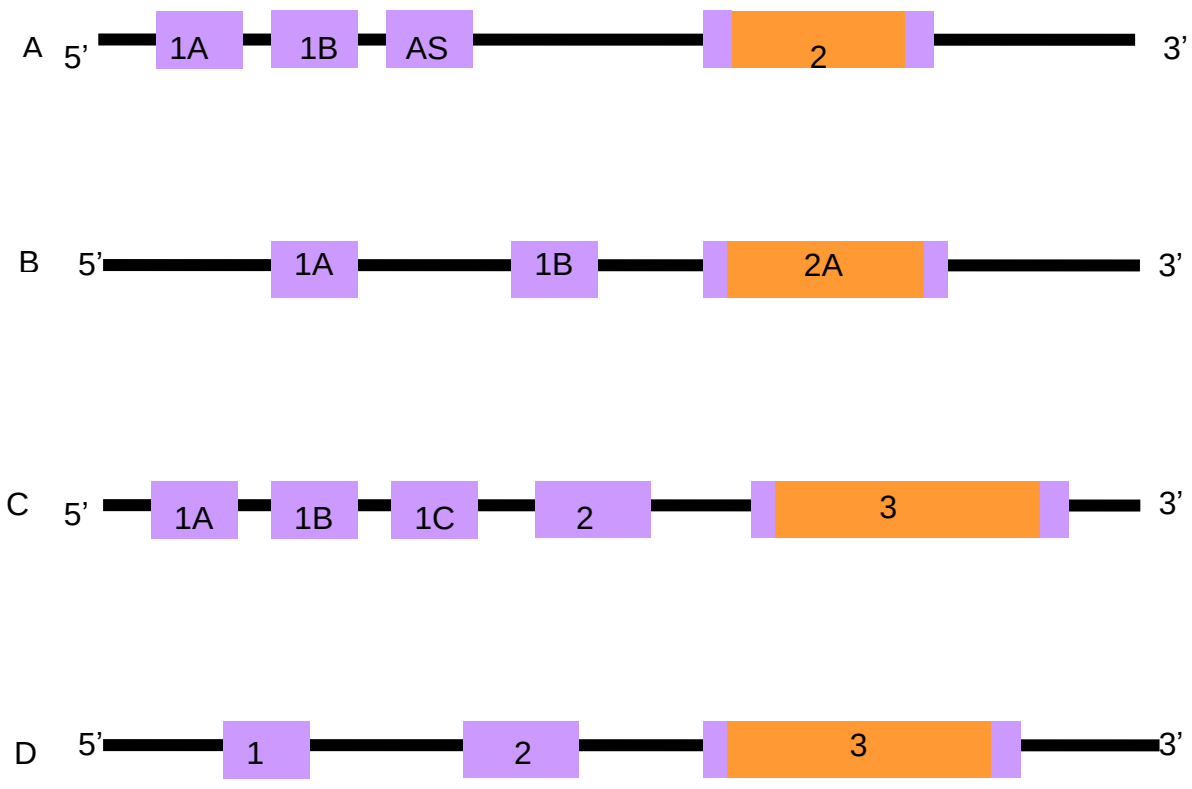

Figure 1.3 Gene structures presented by the most prominent cardiac Cxs, Cx40, Cx43 and Cx45, in human, mice and rats.

A=Mouse Cx40, B=Human Cx40, C=Mouse Cx45, D= Human Cx45;

Parts in orange represent coding regions; the transcript containing exon AS mCx40 is sometimes absent in mice embryos (adapted from Teunissen and Bierhuizen, 2004, Oyamada *et al.*, 2005).

1.3 CONNEXINS IN GAP JUNCTION FORMATION

Connexins, like all eukaryotic transmembrane proteins, are synthesised by ribosomes that are bound to the endoplasmic reticulum (ER) membrane. Thereafter, they are either assembled into connexons and trafficked from the endoplasmic reticulum (ER) to the plasma membrane or are directly inserted in the plasma membrane where they dock head-to-head to form fully functional gap junction channels as shown in Figure 1.4 (Martin and Evans, 2004, Aasen *et. al.,* 2018).

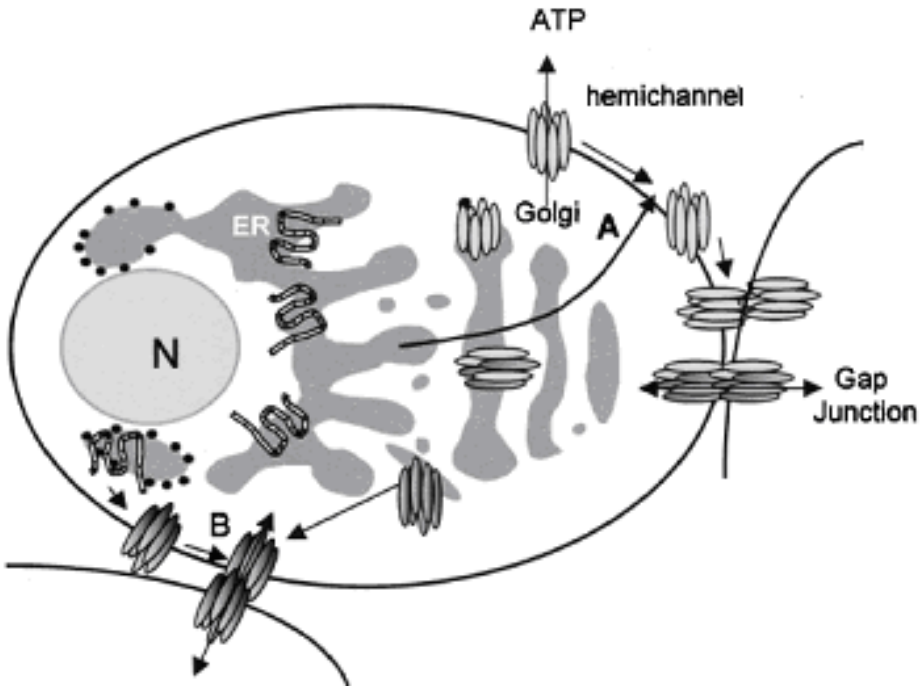

Figure 1.4 Gap junction formation.

After translation, connexins are inserted in the membrane of the endoplasmic reticulum (ER) and oligomerised to connexons in the Golgi apparatus. Thereafter, they are delivered to the plasma membrane where they dock head-to-head to form a functional gap junction channel. N= Nucleus; (A) some Cx proteins are directly inserted in the plasma membrane while others are packaged in the ER transported to the plasma membrane (B) (Evan and Martin, 2002, Aassen *et. al*., 2018).

Gap junctions exist in various configurations of Cx units, which can oligomerise to form homomeric and heteromeric connexons, as well as homotypic and heterotypic

channels as shown in Figure 1.5. Homomeric connexons and homotypic channels form when identical Cxs assemble, while heterotypic channels form when different homomeric connexons dock head-to-head. Biheteromeric channels, on the other hand, form when heteromeric connexons assemble (Moreno, 2004).

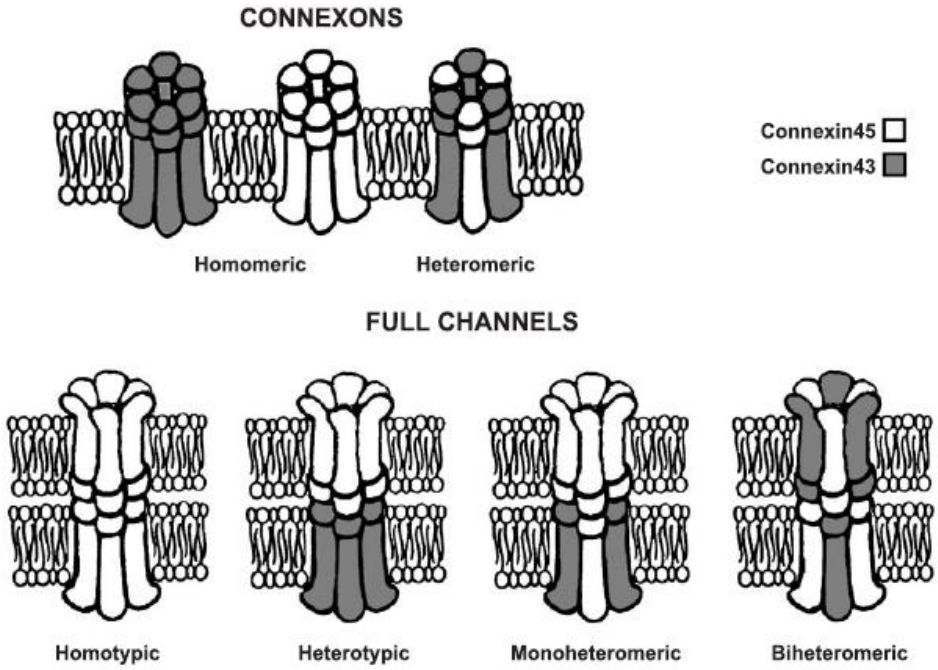

Figure 1.5 Combinations of cardiac Cxs 43 and 45 forming gap junction channels (Moreno, 2004).

These highly variable combinations in connexon oligomerisation may greatly affect permeability of gap junction channels (Elenes *et al*., 1999; Moreno, 2004) where under conditions of mechanical, or ischemic stress, allowing the flux of small molecules like Ca2+, ATP, glutamate, or NAD+ across the plasmamembrane, thereby eliciting signaling cascades and diverse physiological responses (Evans *et al*., 2006; Retamal *et al*., 2015).

1.4 GAP JUNCTIONS AND THEIR ROLE IN CELL-CELL COMMUNICATION

Intercellular communication in multicellular organisms is the basis for all physiological processes. It is mediated by gap junctions, previously perceived as a group of cell junctions which control the direct exchange of cellular metabolites between cells. To date, intercellular communication is known to influence a wide range of cellular and physiological processes (Vinken *et al.*, 2006, Aasen, 2015 and Aasen *et. al*., 2016). For instance in cardiac function, gap junctions facilitate the flow of the action potential from one cardiomyocyte to another, providing rhythmic

contraction of the heart (Veenstra *et al.*, 1990). At some synapses in the brain, they allow the arrival of an action potential at the synaptic terminals to be transmitted across the postsynaptic cell, needed for the release of a neurotransmitter (Kelmanson *et al.*, 2002). Additionally, before childbirth, gap junctions between the smooth muscle cells of the uterus enable coordinated, powerful contractions to begin (Ciray *et al.*, 1994). Essentially, they selectively allow ions and other metabolites to move between cells (Evan and Martins, 2002, Nielsen *et. al*., 2012), electrically connecting and transforming them from individual cells to a highly synchronised organ (Evans and Martins, 2002; Vinken, 2016).

Gap junction channel communication involves the passage of small and hydrophilic molecules, less than 1kDa in size, such as metabolites (eg., adenosine triphosphate or [ATP]), nutrients (eg., glucose), and second messengers (eg., potassium ions (K^+), sodium ions (Na^+) and calcium ions [Ca^{2+}]) (Alexander and Goldberg, 2003). It is regulated at several levels ranging from *Cx* gene transcription to gap junction degradation (Vinken *et al.*, 2006; Hussain, 2014; Vinken, 2016). Gap junction channel communication is regulated via three communication networks, namely, (i) intracellular communication: Cx proteins affect gene expression of a number of regulatory proteins, (ii) intercellular communication: gap junctions mediate passage of signalling molecules between cells and (iii) extracellular communication: hemichannels control paracrine release of cellular metabolites (Vinken *et al.*, 2006; Vinken et. al., 2015; Vinken, 2017). As these communication networks work together, for the purpose of this review, the focus will be on intercellular communication because of the role of gap junctions in cardiac impulse propagation.

Gap junction channel intercellular communication is regulated by two broad factors; namely gating, also described as fast-control, and Cx gene expression, or long-term control (Holder *et al*, 1993). Gating, which can be subdivided into voltage or chemical, is said to be triggered by a number of factors including transmembrane voltage (V_m) and transjunctional voltage (V_j) (voltage gating) and hydrogen ions (H^+) and Ca^{2+} (chemical gating). Phosphorylation of the COOH-terminal of Cx has also been implicated in chemical gating of gap junction channels (Seaz, 2003; Epifantseva and Shaw, 2018). Conversely, long-term regulation involves regulation of *Cx* gene expression by various steps in the pathway from DNA to RNA to protein; steps such as transcription control which is mediated by factors such as T-box transcription factors (Tbx5, Tbx2 and Tbx3), Sp1/Sp3, activator protein 1 (AP-1),

cyclic AMP, Nkx2-5 and epigenetic factors such as DNA methylation (Oyamada *et al*., 2005; Vinken *et al*, 2006; Vinken, 2017). The following sub-sections will thus give an overview of selectivity, as well as fast-control and long-term control, in the regulation of gap junction cell-cell communication.

1.4.1 Selectivity and permeability

Selectivity and permeability of gap junction channels is the pinnacle of gap junction channel intercellular communication and is governed by a number of both physical and electrical factors. It depends primarily on channel physical properties, including pore structure, surface charge and, in some instances, the interaction between the pore and the permeant. Differences in selectivity represent the diversity of mechanisms of conduction in specific combinations of Cxs, which is also influenced by conductance of the specific Cx isoforms (Elenes, 2000; Moreno, 2004, Vinken, 2016). For instance, each homotypic Cx45 gap junction channel has a conductance of approximately 40pS* and a selectivity cation:anion ratio of 10:1, while Cx40 (+/- 200pS*) and Cx43 (+/- 100pS*) have a 2:1 and 4:1 ratio, respectively, which means that each channel allows passage of a certain number of cations per anion (Moreno *et al.*, 1995; Veenstra, 1996; Valiunas, 2002 and Valiunas *et al.*, 2002). From these findings, it can therefore be deduced that channels of low conductance more freely allow passage of cations than channels of higher conductance.

* Unitary conductance results from the amount of current that passes through a single channel and is usually measured in Ohmic Sum (pS) (Frangie, 1997)

1.4.2 Fast-regulation

Voltage-gating

Voltage-gating in gap junctions implies the closing and opening of the channels as a result of voltage differences across the connexons of abutting cells. These differences may also arise as a result of variability in the degree of sensitivity among the constituent Cx isoforms (Spray, 1994). The voltage-sensitivity and potential difference exhibited by gap junctions also have the ability to metabolically uncouple communicating cells (Bukauskas and Verselis, 2004). For instance, when each of the two abutting cells has an equal voltage, no transjunctonal voltage is produced as the voltage amounts in each cell cancel the other out, which results in free passage of particularly large molecules such as cAMP. However, when transjunctional voltage

is produced between the two adjoining cells, the cells are electrically coupled but metabolically uncoupled. All in all, transjunctional voltage electrically couples the cells, but limits the passage of larger molecules (Bukauskas and Verselis, 2004).

Chemical-gating

Chemical-gating in gap junctions is governed by a myriad of factors which, directly or indirectly, affect the interaction of channels with their surrounding membranes. These factors include pH, Ca^{2+} concentration and phosphorylation.

i. pH

Intracellular pH has always been thought to play a major role in gap junction channel gating and has been tested in various cell types expressing different Cx isoforms. When Delmar compared the pH sensitivity in oocyte pairs expressing a range of Cxs, a spectrum of sensitivity that spread from Cx50 to Cx32, as shown in decreasing order -Cx50 >Cx46 >Cx45 >Cx26 > Cx37 >Cx43 >Cx40 >Cx32 (Delmar, 2002) – was observed. It was evident that indeed intracellular pH affected various isoforms in varying degrees. Among the three isoforms predominantly expressed in the heart, Cx45 seemed to be the most sensitive to pH. In other words, Cx45 gap junction channels, closed readily at low pH. This has also been suggested to serve as a mechanism to limit the spread of injury from damaged to normal tissue. In fact, Bukauskas and Peracchia (1997) showed in HeLa cells and in fibroblasts from sciatic nerves transfected with Cx43 and Cx45 that low pH produces full uncoupling of Cx43 and Cx45 gap junction channels, by inducing slow gating transitions between open and closed states (Bukauskas and Peracchia, 1997). They also deduced that gating activity of individual Cxs could be fast, but may not always be synchronous, which gives the false impression that transitions between open and closed states are slow, or consist of a series of resolvable transient sub-transitions.

The most studied mechanism of Cx acidification is the one that occurs by cytoplasmic acidification. The H^+ binding that initiates the gating effect of pH has been shown to be on the cytoplasmic side of the hemichannels, possibly near the entrance of the pore. In fact, several studies performed in *Xenopus* oocytes suggested that the cytoplasmic loop and COOH-terminal domain residues are important in pH gating (Ahmed *et al*., 2001). The COOH-terminal domain has also been suggested to behave like a gating particle that binds to a receptor domain

which leads to channel closure (Girsch and Peracchia, 1991). Furthermore, experiments by Wang and Peracchia in *Xenopus* oocytes demonstrated that replacing the cytoplasmic loop of Cx32 with that of Cx38 increased pH-gating sensitivity to that of Cx38 channels, further supporting the proposal that the cytoplasmic loop is important in pH-sensitive gating (Wang and Peracchia., 1998). It is in fact the first 11 residues of the COOH-terminal domain that significantly modulate pH-gating sensitivity of the Cx channels. These observations were collectively made by groups of Torok and Saez, where they showed that deletion of 272 of up 283 amino acid residues, of the COOH-terminal domain of Cx32 did not affect the kinetics of uncoupling (Saez *et al.,* 1990; Torok *et al.*, 1997). Additionally, Girsch and Peracchia showed that replacing five positively charged arginines (R215, R219, R220, R223 and R224) of the 11, either with polar residues asparagine, histidine or glutamic acid, increased the sensitivity of Cx32 channels to intracellular acidification induced by application of CO_2. Interestingly, the initial segment of the COOH-terminal domain was identified as a calmodulin (CaM)-binding domain (Girsch and Peracchia, 1991) and its basic residues would be expected to be relevant for interaction with CaM, which may plug the channel mouth (Peracchia *et al.,* 1996).

ii. Phosphorylation

Protein phosphorylation is a reversible process in which protein functions are regulated by kinase-mediated addition of a phosphate group, principally to serine (S), threonine (T) or tyrosine residues (Y) (Ciesla *et al*., 2011; Davis, 2011). Many critical events involved in cellular responses are mediated by phosphorylation and dephosphorylation. These include regulation of enzymatic activity, protein conformational change, protein–protein interaction and cellular localisation (Huttlin *et al*., 2010; Davis, 2011; Nishi *et al*., 2011). Abnormal phosphorylation has been implicated in many diseases such as cancer (Grek *et al*.,, 2016; Banerjee *et al*., 2016; Kitini et al., 2015; Boucher et al., 2017; Philips *et al*.,, 2017, Stoletov *et al*., 2013), brain disorders (Nakase *et al*., 2004; Giaume *et al*., 2013; Cotrina *et al*., 2012), obesity (Ganesan *et al*., 2015), diabetes (Wright *et al*., 2012) and immunological disorders influencing inflammatory responses (Wong *et al*., 2017), activation of T lymphocytes (Oviedo-Orta *et al*., 2010; Kuczma *et al*., 2011 and Ni *et al*., 2017) and haematopoietic stem cell maintenance (Ishikawa *et al*., 2012; Genet *et al*., 2018;Saez *et al*., 2003; Colomer and Means, 2007). Connexins 26, 31, 32, 36, 37, 40, 43, 45, 46, 50 and 56 have been shown to be be regulated by

phosphorylation (Saez *et al*., 1998; Lampe and Lau, 2000; Lampe *et al*., 2000; Locke *et al*., 2009).

A number of Cx-phosphorylation studies focussed on serine (S), threonine (T) and tyrosine (Y) amino acids via protein kinase B (PKB/Akt) (Dunn *et al*., 2011), c- and v-src, mitogen-activated protein kinase (MAPK), protein kinase C (PKC), p34cdc2, casein kinase 1 (CK1), protein kinase A (PKA) or calmodulin-dependent protein kinase pathways (Saez *et al*., 1998; Lampe *et al*., 2000; Lampe and Lau, 2004; Solan and Lampe, 2005, 2009). Basic amino acid phosphorylation for Cxs has not been reported.

In Cxs, phosphorylation of cytoplasmic residues mainly occurs in the C-terminal domain (Cooper *et al*., 2000; Rikova *et al*., 2007; Wisniewski *et al*., 2010), and occasionally in the N-terminal domain (Wisniewski *et al*., 2010; Chen *et al*., 2012) or cytoplasmic loop domain (Berthoud *et al*., 1997; Alev *et al*., 2008; Rigbolt *et al*., 2011).

In multiple tissues, Cxs are regulated by multi-site phosphorylation resulting in altered Cx-protein synthesis and turnover, trafficking, membrane insertion and aggregation. Hence, Cx phosphorylation is involved in the efficient delivery of hemichannels to the gap junction plaque (Palatinus *et al*., 2011a; Johnson *et al*., 2012), gap junction channel assembly, function and turnover under both normal and disease conditions (Saez *et al*., 1998; Lampe and Lau, 2000, Saez *et al*., 2003; 2004; Laird, 2005; Solan and Lampe, 2005, 2007, 2009; Marquez-Rosado *et al*., 2011). However, it is suggested that phosphorylation is neither required for Cx insertion to the membrane (Musil *et al*., 1990; Solan and Lampe, 2005) nor for the formation of functional channels (Martinez *et al*., 2003; Johnstone *et al*., 2009).

Studies of truncation constructs of Cx43 showed that truncated at aa 236 was not trafficked to the to the membrane, whereas Cx43 truncated at aa 239 remained able to traffic to the membrane and form functional gap junction channels, but not functional hemichannels (De Vuyst *et al*., 2007; Wayakanon *et al*., 2012). Thus, only a portion of the Cx43 C-terminal domain is shown to be required for its trafficking.

To date, the effects of phosphorylation on Cx43 structure and function have been extensively reviewed (Solan and Lampe, 2009; Jeyaraman *et al*., 2011; Marquez-Rosado *et al*., 2011; Johnstone *et al*., 2012; Yeganeh, 2012; Slavi, 2018). There is a

paucity of studies investigating the phosphorylation of other Cx isoforms. Cx45 phosphorylation in the C-terminal domain differentially regulates electrical intercellular conductance via Cx45 gap junctions. Yet, regulation does not alter the single channel conductance, but most likely modulates the open probability of Cx45 gap junction channels (van Veen *et al*., 2000). Phosphorylation of Cx45 occurs at S381, S382, S384 and S385. Mutating these serine residues into phosphodead mutants, in order to disable Cx45 phosphorylation, increased the turnover rate of Cx45 (Hertlein *et al*., 1998).

iii. Calcium ion concentration

In 1877, Engelmann reported that cardiac cells in direct contact with each other during life became independent as they died (Engelmann, 1877), a phenomenon believed to result from the formation of ionic barriers between injured and uninjured cells (reviewed by Peracchia *et al.*, 2004). Approximately a century later, Délèze (1970) reported that cut heart fibres from rats do not heal in the absence of extracellular calcium (Ca^{2+}), but do so rapidly when Ca^{2+} is supplied as a result of Ca-induced cellular uncoupling which limits the spread of injury to other parts of the tissue. This observation, suggested for the first time the role of Ca in the regulation of gap junctional communication. Later, the role of Ca^{2+} in cell uncoupling was confirmed through a study correlating loss of electrical and dye coupling among cells exposed to treatments known to increase intracellular Ca^{2+} concentration (Paracchia, 1980). Additional evidence of the importance of Ca^{2+} was provided by studies of Rose and Lowenstein, where they showed that in insect gland cells, monitored by the Ca^{2+} indicator aequorin (a photoprotein isolated from luminescent jellyfish, *Aequorea* species), electrical uncoupling coincides with an increase in Ca^{2+}concentration (Rose and Loewenstein, 1975, 1980).

In various cells, Ca is said to self-limit its cell–cell diffusion. Initially, it was reported in pancreatic acinar cells (Yule *et al.*, 1996) then another report by Leite *et al.*, (2002) confirmed this observation in human hepatoma (SK-Hep1) cultured cells. The latter authors, showed Ca^{2+}, uncaged by photolysis in one SK-Hep1 cell expressing either Cx32 or Cx43, to be restricted to one cell and never to spread to its neighbouring cells. These findings further suggested that an increase in intracellular Ca^{2+} concentration closes gap junction channels and completely uncouples the abutting cells (Peracchia *et al.*, 2004).

Additionally, Ca^{2+} has also been shown to indirectly interact with the constituent Cxs via an intermediate component. Girsch and Peracchia (1991) and Lurtz and Louis (2003) collectively made the following observations when studying the mode of interaction between Cxs and Ca^{2+}. Since Cxs typically contain only one acidic residue facing the cytosol, Ca^{2+} could not directly interact with Cxs. Furthermore, this residue was a glutamate situated in between the TM4 and the COOH-terminal domains (residue 208 in Cx32) and was believed to be incapable of binding Ca^{2+} with sufficiently high affinity to affect gating. This residue was unable to distinguish between $Ca^{2+}$and magnesium ions (Mg^{2+}), and was not near the pore. Thus, they postulated that the Ca^{2+} effect on gating was mediated by an intermediate component, possibly CaM (reviewed by Peracchia *et al.*, 2004).

1.4.3 Long-term regulation

As previously indicated, long-term regulation of gap junction channel communication is one of the two routes believed to contribute to gap junction channel gating. As the term suggests, it is based on the length of time required to effect regulatory changes in function, ranging from a few minutes to hours, and mainly involves *Cx* gene expression (Vinken *et al*., 2006, 2015).

The general *Cx* gene structure contains different promoter sites for specific transcription factors (section 1.1.2), which ultimately control gap junction channel activity. These factors include TATA box binding-protein, Sp/Sp3, AP-1, Nkz2-5, GATAA4 and Tbx5 (Oyamadu *et al*., 2005), to name but a few. These factors may suppress or enhance *Cx* gene expression. For instance, cardiac specific Nkx2-5, a transcription factor critical for cardiac development (Bruneau, 2002), also associated with the development of cardiac conduction defects such as atrial septal defects (ASD) (Shiojima *et al*., 1995) and heart block, down-regulates the expression of *Cx43* (Jay *et al*., 2004). Tbx5, also implicated in the development of Holt-Oram syndrome (HOS) (to be discussed later in section 1.1.9), up-regulates *Cx40* gene expression (Bruneau *et al*., 2001).

Apart from cis/trans regulation, *Cx* gene expression is also controlled by epigenetic factors such as DNA methylation of the *Cx* gene promoters. DNA methylation of *Cx32* and *Cx43* promoter regions has been shown to result in *Cx* gene silencing (Piechocki *et al*., 1999; Tan *et al*., 2002; D'hondt et al., 2013). Apparently, promoter methylation interferes with the binding of some activators resulting in lack of *Cx* gene

expression. Although no clear correlation has been made between promoter methylation and *Cx* gene expression, down-regulation of *Cx26* in breast cancer cells (Singal *et al*., 2000), of *Cx32* in human renal carcinoma cells (Yano *et al*., 2004) and *Cx32* in human renal carcinoma cells (Yano *et al*., 2004) has been observed.

In short, evidence suggests that regulation of *Cx* gene expression by both transcription and epigenetic factors plays a vital role in cell-cell communication. It can be speculated that, for instance, if gene expression of certain Cxs is down-regulated or suppressed, this would ultimately disrupt Cx oligomerisation, which in turn may result in the development of disease.

Summary of section 1.4

In summary, from gating factors discussed from section 1.1.4.1 to section 1.1.4.3, it can be deduced that gap junction channel communication has layers of complexity. In most cases, it is simultaneously regulated by many of the factors discussed, by varying mechanisms, which makes it challenging to tease out individual components, in order to understand gap junction intercellular communication. However, findings from studies such as those mentioned above have, to a certain extent, shed some light in this phenomenon, making Cx proteins plausible platforms for gaining an understanding of the role of ion channels in cell-cell communication.

1.5 CONNEXINS AND PROTEIN-PROTEIN INTERACTIONS

Connexins have been shown to interact with a diverse array of proteins to form multi-protein complexes (Duffy *et al.,* 2002; Herve *et al.,* 2004; Epifantseva and Shaw, 2018). Such interactions are likely to regulate Cx function at several levels, including gating. Studies have also shown the possible involvement of these interactions in the modulation of Cx function in response to physiological stimulation and pathological conditions, to be introduced below (Thomas *et al.*, 2002; Fu *et al*, 2004; Aasen et al., 2018).

1.5.1 Adherens Junction-Associated Protein interactions

Gap junctions have been shown to form a close association with cadherin-based adherens junctions. Cadherins comprise a major family of transmembrane glycoproteins known to play an important role in the regulation of cell adhesion and

cell motility (Juliano, 2002; Wheelock and Johnson, 2003). Cadherins have the ability to disrupt cell-cell coupling and have been shown to play a vital role in gap junction formation. In fact, inhibition of cadherin function by anti-cadherin antibodies disrupts cell-cell coupling (Frenzel and Johnson 1996; Hertig *et al*., 1996; Kostin *et al*., 1999; Meyer *et al*., 1992; Zuppinger *et al*., 2000). Cadherin-mediated cell adhesion is also regulated by signaling through the Rho-Guanosine triphosphatases (Rho-GTP)-ases and receptor tyrosine kinases (Wheelock and Johnson, 2003), as well as through a variety of extracellular signals that include signals passed through gap junctions (Paul *et al*., 1995). The cytoplasmic domains of cadherins bind *α*/*β*-catenins and other F-actin binding proteins, including *α*-actinin, vinculin, and zonula occludens-1 (ZO-1) and thus provides linkage to the actin cytoskeleton (Nagafuchi, 2001). In rat cardiac myocytes, *β*-catenin interacts with Cx43 (Ai *et al*., 2000), and the formation of the Cx43/ZO-1/*β*-catenin complex is required for targeting of Cx43 to the plasma membrane (Wu *et al*., 2003).

Another study also suggests that *α*-catenin is important for Cx43 trafficking and assembly (Govindarajan *et al*., 2002). Given that N-cadherin and catenins are co-assembled in the ER/Golgi compartments (Wahl *et al*., 2003), this raises the possibility that Cx43 is assembled as part of a multi-protein complex that may regulate both adherens and gap junction assembly. It should also be borne in mind that most Cxs follow this route of assembly (section 1.1.4), which suggests that Cx45 and other Cxs may play a role in gap junction assembly, as part of the multi-protein complex.

It is also interesting to note that another adherens junction protein interacts with one of the major cardiac Cx isoforms. Mussini *et al*., (1999) provided evidence for colocalisation of Cx43 and myotonic dystrophy protein kinase (DMPK), the product of the mytonic dystrophy gene (*DMPK*), in rat cardiac muscle. Mytonic dystrophy protein kinase is found to localise in specialised structures in both heart and skeletal muscle, particularly in intercalated disks (van der Ven *et al.*, 1993, Whitney *et al*., 1995, Salvatori *et al*., 1997). The manner in which Cx43 and DMPK interact is unclear, however, Mussini *et al*. (1999) showed, with the use of polyclonal antibodies, the interaction to be on the cytoplasmic face of the gap junction. From the data presented by this study, they further suggested the participation of this interaction is a regulatory mechanism of connexon activity (Mussini *et al*, 1999). These findings have in fact formed part of the rationale for our current study, which

was to identify ligands of cardiac Cx45 in order to gain further understanding of the functional specificity cardiac Cxs – and to investigate their possible role in cardiac conduction disturbances, details of which will be discussed in section 1.1.11.

1.5.2 Cytoskeletal Protein Interactions

A number of investigations indicate that gap junctions constituted exclusively of Cx43, *in vitro,* may be closely associated with cytoskeletal proteins. One study, in Morris hepatoma H5123 cells, showed that formation of functional Cx43 gap junctions required elevated cAMP and intact microfilaments, which suggests the possibility that clustering of Cx43 gap junctions may involve protein kinase A (PKA) and actin filaments (Wang and Rose, 1995). The association of Cx43 with actin filament, and perhaps other actin-binding proteins, was also implicated in studies with cultured astrocytes, where microinjection of anti-actin antibody impaired Cx43 membrane trafficking and inhibited gap junctional communication (Theiss and Meller, 2002). Direct interaction of Cx43 with microtubules also has been demonstrated in lysates from rat liver epithelial T51B cells, human fibroblasts, and HEK293 cells (Giepmans *et al*., 2001, Guo *et al*., 2003). Although the nature of this interaction is still unclear, it is possible that Cx43 acts as an anchor to stabilise microtubules, or it may serve to regulate Cx43 expression and distribution via the integrin-mediated cell signaling pathway (Giepmans *et al*., 2001; Guo *et al*., 2003; Dunn and Lampe 2014).

1.5.3 Tight junction Associated Proteins

As mentioned in subsection 1.1.5.1, Laing *et al.*, (2001) showed that the COOH-terminal domain of Cx43 binds ZO-1 in osteoblastic cells. Connexin 43 has also been shown to bind to ZO-1 in several cells, such as KEK 293 and COS7 cells, and this interaction is regulated by phosphorylation of Cx43 by Src tyrosine kinases (Giepmans *et al*., 2001; Toyofuku *et al*., 1998). Zonula occludens-1 is a peripheral membrane scaffolding protein that is specifically enriched at the tight junctions of epithelial and endothelial cells (Stevenson *et al*., 1986). It functions to tether transmembrane proteins to the actin cytoskeleton (Denker and Nigam, 1998) and is also part of adherens junctions (Itoh *et al*., 1993). Although the role of ZO-1 in the functioning of both Cx43 and Cx45 is not clear, it is possible that ZO-1 serves as a scaffold to recruit signaling molecules and/or actin filaments to members of the Cx family, which may help in regulating gap junction formation, with the conversion of the actin cytoskeleton or with intracellular signaling (Wei *et al*., 2004).

1.5.4 Caveolin and Membrane Microdomain

Connexin 43 has also been shown to interact with caveolin-1 (CAV-1), a structural protein that resides in a specialised lipid raft domain known as a caveolae (Schubert *et al*., 2002). Lipid rafts are membrane microdomains enriched in cholesterol and glycosphingolipids, which serve as a platform for a number of diverse cellular processes such as signal transduction, endocytosis, and cholesterol trafficking (Pike, 2004). The functional significance of Cx43's interaction with CAV-1 is still unclear, while Cx45 has not yet been shown to have a role in cholesterol trafficking or any of the above-mentioned processes. Extrapolating from the polarity of Cxs in general, and structural similarities between Cx43 and Cx45, it is possible that Cx45 is also involved in regulating cholesterol trafficking through a non-specific association.

In summary, it can be deduced from the findings discussed in subsections 1.1.5.1 – 1.1.5.4, that Cxs interact with a variety of proteins and molecules to facilitate efficient functioning of physiological processes. It is also evident that most of these findings are derived from studies with Cx 43 and it is therefore important to delineate ligands of other predominant Cx isoforms, such as Cx 45, the subject of the present study. This would aid in elucidating the role of gap junction mediated cell-cell communication.

1.5.5 A speculative model of protein-protein interactions

The characterisation of protein-protein interactions of Cxs and their functional importance has been extensively studies. As a result, studies such as those described above have contributed to the construction of a speculative model based on Cx43 (Wei *et al*, 2004), in order to further elucidate the protein-protein interaction phenomenon in Cxs. Thus, to date, it is known that gap junction channels are associated with a variety of molecules to achieve their physiological functions. In addition to coupling to supporting subunits that regulate biophysical properties of the pore-forming subunit, the channels have also been shown to interact with scaffolding proteins and the cytoskeleton and such interactions are essential for the channel regulation and targeting (Giepmans *et al.*, 2001, Sorgen *et al*., 2018).

Taking all the information discussed from section 1.1.5.1 to 1.1.5.4 into account, Wei *et al.* (2004) proposed that Cx43 interacts with a diverse array of protein-binding

partners which may include signaling proteins (*α*/*β*-catenin, p120ctn), structural proteins (ZO-1, caveolin-1), membrane proteins (cadherins), and proteins that interact with, or are part of, the cell cytoskeleton (*α*-actinin, microtubule). This network of proteins may cross talk with cell signaling pathways that regulate cell adhesion, cell motility, and the actin cytoskeleton (Figure 1.6). Additionally, several protein kinases, including Src tyrosine kinase, PKC, and MAPK can phosphorylate the COOH-terminal of Cx43, potentially altering not only gating of the channel but also protein interactions that may be important in cell signaling. Transcriptional effects may also be elicited via the p120ctn/Kaiso receptors, resulting in additional long-term effects through gene expression changes (Wei, Xu and Lo, 2004).

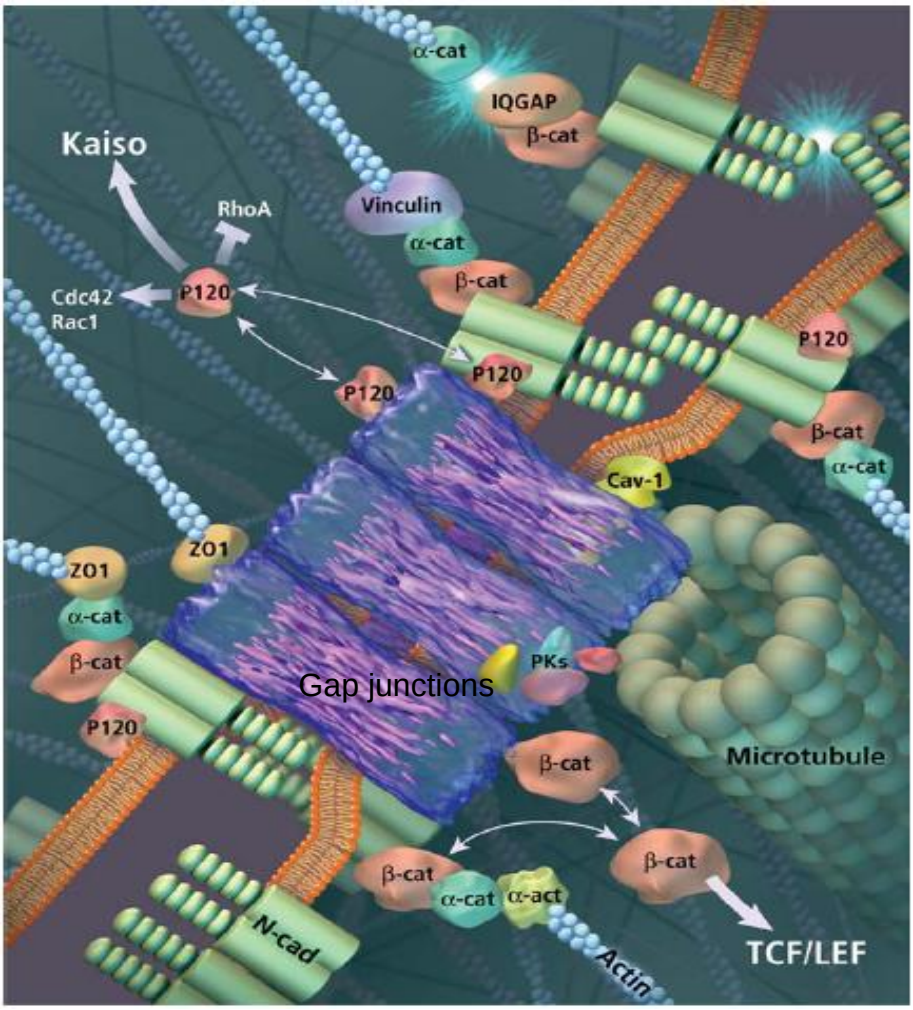

Figure 1.6 Model proposing protein-protein interactions in connexins.

Connexin 43 gap junction interacts with other several members of the signaling complex that include *β*-catenin (*β*-cat), p120ctn, N-cadherin (N-cad), T-cell factor/lymphocyte enhancer binding factor (TCF/LEF), and a host of other proteins,

and together, they facilitate cross talk to affect the coordinate regulation of cell-cell communication (Wei, Xu and Lo, 2004).

Subsequent to the model proposed by We et al., 2004; numerous studies have been conducted to show the role played by the Cx43 carboxyl terminal (Cx43CT) domain in the trafficking, localization, and turnover of gap junction channels via numerous post-translational modifications and protein–protein interactions (Nielsen et al., 2012; Laird, 2010; Herve et al., 2007; Thevenin et al., 2013). Close to 50 proteins have been identified to date to interact with Cx 43 (Sorgen et al., 2018)

1.6 CONNEXINS IN CARDIOVASCULAR FUNCTION

Connexins have been shown to play a role in numerous physiological systems, such as the, digestive, reproductive, immune and cardiovascular systems (Saez *et al*., 2003; Srinivas et al., 2018). A range of studies has been conducted in order to assess the various roles played by Cxs in these systems. However, since the main objective of the current study is to gain further understanding of the functional specificities of cardiac Cxs and their possible involvement in the development of cardiac conduction disorders, only Cx40, Cx43 and Cx45 will be discussed, focusing on their distribution patterns and their speculative roles in cardiac function.

1.6.1 Cardiac conduction system and gap junctions

Cardiac contraction is initiated by an electrical impulse originating from the pacemaker cells of the sinoatrial node (SAN), which is located at the junction of the superior vena cava and the right atrium (Figure. 1.7). The impulse rapidly spreads from the SAN through both atria but its transmission to the ventricular myocardium is prevented by a nonconducting band, the annulus fibrosus. The atrioventricular node (AVN) is located at the junction of the atria and ventricles and is the only conducting route towards the ventricles. The impulse is then transmitted from the AVN to the bundle of His, which is located at the top of the interventricular septum and which divides on either side of the septum into a highly ramified network of Purkinje fibres that activate both ventricular chambers simultaneously. The SAN and AVN node are pace-making and slow-conducting, whereas the bundle of His and Purkinje fibres are fast-conducting pathways (Gaussin, 2004).

Immunohistochemistry and confocal microscopy studies conducted by Yamada and co-workers (2004), on Cx43 and Cx45 gap junctions, have shown that cardiac tissues that differ in their conduction properties show remarkable differences in their relative abundance of gap junctions. They, in fact, showed Cx43 expression in mice hearts to be significantly greater in the endocardial and midmyocardial, compared to the epicardial, layers of the mouse heart, while Cx45 was evenly expressed throughout the ventricles.

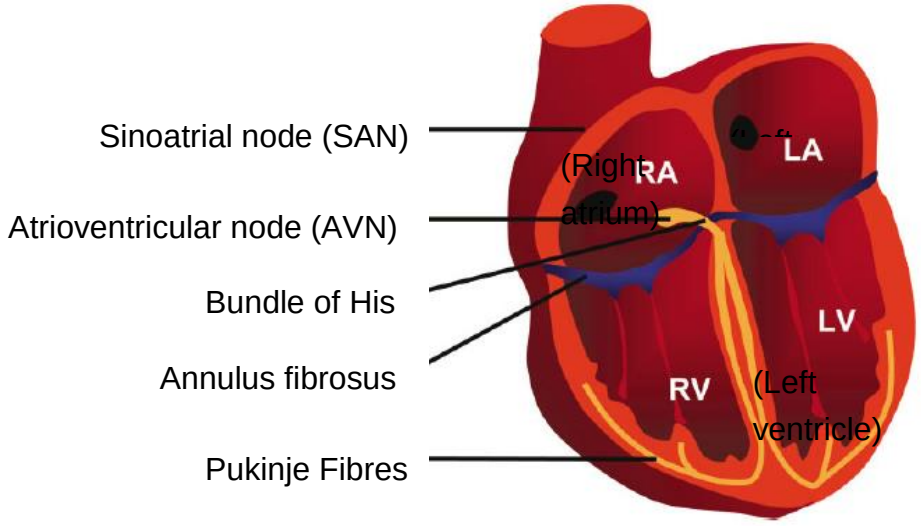

Figure 1.7 Cardiac conduction system (Gaussin, 2004).

Cardiac contraction is initiated by an electrical impulse originating from the pacemaker cells of the sinoatrial node (SAN) then through both atria, the bundle of His and ultimately to Purkinje fibres that activate both ventricular chambers simultaneously.

These findings support the notion that differences in expression patterns of Cxs could contribute to differences in cardiac conduction abilities of different areas of the heart's conduction system (Yao *et al.,* 2003).

1.6.2 Connexin distribution in the heart

Connexin 40, Cx43 and Cx45 are the major Cx isoforms expressed in the heart, which have been shown to exhibit different distribution patterns in specialised cardiac tissues. The absolute amounts of different Cxs in cardiac myocytes have not been determined; rather, their relative distribution has been derived from the intensity of immunostaining (Severs *et al*., 2001). Connexin 43 appears to be the major Cx in the working myocardium of the ventricle (Becker and Davies, 1995),

whereas in atrial myocytes Cx43 is coexpressed with Cx40 (Severs *et al*, 2001). Studies of cardiac tissues from several different species (human, dog, cow, rabbit) have shown that Cx43 is rare or absent in cells of the specialised conducting regions of the SAN and AVN (Figure 1.8A and 1.8B) (Teunissen and Bierhuizen, 2004). However, some studies have found Cx43-expressing cells that might form specialised pathways for electrical conduction out of nodal zones (Severs *et al.*, 2004). Although it varies from animal to animal and stage of developments, expression of Cx40 in the heart is more restricted than that of Cx43. It is abundant in atrial myocytes and cells of the His-Purkinje system and is also found in cells of the SA and AV nodes (Bukauskas *et al*, 1995). Connexin 45 expression is detectable in cells of the atria, ventricle, SAN and AVN, and His bundle (Coppen *et al.*, 1999).

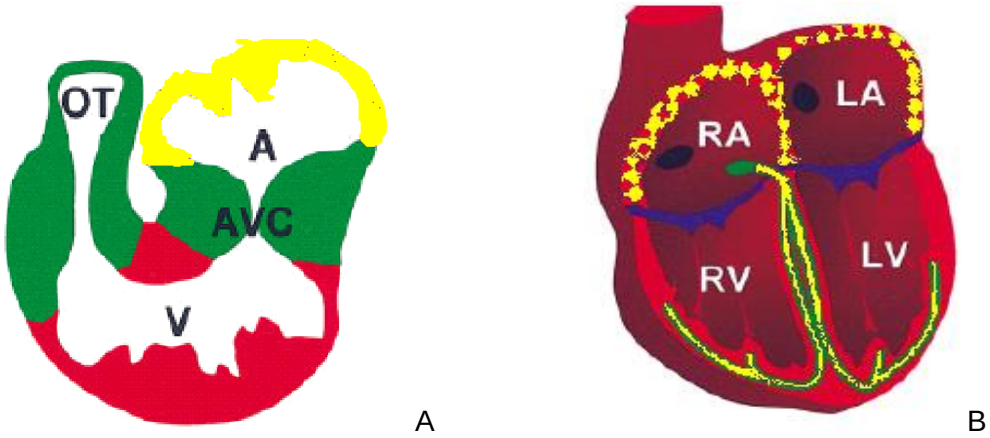

A B

Figure 1.8 Distribution of major cardiac connexins

(A) during heart development, (B) in the adult heart. A=atrium, V=ventricle, AVC=Atrioventricular canal, OT=Outflow Tract, RA and LA=Right and left atria, RV and LV=Right and left ventricles, Cx 45=green, Cx 40=yellow, Cx 43= red (Gaussin, 2004).

Generally, all types of blood vessel wall cells express Cx43, *in vivo* and *in vitro*. *In vivo*, Cx40 mRNA or protein has been demonstrated in large and small vessel endothelium and in smooth muscle from several species (Bastide *et al.*, 1993 and Gros *et al.*, 1994). Cx40 is a major gap junction protein of endothelial cells of the adult vasculature in most organs (van Veen, 2004; Hucker *et al*., 2008 and Greener *et al*., 2011). While arterial smooth muscle cells abundantly express Cx43, they may also express Cx40 (Severs *et al.*, 2001; Chandler *et al*., 2009 and Kreuzberg *et al*., 2009) and Cx45 (Coppen *et al.,* 1999; Kreuzberg *et al*., 2009 and Greener *et al*., 2011).

1.7 DISEASES ASSOCIATED WITH CONNEXIN MUTATIONS

The importance of connexin-based signalling in human physiology has been highlighted by the discovery of numerous mutations in connexin genes causing severe disorders in a wide range of tissues and systems (Pfenniger *et al*, 2011). These disorders can be broadly grouped into six classifications, namely hearing loss, myelin-related disorders, oculodentodigital and craniometaphyseal dysplasias, cataracts, skin disorders and cardiovascular disorders (Kelly *et al*., 2015). These diseases can either present themselves in a non-sydromic (only one phenotype associated with the disease) or syndromic (more than one phenotype) manner. These diseases can be caused by a by a range of missense, nonsense, insertion, deletion and frame-shift mutations and can be inherited in an autosomal dominant, recessive or X-linked fashion (Kelly *et al*., 2015; Srinivas *et al*., 2017).

To date, twenty eight (Table 1) distinct human disorders have been linked to mutations in ten connexin genes (Srinivas *et al*., 2017). Eight of these disorders result from mutations in Cx26, and an additional six disorders are caused by mutations in Cx43. The highest number of distinct mutations has been identified in Cx32. Chromosome-X-linked Charcot-Marie-Tooth disease was the first disease to be linked to a Cx, when it was shown that point mutations in Cx32 gave rise to abnormal Cx32 trafficking, which ultimately led to distorted gap junction channel assembly and abnormal gating properties (Latour *et al*., 1997, Sun *et. al*., 2016). However, because of the broad range of phenotypes across which these diseases extend, only cardiovascular diseases will be discussed, as they are pertinent to the scope of this study.

Table 1.1: Genetic disorders caused by human connexin mutations (Adapted from Srinivas et al. 2018)

Protein	Chromosome	Disorder	OMIM
Cx 43	6q22.31	Craniometaphyseal dysplasia,	218400
		autosomal recessive Erythrokeratodermia variabilis et progressiva	133200
		Oculodentodigital dysplasia	164200
		Oculodentodigital dysplasia,	257850

Protein	Chromosome	Disorder	OMIM
		autosomal recessive	
		Palmoplantar keratoderma with congenital alopecia	104100
Cx 46	13q12.11	Cataract	601885
Cx 37	1p34.3		
Cx 40	1q21.2	Atrial fibrillation, familial, 11	614049
		Atrial standstill, digenic (GJA5/SCN5A)	108770
Cx 50	1q21.2	Cataract	116200
Cx 59	1p34.3		
Cx 62	6q15		
Cx 32	Xq13.1	Charcot-Marie-Tooth neuropathy, X-linked 1	302800
Cx 26	13q12.11	Bart-Pumphrey syndrome	149200
		Deafness, autosomal dominant 3A	601544
		Deafness, autosomal recessive 1A	220290
		Hystrix-like ichthyosis with deafness	602540
		Keratitis-ichthyosis-deafness syndrome	148210
		Keratoderma, palmoplantar, with deafness	148350
		Vohwinkel syndrome	124500
		Porokeratotic eccrine ostial and dermal duct nevus	
Cx 31	1p34.3	Deafness, autosomal dominant 2B	612644
		Deafness, digenic, (GJB2/GJB3)	220290
		Erythrokeratodermia variabilis et progressiva	133200
Cx30.3	1p34.3	Erythrokeratodermia variabilis et	133200

Protein	Chromosome	Disorder	OMIM
		progressiva	
Cx31.1	1p34.3		
Cx 30	13q12.11	Deafness, autosomal dominant 3B	612643
		Deafness, autosomal recessive 1B	612645
		Deafness, digenic (GJB2/GJB6)	220290
		Ectodermal dysplasia 2, Clouston type	129500
Cx 25	6q14.3-q15		
Cx 45	17q21.31		
Cx 47	1q42.13	Leukodystrophy, hypomyelinating, 2	608804
		Spastic paraplegia 44, autosomal recessive	613206
		Lymphedema, hereditary, IC	613480
Cx30.2	7q22.1		
Cx 36	15q14		
Cx 31.9	17q21.2		
Cx 40.1	10p11.21		
Cx 23	6q24.1		

Connexin 40 gene mutations have been found to be associated with atrial fibrillation, whereas Cx43 gene mutations have been linked to both atrial fibrillation and sudden infant death syndrome (SIDS) (Van Norstrand *et al*. 2012). Connexin 40 has been argued to be the dominant connexin required for impulse conduction in the atria and, thus, both somatic and germ-line mutations in this connexin have been shown to predispose patients to atrial fibrillation (Christophersen *et al*. 2013; Gollob *et al*. 2006). Atrial fibrillation is characterised by uncoordinated electrical activity in the atria of the heart, causing the heartbeat to become fast and irregular, in addition to increasing the risk of stroke and sudden death (Molica *et al*., 2014). These observations have also been summarised in a mouse model of atrial fibrillation that expresses the human Cx40-A96S mutation and in which the mouse heart exhibits significantly reduced atrial conduction velocities and prolonged episodes of atrial

fibrillation (Lubkemeier *et al*. 2013). To date, three somatic mutations and six autosomal dominant germline mutations in Cx40 (and one somatic mutation in Cx43) have been identified in 23 lone atrial fibrillation patients (Bai 2014).

Sudden infant death syndrome (SIDS) is a poorly understood disease that leads to the death of as many as 2000 children per year under the age of one in the USA (Kochanek *et al*. 2011). Mutations in the E42K and S272P regions of Cx43 have been found to be associated with SIDS (Van Norstrand *et al*. 2012). Although both mutations are found in highly conserved regions, the E42K mutation clearly disrupts normal Cx43 properties, whereas the S272P mutant has been found to traffic and function normally. Therefore, Van Norstrand *et al*. (2012) suggested that the S272P mutation cannot be considered as a sudden-death predisposing mutation, whereas Cx43-E42K, although rare, is the first connexin mutation to be implicated in the pathogenesis of SIDS.

1.8 CONNEXIN-DEFICIENT ANIMAL MODELS

A variety of experimental approaches have been used to identify molecules and regulatory factors involved in cardiac development and function. Some of these approaches include transgenic mouse models which have proven useful, particularly in determining the roles played by various Cx isoforms in the heart. A range of alterations in their number and distribution has been observed in Cx-deficient animals and this has been correlated to cardiac abnormalities similar to those reported in known cardiac Cx-associated human diseases, as detailed below (Gutstein *et al.*, 2001, Reame *et al.*, 1995, Oyamadu *et al.*, 2005; 2013).

Cx43 knock-out mice

Reaume and colleagues used knock-out mice to determine the function of Cx43 in cardiogenesis and cardiac function (Reaume *et al.*, 1995). These mice survived until birth and presented a relatively normal heart structure and contractile function. However, at birth they appeared cyanotic and died shortly thereafter, apparently due to a lack of blood flow to their lungs caused by swelling and obstruction of the right ventricular outflow tract (Reaume *et al.*, 1995). Gutstein and co-workers further verified these observations by generating heart specific knock-outs of Cx43 (Gutstein *et al.*, 2001). The Gutstein study also showed the down-regulation of other isoforms, such as Cx45 (Gutsein *et al.*, 2001), suggesting co-expression of these two Cx

isoforms. Furthermore, a series of transgenic experiments (using wild-type or mutant Cx43) by Lo and colleagues (1999) have emphasised the role of Cx43 expressed by cardiac neural crest cells for the proper development of the heart (Lo *et al.*, 1999). Heart looping defects have also been described in Cx43-null mice, although these abnormalities disappeared by embryonic day (E) 12 (E12) (Ya *et al.*, 1998). These observations, therefore, suggested that the presence of Cx43, although important, is not an absolute requirement for the heart to beat, or for the anatomic development of the heart. It thus can be speculated that Cxs do replace one another in certain processes.

Cx40 knock-out mice

Cx40-null mice, on the other hand, were shown to present prolonged atrioventricular conduction (as shown by widened QRS complexes on electrocardiograms), right bundle branch block and were prone to develop arrhythmias (Kirchhoff *et al.*, 1998, Simon *et al.*, 1998). These animals developed to adulthood and reproduced normally, which indicated that Cx40 may not be necessary for cardiac development, since the cardiac structure and chambers appeared normal (Simon *et al.*, 2004). These mice also retained gap junctional communication between aortic endothelial cells, despite altered characteristics with respect to wild-type mice. Additionally, Cx37 and Cx43 were upregulated and redistributed (Simon *et al.*, 2004), suggesting a compensatory mechanism, to be discussed below.

Cx45-knock out mice

Among the three predominant cardiac Cxs, Cx45 is the only isoform expressed in earliest cardiomyocytes (Alcolea *et al.*, 1999) and its knock-out experiments have been useful in gaining understanding of the physiology of early cardiomyocytes. Independent studies by Kruger *et al.,* (2000) and Kumai *et al.*, (2000) showed Cx45-null mice to die during embryogenesis, due to abnormalities of vascular development and cardiogenesis (Kruger *et al.*, 2000). Endothelial cell development and positioning appeared normal, but further formation of vascular trees was impaired and the smooth muscle layer of major arteries failed to develop. The hearts of these animals were dilated, and apoptosis was observed in almost all tissues by E9.5, which contributed to their death by E10.5. Their hearts also showed a looping defect, reduced trabeculation, and disrupted formation of the endocardial cushions and a conduction block (Kumai *et al.*, 2000; Kruger *et al.*, 2000; Nishii *et al.*, 2003). Significantly, expression of the calcium-dependent transcription factor, NF-ATc1,

was inactivated in the endocardium. NF-ATc1-deficient mice were also seen to present defects associated with formation of endocardially-derived valve tissues (de la Pompa *et al.,* 1998; Kruger *et al.,* 2000; Kumai *et al*., 2000; Ranger *et al.,* 1998), suggesting the possibility that Cx45 has a role in modulating calcineurin signaling required for NF-ATc activation.

Functional equivalence of connexins

As discussed throughout section 1.1.8, all Cx isoforms present unique molecular structures, implying that they possess unique functions. However, mice knock-out studies have shown some Cxs to have overlapping functions. For instance, Cx40 knock-out/Cx45 knock-in mice (Cx40KO/Cx45KI) presented normal impulse propagation in the RA, AV note and the left His bundle branch, suggesting that Cx45 is sufficient to partially compensate for lack of Cx40 (Alcolea *et al.,* 2004). Furthermore, as previously discussed, Cx45 knock-out mice die at E10 and, as Cx45 is widespread during heart development, it was surprising when Kumai *et al.*, (2000) detected heart contractions at E8.5, implying that other Cx isoforms were functional in the heart tube. In addition, Verheula *et al*., (1999) found Cx43 knock-out mice to survive early stages of heart development due to Cx40 and Cx45 expression, they, however, die due to the migration of neural crest cells to the pulmonary outflow tract.

Summary of section 1.1.8

In summary, knock-out mice studies show the importance of gap-junction mediated communication in normal embryonic development and suggest both common and unique functions for various Cx isoforms during cardiac development. It is also evident that while some Cxs can partially replace other isoforms, morphological differences observed in knock out mice suggest that they are functionally inequivalent. These studies also may give an indication of possible cardiac disorders that may ensue as a result of mutations in any of the Cx isoforms and/or possibly their binding partners.

1.9 SELECTED INHERITED CARDIAC CONDUCTION DISORDERS

Almost every person's heart will occasionally produce an extra beat or two, and the distressing symptoms that may accompany the extra beats such as dizziness and palpitations do not necessarily signal a serious health problem (McPherson *et al.*, 2003). However, more serious disorders may ensue as a result a malfunction in the

heart's conduction system. Furthermore, the conduction system is crucial in the synchronised coordination of cardiomyoctes, allowing the passage of electrical impulsewhich ultimately cause the heart to beat.

The pathophysiological mechanisms underlying these conditions are diverse (Michaelson *et al*., 1995). Previously, cardiac conduction disorders were viewed as a structural disease of the heart in which macro- or microscopical structural abnormalities in the conduction system underlay disruption of normal impulse propagation. Conduction disturbances were later observed to be present in the absence of anatomical abnormalities. To date, it is believed that functional, rather than structural, alterations underlie most conduction disturbances (Wilde and Bezzina, 2005; Jansen, 2010; Mezzano, 2014; Nademanee, 2015). The molecular causes of most of these disorders have been identified inherited forms of which are believed to be from abnormalities in cardiac conductive pathways which are governed by electromechanical factors. The following sub-sections, will therefore give an overview of two inherited syndromic diseases associated with cardiac conduction abnormalities, among other features; namely: Myotonic Dystrophy (DM) (Gatchel and Zoghbi, 2005), Holt-Oram Syndrome (HOS) (Bruneau *et al.*, 2001), and Progressive Familial Heart Block type II (PFHBII), identified in South Africa, whose primary clinical features include cardiac conduction disturbances as well as heart block (Brink and Torrington, 1977).

A. Myotonic dystrophy (DM)

Myotonic dystrophy, or Steinert's disease, an inherited condition showing an autosomal dominant mode of inheritance, is the most prevalent form of muscular dystrophy with a frequency of 1 in 8000 individuals worldwide. Affected individuals express highly heterogeneous, multisystemic symptoms including myotonia, progressive muscle weakness and wasting, cataract development, testicular atrophy, and cardiac conduction defects (Gatchel and Zoghbi, 2005). The molecular mechanism of this disorder was determined from its linkage to chromosome 19q13.3 and subsequent identification of an expanded CTG repeat in the 3′ UTR of the myotonic dystrophy protein kinase gene *DMPK* in patients with DM (Brook *et al*., 1992). Furthermore, studies revealed that disease severity generally correlates with repeat length. Notably, non-mutant carriers have 5–38 CTG repeats at this locus, whereas DM-affected individuals have repeats in the hundreds to thousands.

This condition was later divided into two forms, DM1 and DM2, for after the genetic cause of DM1 was revealed, a group of DM patients who did not have CTG expansions at the known DM locus were identified (Liquori *et al*., 2001). Despite common clinical features, such as myopathy, myotonia, cataracts, and cardiac disturbances and a common mode of inheritance, these patients also presented proximal muscle weakness, often involving hip flexors and extensors. Hence, proximal myotonic myopathy (PROMM) was the initial term used in diagnosis for those who did not have DM1 (Thornton *et al*., 1997, Ricker *et al.,* 1995, Day *et al.,* 2003). Almost a decade after the discovery of unstable CTG repeats in 3′ UTR of *DMPK*, in 2001 Liquori and colleagues revealed that a CCTG expansion in intron 1 of the zinc finger protein 9 gene *ZNF9,* on chromosome 3q21, is associated with individuals who were diagnosed with having PROMM/DM2 (Liquori *et al*., 2001). This new locus associated with the myotonic dystrophy disorder PROMM was then designated DM2.

Both the DM1- and DM2-causing genes share repeat expansions in noncoding regions of genes (*DMPK* and *ZNF9*, respectively) that are expressed in tissues affected by this disease. The fact that both genes were associated with repeat expansions in transcribed but untranslated regions suggested that the mutant RNA might have a significant role in the disease process (Harper, 2004). However, another recognised difference between DM1 and DM2 is that only the DM1 locus presents a congenital form of this disorder (reviewed by Cho and Tapscott, 2006).

B. Holt-Oram syndrome (HOS)

Holt-Oram syndrome was first clearly described by Holt and Oram (1960), who observed cardiac atrial septal defect in four generations of a family whose affected members also presented with a congenital anomaly of the thumbs which lay in the same plane as the fingers, and inwardly curved terminal phalanges (reviewed by Davies, 1992). McKusick and co-workers (1961) reported a mother and daughter with atrial septal defect and absent or triphalangeal, fingerlike thumbs (McKusick *et al.,* 1961). In 1966, the daughter gave birth to a male infant with flipper-like hands and ventricular septal defect. The involvement of the arm was more extensive and the cardiovascular involvement more varied in the families described by Lewis *et al*. (1965) and Harris and Osborne (1966) than in the family of Holt and Oram (1960). These studies clarified the autosomal dominant pattern in which HOS is inherited, as well as the clinical manifestation of the disease.

Basson and co-worked (1994) validated previous clinical findings described in the 60s in patients with HOS. These authors found the affected individual to have upper limb malformations and a high incidence of congenital heart disease, accompanied by abnormal cardiac electrophysiology, including AV block (Basson *et al*., 1994). The HOS causative gene, *TBX5* gene, a T-box transcription factor, has been linked to the development of the heart and upper limbs before birth. This gene's product was also suggested to be important particularly for cardiac septation and possibly the development of bones in the arms and hands (Basson *et al*., 1997; Li *et al*., 1997). These findings were further validated in heterozygous knock-out mice, which exhibited the morphological defects of the HOS, as well as conduction defects (Bruneau *et al*., 2001). Additionally, the TBX domain has been proposed to act as a DNA-binding domain (Basson *et al*., 1999). In another study, Hiroi *et al*., (2001) found that TBX5 associated with NKX2-5 and synergistically promotes cardiomyocyte differentiation. TBX5-binding has also been found in a number of cardiac expressed genes, such as α-actin, α-cardiac myosin heavy chain (*MYH)* and β-cardiac myosin heavy chain *MYH* genes, which suggests a role by TBX5 in their regulation (Ghosh *et al*., 2001).

C. Progressive familial heart block I and II (PFHBI and PFHBII)

Progressive familial heart block type I (PFHBI) is an autosomal dominantly inherited disease of the cardiac bundle branch, first described by Brink and Torrington in 1977. It segregates in a large South African pedigree of Portuguese descent and two smaller pedigree (Figure 1.9). Clinically it is characterised by right bundle branch block, left anterior or posterior hemiblock, or complete heart block detected on ECG by the presence of broad QRS complexes (Brink and Torrington, 1977; Van der Merwe *et al.*, 1986; Van der Merwe *et al.*, 1988).

Initial linkage studies mapped the PFHBI causative-gene to a 10cM region between genetic markers *D19S412* at the centromeric limit, and *D19S866* at the telomeric limit of chromosome 19q13.3 (Brink *et al.* 1995). Concomitantly, another conduction disorder known as isolated cardiac conduction disease (ICCD) was mapped in a Lebanese family to the same region as PFHBI (Stephan *et al*., 1995). However, since these two conditions shared common clinical symptoms and genetic loci, they later were regarded as the same disease (Brink – personal communication, reported by Arieff, 2004). Fine-mapping strategies later reduced the PFHBI locus to about 7cM (De Jager - personal communication, reported by Arieff, 2004), and further fine-

mapped it to the 4cM (2.42Mb) region of chromosome 19q13.3 which ultimately set the centromeric limit to *D19S606* (Figure 1.10) (Arieff, 2004). The genetic cause for PFHBI was found to be caused by the mutation c.19G-->A in the transient receptor potential cation channel, subfamily M, member 4 gene (TRPM4) at chromosomal locus 19q13.3 (Kruse *et al*., 2009).

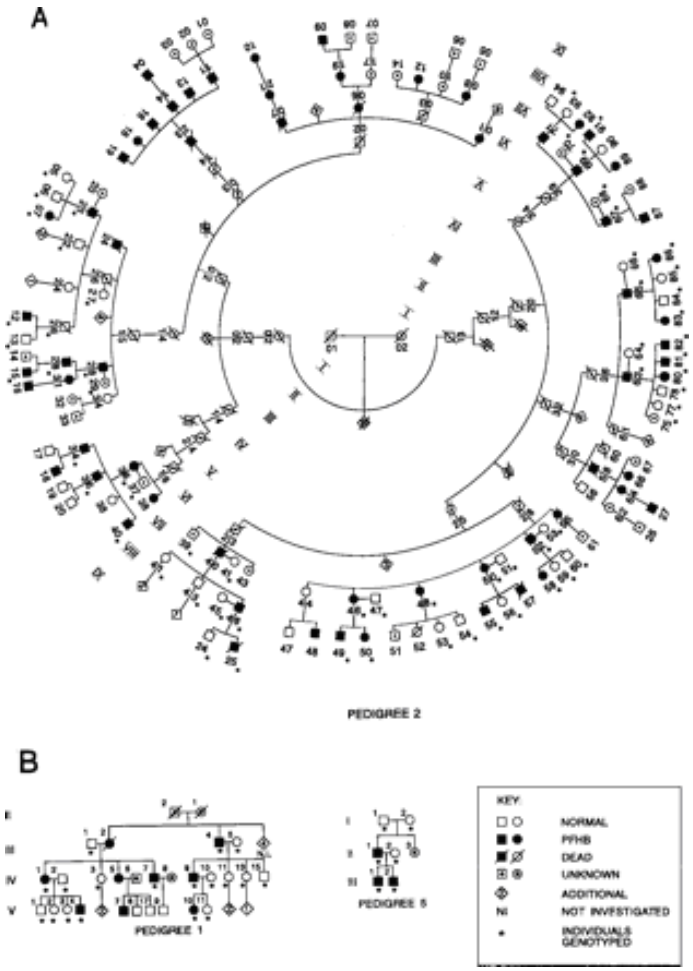

Figure 1.9 Pedigrees (1, 2 and 5) in which PFHBI segregates.

A. Pedigree 2 is a nine generation pedigree traced back to a single male of Portuguese descent (I.01) and his wife (I.02), who married in 1735. B. Pedigrees 1 and 5, are smaller pedigrees of individuals who presented the same phenotype as PFHBI-affected individuals and share the same haplotype, although no genealogical links have been established with pedigree 2 (Brink *et al*, 1995).

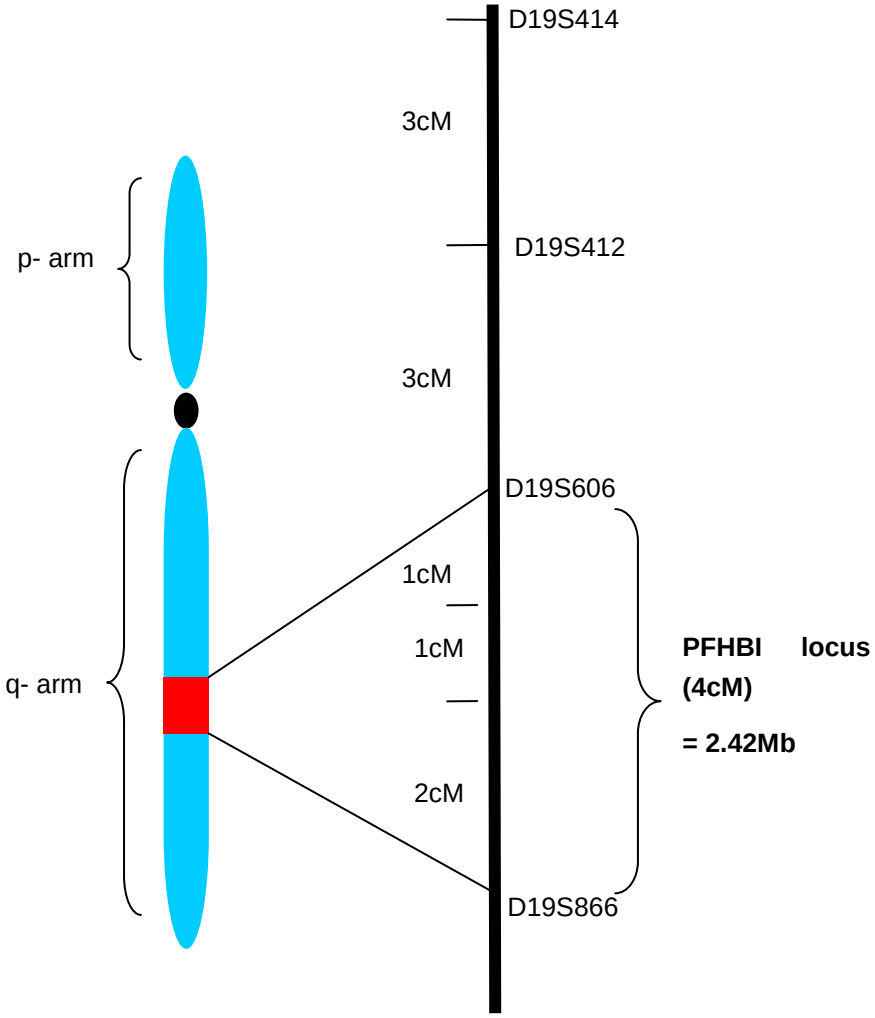

Figure 1.10 The PFHBI locus

Flanked by the *D19S606* and *D19S866* markers is harboured in the 4cM region in chromosome 19q13.3 (Arieff, 2004 – PhD thesis).

Progressive familial heart block type II (PFHBII) segregates in a South African Afrikaner family of Dutch descent (Figure 1.12). Like PFHBI, it is inherited in an autosomal dominant manner (Brink and Torrington, 1977). However, its clinical features include sinus bradycardia and left posterior hemiblock which later progresses to complete heart block, detected as narrow QRS complexes on ECG (Brink and Torrington, 1977). Progressive familial heart block type II is associated with syncopal episodes, Stoke-Adam seizures (light-headedness) (van der Merwe, 1986) and dilated cardiomyopathy (Fernandez *et al.*, 2004). The genetic cause for PFHBII is still illusive ; however, it was found to be located within a 2.85Mb region on

chromosome 1 between q32.2 and q32.3, a region flanked by the *D1S70* and *D1S505* markers (Fernandez *et al.,* 2005).

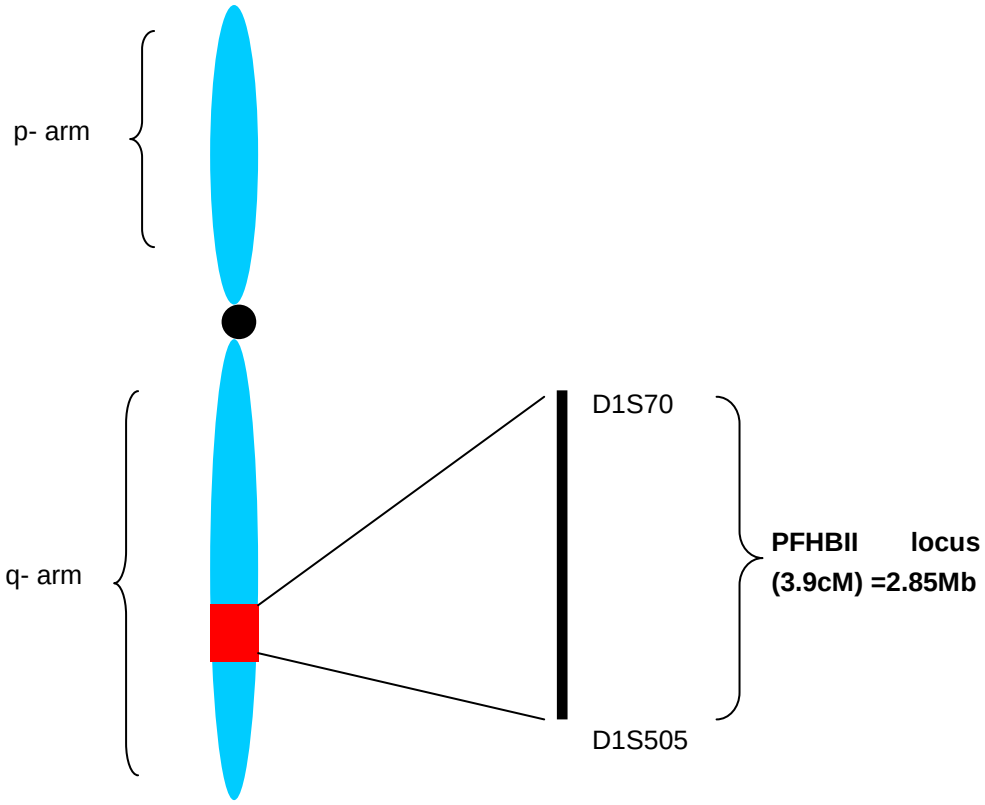

Figure 1.11 The PFHBII locus, flanked by the *D1S70* and *D1S505* markers is harboured in the 2.85Mb region in chromosome 1q32.2 – q32.3 (Fernandez *et al*., 2005).

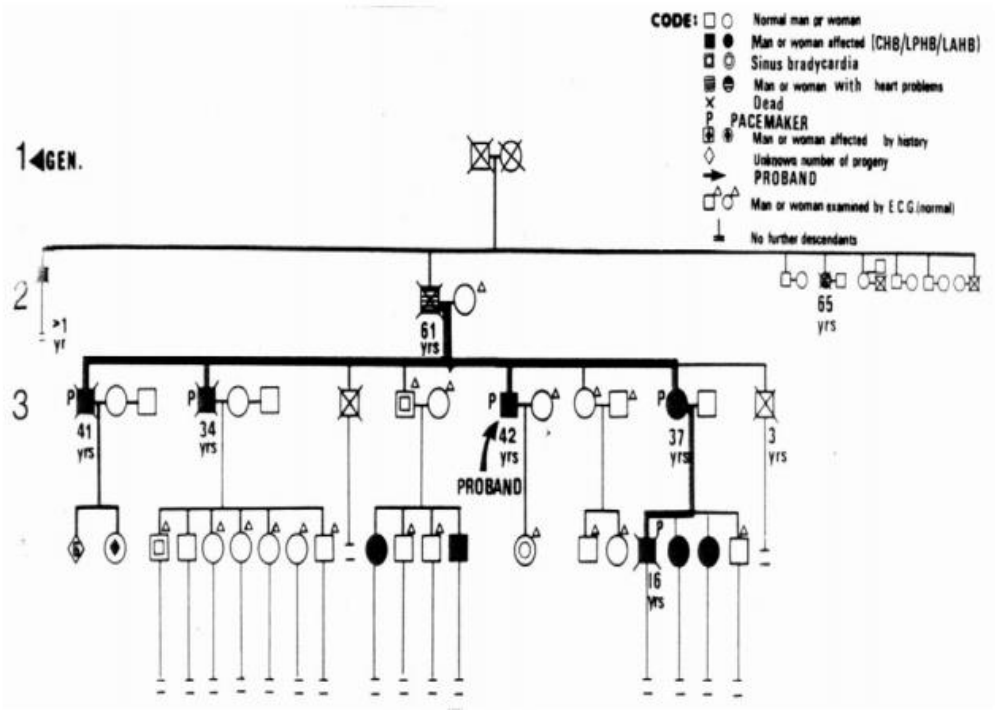

Figure 1.12: A four-generation pedigree in which PFHBII was identified and described (Brink and Torrington, 1977).

Twenty four members of the family were clinically evaluated in the original study and 10 of them were affected.

1.9.1 Exclusion of connexins as FHBII causative genes

A number of cardiac ions channels which control the flow of ions, such as Na^+, Ca^{2+}, K^+ and Cl^- ions, are present in membranes of cardiomyocytes. These channels facilitate the passage of electrical potential which ultimately causes the heart to beat. However, when conduction pathways are dysfunctional and the electrical flow is disrupted, cardiac conduction disorders, such as PFHBII, may ensue. It therefore seemed plausible to deduce that genes encoding proteins of channels physically and electrically joining cardiac myocytes such as the *Cxs* would be good candidates for PFHBII. Hence, Cxs were included in a list of putative candidate genes for PFHBII. However, independent bioinformatic and genetic mapping analyses conducted by Fernandez (2004) excluded Cx as aetiological genes, as they were not found within the genetic loci of PFBHII. However, it was intriguing to note that DMPK, encoded by the *DMPK* gene, colocalises with Cx43, a prominent cardiac Cx (Mussini *et al.*, 1999). Hence, an explanation for the conduction disturbances that are part of the DM syndrome could be that functional defects caused by mutated DMPK may affect Cx-binding. Since DM is characterised by conduction disturbances similar to those in

PFHBII -affected individuals, it seemed plausible to hypothesise that other proteins that interact with Cxs could contribute to the aetiology of either conduction disorder.

1.10 METHODS TO STUDY PROTEIN-PROTEIN INTERACTIONS

As discussed in previous sections, cardiac Cx isoforms have, in part, been linked to numerous diseases. For instance, Cx40 was associated with the development of DCM in mice (Richardson et al., 1999), which is also a clinical manifestation in PFHBII-affected individuals (Fernandez *et al*., 2004). Myotonic dystrophy, characterised among other clinical features, by cardiac conduction disturbances, is another interesting condition whose causative protein, DMPK co-localises with Cx43 (Mussini *et al*., 1999). As mentioned above, this DMPK-Cx43 association is, in fact proposed, though not proven, to play a role in the development of cardiac conduction disturbances in DM-affected patients (Mussini *et al*., 1999). Since the causative gene of PFHBII has not yet been identified, it seemed plausible to hypothesise that other Cxs or Cx-interacting proteins could lead to the development of either of thiscondition.

A number of methods have been applied to identify protein interactions in order to further understand the biochemical nature of the interactors and their possible roles in physiological processes. In the following subsections, principles of the two techniques employed in the current study, the yeast-2-hybrid (Y2H) and mammalian-2-hybrid (M2H) analyses will be discussed. Additionally, advantages and disadvantages of both of these techniques will be outlined.

A. YEAST TWO-HYBRID (Y2H)

The Y2H method, developed by Fields and Song (1989), exploits the principle of transcription (Fields and Song, 1989). Yeast two-hybrid uses two protein domains of a transcription factor that have specific functions: a DNA-binding domain, that is capable of binding to DNA, and an activation domain, that is capable of activating transcription of the downstream reporter gene (Figures 1.13 and 1.3) (Ma and Ptashne, 1988). The binding domain and the activation domain do not necessarily have to be on the same protein. In fact, an engineered protein with a binding domain can activate transcription when bound to any other engineered protein containing an activation domain (Fields and Song, 1989).

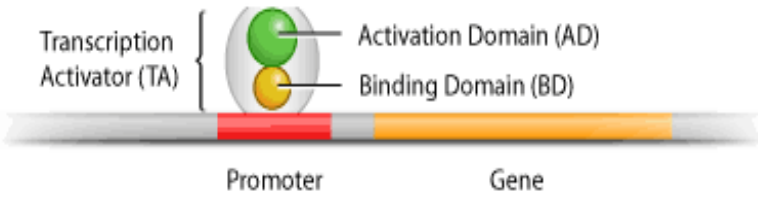

Figure 1.13 Normal transcription requires both the DNA-binding domain (BD) and the activation domain (AD) of a transcriptional activator (TA) (Sobhanifar, 2005).

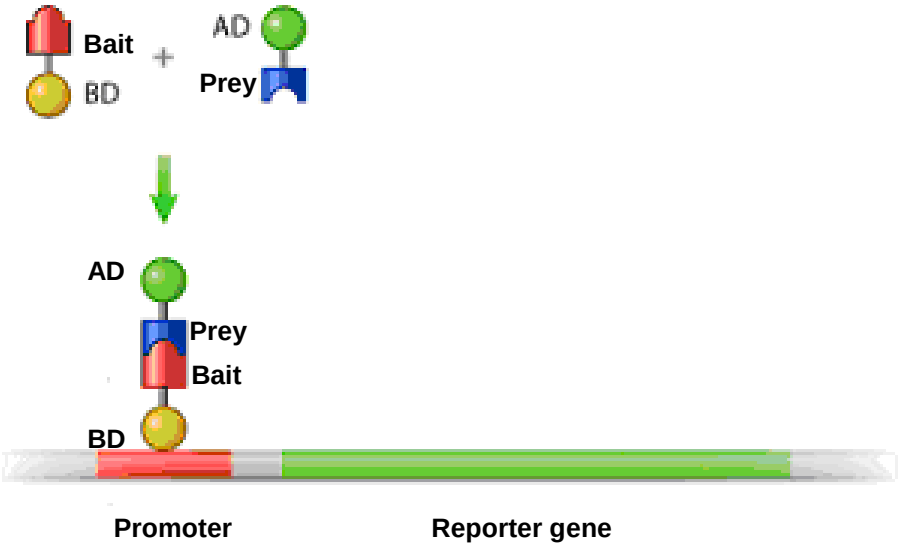

Figure 1.14 Yeast two hybrid transcription.

The yeast two-hybrid technique measures protein-protein interactions by measuring transcription of a reporter gene. If the bait protein and the prey protein interact, then their DNA-binding domain and activation domain will come to close proximity to form a functional transcriptional activator. The transcriptional activator will then proceed to transcribe the reporter gene that is paired with its promoter (Sobhanifar, 2005).

In the Y2H assay, two fusion proteins are created: the **bait** construct is constructed to have a DNA binding domain, commonly derived from the yeast Gal4 protein (Chien *et al.,* 1991, Durfee *et al*., 1993), attached to its NH_2-terminus, while the **prey** construct, is fused to an activation domain. These fusion proteins are co-expressed in yeast, where a physical interaction between the bait and prey leads to the reconstitution of a functional transcription factor, derived from the Gal4 protein

(Chien *et al.,* 1991, Durfee *et al*., 1993), which binds to the upstream activatory sequence of the promoter of the receptor gene (Figure 1.14). Thereafter, transcription of the reporter gene occurs. A protein-protein interaction is therefore translated into reporter gene activity which can be measured, usually involving selectable yeast genes such as *HIS3* (Durfee *et al.,* 1993) and *LEU2* (Fusco *et al*., 1999).

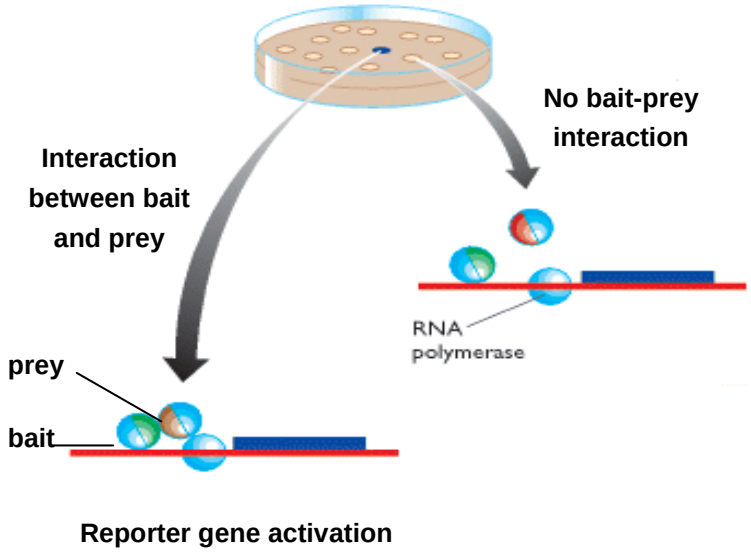

Figure 1.15 Y2H library screening.

The bait and prey constructs are mated and co-transfected into yeast. A colony in which the reporter gene is expressed contains fusion proteins whose bait and prey interact, thereby bringing the DNA-binding and activation domains into proximity and stimulating the RNA polymerase to drive nutritional reporter gene activation. This in turn allows auxotrophic yeasts to grow in selective growth medium. However, if there is no interaction between the bait and prey fragment, no growth of the yeast will be observed (Adapted from Brown, 2002).

In a typical Y2H experiment, *S. cerevisiae* cells are transfected with plasmid constructs bearing genes usually encoding either the bait or the prey (the latter may be individual recombinant clones from a cDNA library) portions of the hybrid proteins. The two, bait and prey, yeast strains are mated and the mixtures plated onto primary selection media (lacking histidine, tryptophan and leucine) (Figure 1.15). Diploid colonies expressing tryptophan (*TRP1*), leucine (*LEU2*) and histidine (*HIS3*) reporter genes are then transferred to more stringent selection media (lacking adenine, histidine, tryptophan and leucine) and diploid colonies expressing the *TRP1*, *LEU2,*

HIS3 and adenine (*ADE2*) reporter genes then tested, by nutritional selection. For the expression of the *MEL1* reporter gene a colourmetric assay which also indicates the strength of the bait-prey interaction is used (Fields and Songs, 1989).

The Y2H technique is one of the most favoured methods for studying protein-protein interactions. One of its most prominent benefits is that it mimics an *in vivo* system using the yeast host cell as a “live test tube”. It more closely resembles the higher eukaryotic system than most *in vitro* techniques based on bacterial expression. Another advantage to Y2H is that only the cDNA, be that full-length or a partial region, of the gene of interest is needed, in contrast to sometimes-high quantities of purified proteins needed in classical biochemical techniques (Ma and Ptashne, 1998). Weak interactions can also be detected since the genetic reporter gene strategy results in a significant amplification. Apart from the ability to screen libraries, this system also allows for the analysis of specific or suspected interactions (Guthrie and Fink, 1991).

However, in spite of improvements to increase it applicability, the Y2H method has numerous disadvantages, one of these being the risk of using artificially engineered fusion proteins. The fusion protein might change the actual conformation of the bait and/or prey and consequently alter functionalities increasing the possibility of obtaining false positives or negatives. This change in conformation might result in a limited activity or in the inaccessibility of binding sites (Ma and Ptashne, 1988). Another disadvantage of Y2H is that it makes use of yeast, *S. cerevisiae*, and not mammalian cells as a host. At times the bait protein may not fold correctly nor exist as a stable protein inside the yeast cells (Ma and Ptashne, 1988). Additionally, another disadvantage of assaying protein-protein interaction in a heterologous system is that some interactions depend on post-translational modifications, such as phosphorylation, that do not occur in yeast (Greener and Perkel, 2005). Since the two-hybrid system needs the fusion proteins to be targeted to the yeast nucleus, it might be a disadvantage for extracellular proteins or proteins that contain strong targeting signals to other subcellualr regions (Greener and Perkel, 2005), as transcription would not occur. Furthermore, some proteins might become toxic upon expression in yeast. Other proteins might proteolyse essential yeast proteins or proteins essential for the system like the DNA-binding domain or the activation domain (Greener and Perkerl, 2005).

From the above discussion, it is evident that the Y2H method, like any other method, is not problem-free. In spite of all this, it still is the method of choice for most

molecular scientists. Many disadvantages may not be detrimental to the overall output of protein-protein studies, as they may be circumvented by conducting any of a battery of verification assays, one of which is the M2H technique.

B. MAMMALIAN TWO-HYBRID (M2H)

The M2H system was developed using a strategy similar to that used in the Y2H system (Vasavada *et al*., 1991). Just as in the Y2H system, a reporter gene transcription factor is functionally and physically divided into an activation domain and a DNA binding domain. The recombinant vectors that express both the **bait** and **prey** fusion proteins are co-transfected into the mammalian cell with a reporter plasmid (Figure 1.15). So if these fusion proteins interact, the reporter gene will be expressed (Figure 1.17).

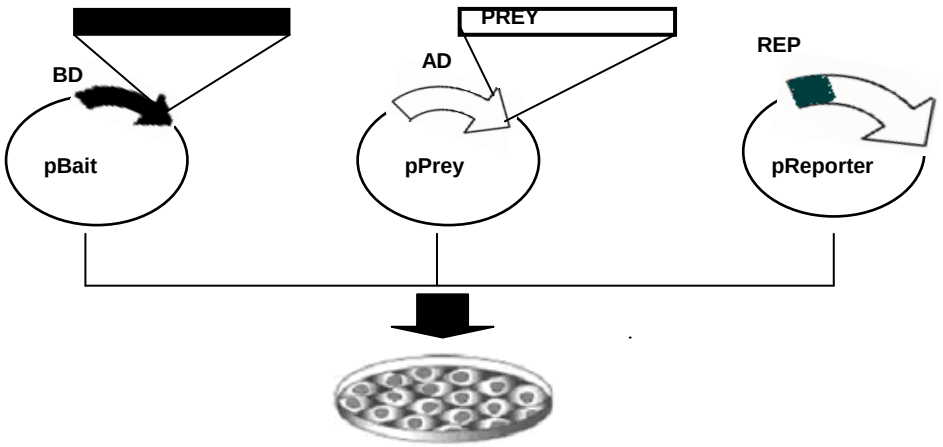

Figure 1.16 In M2H mammalian cells are co-tranfected with three plasmids.

p-Bait construct, p-Prey construct and p-Reporter construct, and then incubated to allow reporter gene expression (Luo *et al.*, 1997).

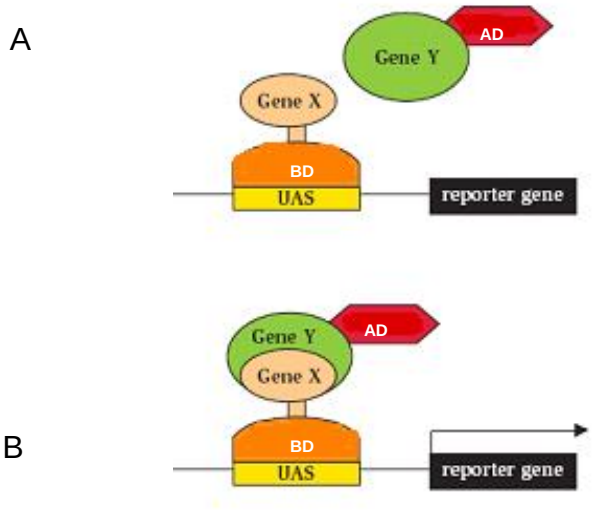

Figure 1.17 The principle behind both Y2H and M2H.

(A) Gene X is cloned downstream of the binding domain (BD) to form the bait construct. Gene Y is cloned downstream of the activation domain (AD) to form the prey construct. As indicated in figure 1.15 bait, prey, and reporter constructs are co-transfected into a mammalian cell line. If protein X interacts with protein Y, the AD is brought together with the DNA-binding domain, which will turn on the reporter gene; UAS = Upstream activation sequence (Fan and Lui, 2002).

The M2H method has been shown to be useful in verifying protein-protein interactions in order to rule out false positives. Protein interactions in mammalian cells are said to mimic the *in vivo* situation better than in yeast cells, as in mammalian cells they are believed to assume their native conformation. As previously mentioned (1.1.10A), some of the post-translational modifications, such as phosphorylation, that do not occur *in vitro* or in yeast are accommodated by the M2H system. Another advantage to using the M2H system is that this assay is less time-consuming than the Y2H. In M2H, the reporter gene assay can be completed within 48 h of transfection. Quantitative results are also immediately available (Luo et al, 1997).

It has been suggested that the M2H exhibits some disadvantages of the Y2H methods as both are based on the same principle of transcription. Since M2H makes use of hybrid proteins, its output may not necessarily be the true reflection of interactions that take place in nature. A significant drawback of M2H is that it can not be used for library screen, only known or suspected pair-wise interactions can be

tested. Additionally, the hybrid proteins may be misfolded which increases the possibility of obtaining false positives or negatives.

1.11 WHOLE EXOME SEQUENCING

Compared with Sanger sequencing, NGS had been reported to have many advantages, including high speed, low cost, less time consuming, high sensitivity, need of less amount of sample, and sequencing multiple genes at a higher coverage (Garraway, 2013). Whole Exome sequencing (WES), involves exome capture, which limits sequencing to the protein-coding regions of the genome, composed of about 20,000 genes, 180,000 exons, and constituting approximately 1% of the whole genome (Choi *et al*., 2009).

A typical workflow of WES analysis consists of the following steps: raw data quality assessment, pre-processing, alignment, post-processing, variant calling, annotation, and prioritization (Bao *et al*., 2014).

Whole exome sequencing (WES) has been used to reveal genetic variants in affected individuals with various forms of cardiomyopathies such as hypertrophic cardiomyopathy (HCM) as well as dilated cardiomyopathy (DCM) (Table 2). Seidman *et al*, 2001 and Colombo *et al*., 2008 studied family histories of HCM and DCM patients, respectively. Studies by Voelkerding *et al*., 2010; Dellefave and McNally, 2010 found mutations of genes encoding sarcomere proteins in HCM etiologies and showed a more heterogeneous etiology of DCM (Voelkerding *et al*., 2010; Dellefave and McNally, 2010). Meder *et al*., 2011 established a comprehensive genetic screening in patients with hereditary DCM and HCM in a cost-efficient manner using array based subgenomic enrichment systems. They found two microdeletions and four point mutations in six patients.

Whole exome sequencing has also been used to characterise the causal gene of familial combined hypolipidemia (ANGPTL3) (Musunuru *et al*., 2010), severe hypercholesterolemia (ABCG) (Rios *et al*., 2011) and familial dilated cardiomyopathy (BAG3) (Norton *et al*., 2011). The use of this technology promises to revolutionise genetic research in cardiovascular diseases as it has potential to indentify rare SNPs susceptible to cardiovascular diseases (Table 2).

Obscurin has been somewhat neglected in these studies, largely because its functional role is far from clear. There was an isolated report in 2007 of obscurin mutations associated with HCM but this was not followed up for several years. Recently, whole exome sequencing methodology (WES) has been used to address mutations in OBSCN, the gene for obscurin, and OBSCN variants were found to be relatively common in inherited cardiomyopathies. Marston *et al*.'s (2015) study found 5 OBSCN unique variants in 4 individual hearts from a group of 30 end-stage failing hearts, Xu *et al*. (2015) found 6 OBSCN unique variants in 74 HCM cases and Rowland *et al*. (2016) found 4 OBSCN unique variants in 335 DCM and LVNC patients, of which OBSCN variants were associated with 3 out of 11 LVNC cases (Marston, 2017).

Table 1. 2: Reported WES approaches in cardiovascular diseases (Rabbani et al., 2014 and Marston, 2017).

Category	Disease (Inheritance)	Identified gene	Studied subject	References
Cardiomyopathy	Recessive HCM	MRPL44	Two siblings	Carroll *et al*., 2013
	Recessive HCM	MTO1	Two unrelated Families	Ghezzi *et al*., 2012
	Dominant ARVC	DES	One family	Hedberg *et al*., 2012
	Recessive HCM Sengers syndrome	AGK	One individual	Mayr *et al*., 2012
	Recessive DCM	GATAD1	One family	Theis *et al*., 2011,
	Recessive HCM	MRPL3	One family	Galmiche *et al*., 2011
	Recessive HCM	AARS2	One family	Gotz *et al*., 2011
	Dominant DCM	BAG3	One	Norton *et al*., 2011
	DCM	OBSCN	Four individuals	Marston *et al*., 2015

Category	Disease (Inheritance)	Identified gene	Studied subject	References
	HCM LVNC		Six individuals 3 individuals	Xu *et al*., 2015 Rowland *et al*., 2016
Heterotaxy Cardiovascular	Recessive	SHROOM3	One	Tariq *et al*., 2011
Familial combined hypolipidemia	Recessive	ANGPTL3	Two families	Musunuru *et al*., 201
Channelopathy	X-linked intellectual disability, atrial fibrillation, cardiomegaly, congestive heart failure	CLIC2	Two males	Takano *et al*., 2012

1.12 THE CURRENT STUDY

Numerous studies have been conducted to date to establish the causative genes of cardiac conduction disorders associated with dilated cardiomyopathy (DCM) (Graber *et al*. 1986; Mestroni *et al*. 1990; Gavazzi *et al*. 2001; Oropeza and Cadena 2003). In some families, a single gene defect has been identified as the cause of the disease. However, the causative genes underlying a number of inherited cardiac conduction, DCM associated disorders such as Progressive Familial Heart Block Type II (PFBH II) remain elusive (Towbin and Bowles, 2002; Antzelevitch 2003; Fernandez *et al*, 2004). The identification of the causative mutations of these disorders will enable precise diagnosis and provide guidelines to effectively treat them.

Connexins 40, 43 and 45, predominantly expressed in the heart, have been shown to exhibit specific as well as shared functions (Section 1.1.6.2). Animal studies and even human studies have highlighted that Cxs may substitute for one another if one is inactivated (Oyamada *et al*., 2005, 2013). To date, most studies have focused on Cx43; hence the aims of this study which are to:

1) Assess functional specificity of cardiac Cx45 to further understand its role in cardiac function and possibly in the development of cardiac conduction diseases.
2) Prioritise ligands that would possibly map to the PFHBII locus as candidate genes for PFHBII.
3) Identify and prioritise putative PFHBII-causing mutations using whole exome sequencing (WES).

In search of the PFHBII locus, our research group found by linkage analyses, that the specific causative gene for PFHBII was harboured in a 3.9cM region between q32.2 and 32.3 on chromosome 1 (Fernandez *et al*., 2005). Cardiac Cx knock-out studies pointed towards the cardiac Cxs as attractive candidate causative genes of these cardiac conditions. For instance, Cx40 and 45 knock-out mice presented cardiac conditions similar to those of known human disorders (Moreno, 2004), Cx40 knock-outs presented prolonged atrioventricular conduction and Cx45 knock-out mice die at E10 of conduction block symptoms which could be related to the PFHBII phenotype. However, no Cx genes were identified in this locus nor did any mutation screening identify other causative genes (Fenandez, 2004, PhD thesis – University of Stellenbosch).

Nonetheless, it was intriguing to note that DMPK, encoded by the *DMPK* gene, mutations of which were linked to DM, colocalised with Cx43, a prominent cardiac Cx (Mussini *et al.*, 1999). Since DM is characterised by conduction disturbances similar to those in PFHBII-affected individuals, it seemed plausible to identify Cx ligands as causative genes.

As most studies have focused on Cx43, in the present study ligands of the COOH-terminal domain of cardiac Cx45 were identified in order to assess the specific and possibly shared functions of the most prominent Cxs by comparing the ligands of Cx45, with those of Cx40 (R. Keyser, 2007, MSc Thesis – University of Stellenbosch), as well as known ligands of Cx43. In addition, it was planned that any identified ligands that serendipitously mapped to the PFHBII locus would be screened for causing disease in members of affected families. The strategy followed was to employ the Y2H technique to identify ligands of the COOH-terminal domain of Cx45, by screening a cardiac cDNA library. As major differences among the Cx isoforms occur in the COOH-terminal domain and because of its participation in protein-protein interaction, the COOH-terminal domain of Cx45 was chosen as "**bait**" in a "fishing expedition" of the cardiac cDNA for putative "**preys**". Sequences of the identified preys were then identified by conducting sequence homology searches against sequences in Genbank databases which also enabled us to prioritise them according to their chromosomal location, biological relevance and subcellular localisation. Verification of true interactors was then attempted by M2H. Whole exome sequencing was used to further identify putative causative mutations in PFBH II patients.

CHAPTER TWO: MATERIALS AND METHODS

2 MATERIALS AND METHODSPART I: YEAST-TWO HYBRID AND MAMMALIAN-TWO

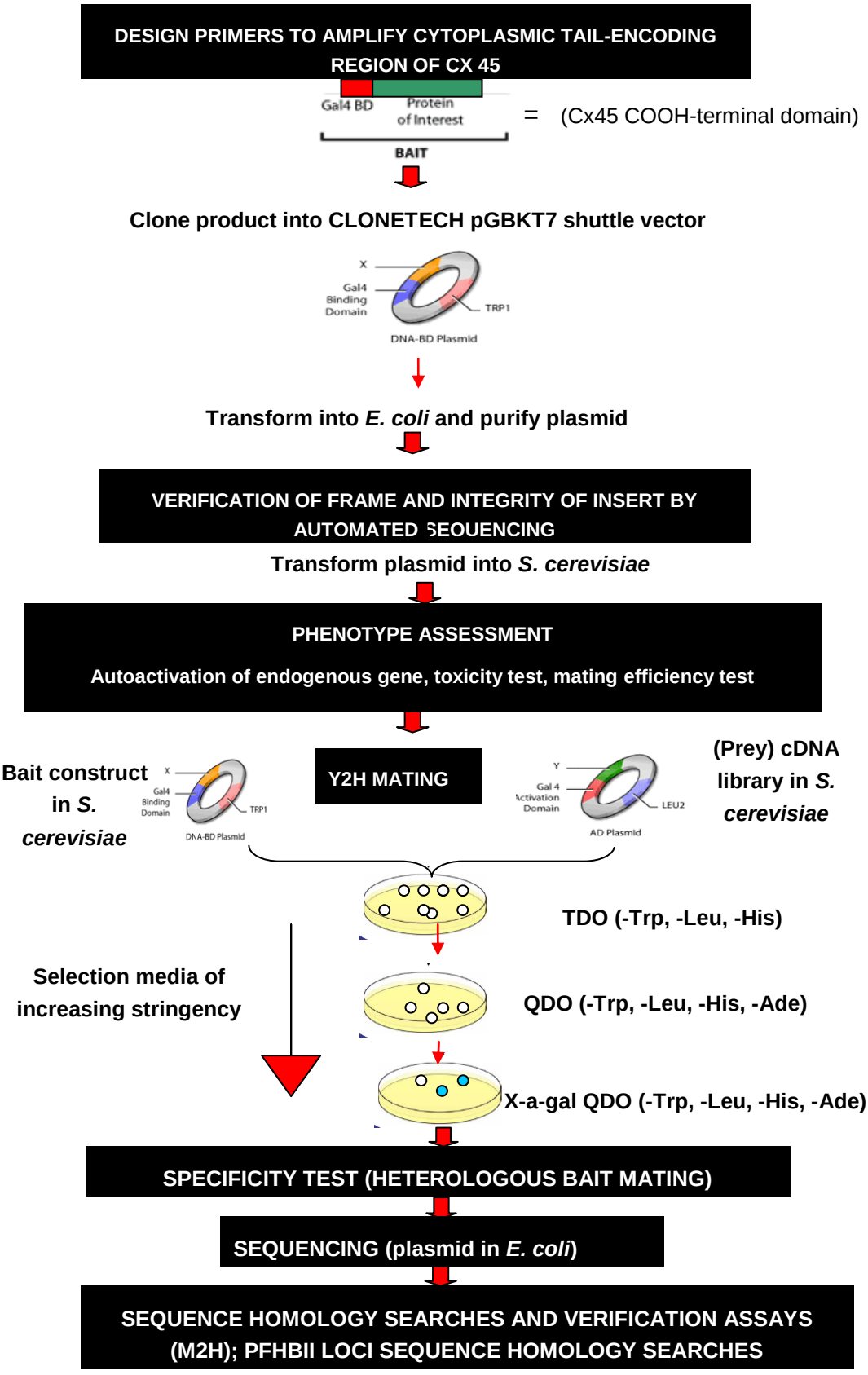

2.1 DNA EXTRACTION

2.1.1 Extraction of DNA from human nuclei.

In order to amplify the region encoding the COOH-terminal domain of Cx45, DNA was extracted from 5ml of an anonymous banked blood sample of a subject enrolled as a control in a project approved by the University of Stellenbosch ethics committee, following a method modified in the Molecules and Genes in Inherited Conditions (MAGIC) laboratory (Corfield *et al*., 1993).

2.2 POLYMERASE CHAIN REACTION (PCR)

The PCR was conducted in order to amplify regions of DNA fragments to be used in the Y2H and M2H screens. Namely, it was firstly used to amplify the region encoding the COOH-terminal domain of cardiac expressed Cx45, to be used as bait in the Y2H screen of a cardiac cDNA library, from human genomic DNA. Thereafter, PCR amplification was used to detect this *Cx45* bait fragment in the recombinant Y2H plasmid constructed and then to amplify fragments of the prey inserts identified. It was also conducted to detect the prey fragments in recombinant M2H vectors.

2.2.1 PRIMER DESIGN

2.2.1.1 Oligonucleotide primer design and synthesis

Oligonucleotide primers were designed using sequence data available either from the Ensembl database (http://www.ensembl.org) or the Genbank database (http://www.ncbi.nlm.nih.gov/Entrez) (see Appendix I for sequences used) or Clontech. Several variables were taking into account when the primers were designed. Among the most critical were; primer length, annealing temperature (T_a), melting temperature (T_m), complementary primer sequences, G/C content and polypyrimidine (T, C) or polypurine (A, G) stretches and 3'-end sequence.

These parameters are interdependent, for instance the longer the primer length, the higher the T_a , which in turn affects the T_m. To optimise the specificity of the primers used and prevent self-annealing, their respective lengths were designed to be between 18 and 24 bases. As each PCR contained two primers, they were designed to have similar annealing temperatures. Furthermore, the primers were designed with no intra-primer homology beyond four base pairs, nor inter-primer homology at the 3' end in order to avoid primer dimer formation. The primers had a base

composition of between 45% and 55% GC-content. Additionally, a G or C residue was also included at the 3' end to ensure correct binding due to stronger hydrogen bonding between G/C residues. All of these parameters were assessed using a computer programme (DNAman™ version 4 software [Lynnion Biosoft Corp©]).

2.1.1.2 Connexin 45 oligonucleotide primers

The region encoding the Cx45 COOH-terminal domain was PCR amplified to generate the 444bp Cx45 COOH-terminal domain-encoding fragment (Figure 2.1). To ultimately facilitate cloning into the appropriate vector, both primers were designed to have engineered restriction enzyme sites on the 5' ends; *Nde*I for the forward primer and *EcoR*I for the reverse primer. In addition, these two primers included "overhang" nucleotides (9bp) at their 5' ends to facilitate restriction enzyme digestion of the engineered *Nde*I and *EcoR*I sites. The reverse primer also contained a "stop" codon upstream of the restriction enzyme site. The sequences of the primers used for this part of the study are shown in table 2.1.

Table 2.1 Primer sequences and annealing temperatures used for the amplification of the COOH-terminal domain of Cx45 gene from genomic DNA.

Primer name	Sequence	T_a
Cx45-*Nde*I(F)	5'- actgcagaa catatg atgcttcatttagggtttgg-3'	56 C
Cx45 *EcoR*I(R)	5'-ATCTCTGCA GAATTC TTA AAATCCAGACGGAGGTC-3'	56 C

Abbreviations: °C, degrees Celsius; Ta, annealing temperature; sequences in black font represent the sequence of the primer that anneals to the DNA in the PCR reaction. The sequences in coloured fonts represent tags for cloning: **Blue, "overhang" tag**; **red, *EcoR*I restriction site**; **brown, stop codon** and **green, *Nde*I restriction site, Cx45-*Nde*I(F)**; connexin 45 forward primer with engineered *Nde*I restriction site, **Cx45-*Nde*I(F)**;connexin 45 reverse primer with engineered *EcoR*I restriction site, Cx45 ***EcoR*I(R)**.

2.2.1.2 Primers for Y2H insert screening

In order to amplify inserts cloned into Y2H cloning vectors, primers were designed to vector-specific sequences flanking the multiple cloning site (MCS) of pGBKT7 Y2H

cloning bait vector (BD Bioscience, Clontech, Paulo Alto, CA, U.S.A) (Figure 2.2). Another set of primers was designed using vector specific sequences flanking the MCS of pGADT7-Rec Y2H cloning prey vector (Figure 2.3) in order to sequence ligands or preys identified from the Y2H screen. The specific vector sequences used in the synthesis of these primers were obtained from the Clontech™ Matchmaker™ vector handbook (www.clontech.com). The sequences of these vector-specific primers are shown in table 2.2.

Table 2.2 Primer sequences and annealing temperatures used for the amplification of inserts from cloning vectors

Primer name	Sequence	T_a (°C)
pGBKT7(F)	5'-TCATCGGAAGAGAGTAG-3'	50
pGBKT7(R)	5'-TCACTTTAAAATTTGTATACA-3'	51
pGADT7-Rec (F)	5'CTATTCGATGATGAAGATACCCCACCAAACC-3'	68
pGADT7-Rec (R)	5'-gtgaacttgcggggtttttcagtatctacga-3'	68

Abbreviations: °C, degrees Celsius; Ta, Annealing temperature; pGBKT7 (F), bait cloning vector forward primer; pGBKT7(R), bait cloning vector reverse primer; pGADT7-Rec (F), prey vector forward primer and pGADT7-Rec(R), prey vector reverse primer.

2.2.1.3 Primers for mammalian two-hybrid analysis (M2H)

Primers were designed in order to amplify the *Cx45*-bait insert from recombinant pGBKT7 and clone it into the pM GAL4 DNA-binding domain vector for M2H screening (section 2.13). Separate sets of primers were designed to amplify Cx45 putative ligands identified during the course of the study from pGADT7-Rec for cloning into the pVP16 GAL4 activation domain vector. The sequence and annealing temperatures of these primers are shown in table 2.3.

Table 2.3 Primer sequences and annealing temperatures used for the amplification of inserts for M2H analysis.

Primer name*	SEQUENCE	Ta(°C)
NADH-*EcoR*1(F)	5'-ATCTAGTGA GAATTC GCCCACGGACTTACATCC-3'	58
NADH-*Xba*I(R)	5'-ATCTCTGCA TCTAGA CTA GGATCCCGTACGATGCC-3'	58
Myo-*BamH*1(F)	5'-ATCTCTGCA GGATCC GAGCACTAACCACAAACG-3'	54
Myo-*Mlu*I(R)	5'-ATCTCTGCA ACGCGT CTA GTATCTACGATTCATCTG-3'	53
Cox1-*EcoR*I(F)	5'-ATCTCTGCA GAATTC ACAGACCGCAACCTCAAC-3'	56
Cox1-*Mlu*I(R)	5'-ATCTCTGCA ACGCGT CTA GTATCTACGATTCATCTG-3'	57
SCF – EcoRI(F)	5'-ATCTCTGCA GAATTC GTGTCCAGGCCGGAGCC-3'	60
SCF – *Hind*III(R)	5'-ATCTCTGCA AAGCTT CTA TCAGTATCTACGATTCATCTG-3'	58
CD63-*EcoR*I(F)	5'-ATGCATCCTG GAATTC ATGGCGGTGGAAGGAGGAATG-3'	66
CD63-*Hind*III(R)	5'-ATCTCTGCA AAGCTTCTA GTATCTACGATTCATCTGCAG-3'	60
Obs-*EcoR*I(F)	5'-ATCTCTGCA GAATTC ATGGGAAAGCAGTGCAGG-3'	56
Obs-*Hind*III(R)	5'-ATCGACTAC AAGCTT CTA GTATCTACGATTCATCTG-3'	53
TX2-EcoRI(F)	5'-ATCTCTGCA GAATTC ATGGCTCAGCGACTTCTTCTG-3	64
TX2-*Hind*III(R)	5'-ATCTCTGCA AAGCTT CTA GTATCTACGATTCATCTG -3'	60

Abbreviations: °C, degrees Celsius; Ta, annealing temperature; sequences in black font represent the sequence of the primer that anneals to the DNA in the PCR reaction. *Prey identification; NADH= NADH dehydrogenase subunit IV, Myo = Myomegalin, CoxI = cytochrome C oxidase subunit I (CoxI), SCF = SCF apoptosis response protein I, CD63 = CD63 antigen, Obs = Obscurin, TX2 = Thioredoxin II. The sequence in coloured fonts represents tags for cloning: **Blue, "overhang" tag**; **red, *Hind*III enzyme restriction site**; **green, *EcoR*I enzyme restriction site**;

orange, *Mlu*I enzyme restriction site; **pink, *Bam*HI enzyme restriction site**; **purple, *Xba*I enzyme restriction site and brown, stop codon.**

2.2.2 PCR-amplification for generation of Cx45 COOH-terminal domain bait fragment.

The generation of the Cx45 COOH-terminal domain bait fragment (Figure 2.1), from 100ng control genomic DNA, was performed using PCR amplification. A PCR reaction mix was made up consisting of 15µl of an equimolar dNTP mixture (2.5mM of each, dATP, dCTP, dGTP and dTTP) solution, supplied by manufacturer (TaKaRa Shuzo Co. Ltd, Shiga, Japan), 50µl Ex Taq^{TM} Mg^{2+}-containing 10x reaction buffer, supplied by manufacture (TaKaRa Shuzo Co. Ltd, Shiga, Japan), 150ng of each primer (Table 2.1) and 395µl ddH_2O. A volume of 1µl of template DNA was added to an aliquot of 46µl reaction mix. Thereafter, 0.5µl ExTaq^{TM}, supplied by manufacturer (TaKaRa Shuzo Co. Ltd, Shiga, Japan) was added. Thermo-cycling was performed in a GeneAmp®, PCR system 9700 thermal cycler (P.E Biosystems, Forster, City CA. U.S.A) using the following cycling parameters: a single denaturing cycle of 94°C for 5min, followed by 30 cycles of 94°C for 30s, 49°C for 30s and 72°C for 1min. PCR conditions are summarised in table 2.4.

Table 2.4 PCR conditions used for amplification of Cx45 insert (Y2H)

Primer set	[$MgCl_2$] mM	TD °C	Time sec	TA °C	Time sec	TE °C	Time sec
Cx45-*Nde*I(F)/ Cx45-*EcoR*I(R)	1.5	94	30	49	30	72	150

Abbreviations: °C, degrees Celsius; $MgCl_2$, magnesium chloride mM, millimolar; sec, seconds; TA, annealing temperature; TD, denaturing temperature; TE, extension temperature. The thermocycler was set to perform 30 amplification cycles; Cx45-*Nde*I(F), connexin 45 forward primer with engineered *Nde*I restriction site, Cx45-*EcoR*I(R), connexin 45 reverse primer with engineered *EcoR*I restriction site.

A

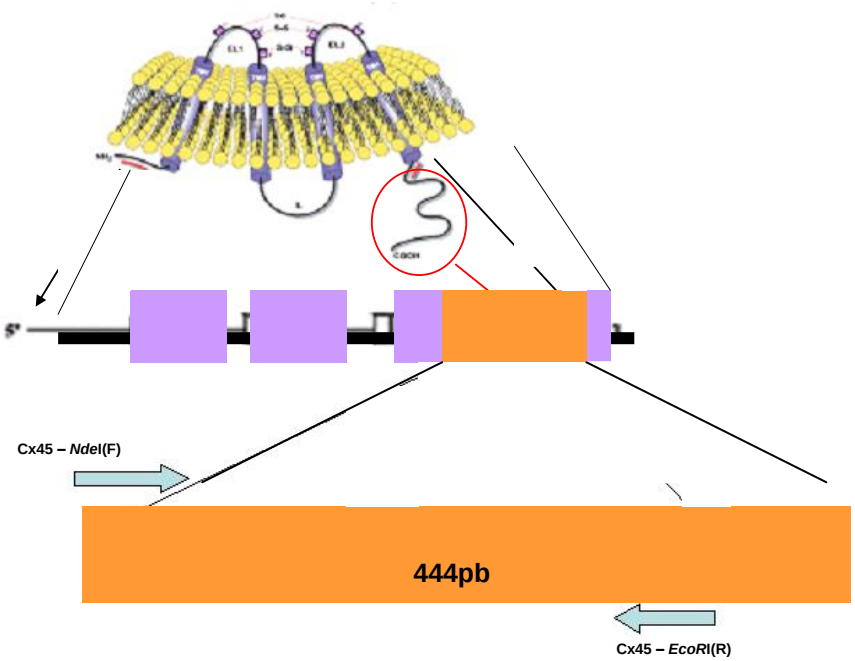

B

Primer Cx45 – *Nde*I(F) 5'- ACTGCAGAA CATATG ATGCTTCATTTAGGGTTTGG-3'

Primer Cx45 – *EcoR*I(R) 5'-ATCTCTGCA GAATTC TTA AAATCCAGACGGAGGTC-3'

Figure 2.1 A. PCR amplification of Cx45 COOH-terminal domain.

B. Nucleotide sequences of forward (Cx45-*Nde*I(F) and reverse (Cx45-*EcoR*I[R]) primers obtained from Genbank database http;//www.ncbi.nlm.nih.gov/Entrez).

2.2.3 Bacterial colony PCR

In order to rapidly identify bacterial colonies harbouring the desired recombinant plasmid to be used in Y2H and M2H analyses, bacterial colony PCRs were performed, as the vectors used did not allow blue/white selection. In these PCRs, instead of using 100ng of genomic DNA as template, a tiny amount of a bacterial colony was picked from an agar plate containing the appropriate antibiotic (Appendix I), and used as template. Y2H vector-specific primers and prey-specific forward primers (M2H) (tables 2.5 and 2.6) were used in conjunction with PCR reaction mixtures identical to those described in section 2.2.2 to perform these colony PCR amplifications. No lysis of the bacterial cells was required prior to the PCR as the high temperatures involved would lyse the cell and release its DNA (template) into the PCR mixture. Amplification was performed in a GeneAmp® PCR system 9700 thermal cycler. The cycling parameters consisted of a single denaturing cycle of 94°C for 5min, followed by 30 cycles of 94°C for 30s, 50°C for 30s and 72°C for

1min. PCR amplified products were subsequently separated on a 1% agarose gel for verification by electrophoresis (section 2.4.1).

Table 2.5 PCR conditions used for bacterial colony PCR (Y2H) analysis

Primer set	[$MgCl_2$] mM	TD °C	Time sec	TA °C	Time sec	TE °C	Time sec
pGBKT7(F)/ pGBKT7(R)	1.5	94	30	50	30	72	150

Abbreviations: °C, degrees Celsius; $MgCl_2$, magnesium chloride mM, millimolar; sec, seconds; TA, annealing temperature; TD, denaturing temperature; TE, extension temperature. The thermocycler was set to perform 30 amplification cycles.

Table 2.6 PCR conditions used for bacterial colony PCR (M2H) analysis

Primer set	[$MgCl_2$] mM	TD °C	Time sec	TA °C	Time sec	TE °C	Time sec
Cx45F-*EcoR*I(F)/ Cx45R-*Hind*III(R)	1.5	94	30	54	30	72	150
SCF-*EcoR*I(F)/ pGADT7-Rec-*Hind*III(R)	1.5	94	30	56	30	72	150
Myo-*BamH*I(F)/ pGADT7-Rec-*Mlu*I(R)	1.5	94	30	56	30	72	150
Obs-*EcoR*I(F)/ pGADT7-Rec-*Hind*III(R)	1.5	94	30	56	30	72	150
NADH-*EcoR*I(F)/ pGADT7-Rec-*Xba*I(R)	1.5	94	30	56	30	72	150
TX2-*EcoR*I(F)/ pGADT7-Rec-*Hind*III(R)	1.5	94	30	56	30	72	150
Cox-*EcoR*I(F)/ pGADT7-Rec-*Mlu*I(R)	1.5	94	30	56	30	72	150
CD63-*EcoR*I(F)/ pGADT7-Rec-*Hind*III(R)	1.5	94	30	60	30	72	150

Abbreviations: °C, degrees Celsius; $MgCl_2$, magnesium chloride mM, millimolar; sec, seconds; TA, annealing temperature; TD, denaturing temperature; TE, extension temperature. The thermocycler was set to perform 30 amplification cycles. Primer sets of respective preys, NADH= NADH dehydrogenase subunit IV, Myo = Myomegalin, CoxI = cychrome C oxidase subunit I (CoxI), SCF = SCF apoptosis

response protein I, CD63 = CD63 antigen, Obs = Obscurin, TX2 = Thioredoxin II, and their engineered restriction enzyme sites **red, *Hind*III enzyme restriction site**; **green, *EcoR*I enzyme restriction site**; **orange, *Mlu*I enzyme restriction site**; **pink, *BamH*I enzyme restriction site**; **purple, *Xba*I enzyme restriction site.**

2.2.4 PCR-amplification for mammalian two-hybrid analysis

The Y2H cloning vector containing the "bait" insert, as well as the vector containing putative Cx45-interacting clones isolated in the Y2H screen, were used as templates for the PCR amplification of the inserts to be cloned into the M2H vectors (pM and pVP-16) for the M2H analysis. Amplification was performed in a 50µl reaction volume containing 0.5µl plasmid preparation (section 2.3.1), 150ng of each primer (table 2.6), 1.5µl of an equimolar dNTP solution, 5µl Ex Taq^{TM} Mg^{2+}-containing 10x reaction buffer supplied by the manufacturer, 2U Ex Taq^{TM} and ddH_2O to a final volume of 50µl. Amplification was performed in a GeneAmp $^{®}$ PCR system 9700 thermal cycler. The PCR conditions for the amplification of the bait-insert and each of the putative ligands are shown below (table 2.7).

Table 2.7 PCR conditions used for amplification of inserts for M2H analysis

Primer set	[$MgCl_2$] mM	TD °C	Time sec	TA °C	Time sec	TE °C	Time sec
Cx45-*EcoR*I (F)/ Cx45-*Hind*III (R)	1.5	94	30	54	30	72	30
SCF-*EcoR*I(F)/ pGADT7-Rec-*Hind*III(R)	1.5	94	30	56	30	72	150
Myo-*BamH*I(F)/ pGADT7-Rec-*Mlu*I(R)	1.5	94	30	56	30	72	150
Obs-*EcoR*I(F)/ pGADT7-Rec-*Hind*III(R)	1.5	94	30	56	30	72	150
NADH-*EcoR*I(F)/ pGADT7-Rec-MluI(R)	1.5	94	30	56	30	72	150
TX2-EcoRI(F)/ pGADT7-Rec-HindIII(R)	1.5	94	30	56	30	72	150
Cox-*EcoR*I (F)/ pGADT7-Rec-*Mlu*I(R)	1.5	94	30	56	30	72	150
CD63-*EcoR*I(F)/ pGADT7-Rec-*Hind*III(R)	1.5	94	30	60	30	72	150

Abbreviations: °C, degrees Celsius; $MgCl_2$, magnesium chloride mM, millimolar; sec, seconds; TA, annealing temperature; TD, denaturing temperature; TE, extension temperature. The thermocycler was set to perform 30 amplification cycles.

2.3 PLASMID PURIFICATION

2.3.1 Bacterial plasmid purification[1]

Bacterial plasmids to be used in restriction enzyme digests were extracted using a standard plasmid purification procedure modified in the MAGIC laboratory. One *E. coli* colony containing the plasmid of interest was picked from an appropriate selection plate and inoculated into 10 ml of Luria-Bertani Broth (LB), supplemented with the correct antibiotic (Appendix I), in a 50ml polypropylene tube. The culture was then incubated at 37°C overnight, while shaking at 250rpm in a YIH DER model LM-530 shaking incubator (SCILAB instrument Co LTD., Taipei, Taiwan).

The following morning, the culture was centrifuged for 10min at 3000rpm in a Beckman model TJ-6 centrifuge, after which the supernatant was discarded and the pellet was resuspended by gently pippeting in 1ml of cell suspension solution. Two millilitres of cell lysis solution was added and the contents were mixed by gentle inversion of the tube which was then incubated at room temperature for 5 minutes. Two millilitres of neutralisation solution was added to the tube and the contents were once again mixed by gentle inversion and thereafter incubated at room temperature for 5 minutes. Following this incubation, 5ml of phenol/chloroform/isoamyl alcohol (25:24:1 [PCI]) (Sigma, St Louis, MO, USA) was added to the tube and the contents mixed by gentle inversion, followed by centrifugation at 3000 rpm for 15 min at 4°C in a Multex centrifuge (MSE Instrumentation, England, UK) in order to allow for phase separation. The upper clear plasmid-containing top (aqueous) phase was transferred into a new sterile 50ml polypropylene tube and approximately 0.7x volume 100% isopropanol (Merck, Darmstadt Germany) was added to the tube, which was mixed well by gentle inversion. This was followed by centrifugation at 4°C for 45 minutes in a Multex centrifuge. After centrifugation, the supernatant was discarded and the pellet was washed twice with 2ml ice cold 70% ethanol and then air-dried. The dried pellet was resuspended in 100-200µl ddH_2O and subsequently 3µl of this plasmid preparation was resolved on a 1% SB agarose gel for verification (2.4.1). [1]

[1] All constituents and make up of solutions used this procedure are in Appendix I

2.3.2 Bacterial plasmid purification using Wizard® Purefection Plasmid DNA purification kit [2]

To reduce impurities which could interfere with the sequencing reaction, the Wizard® Purefection Plasmid DNA purification kit was used to extract and purify bacterial plasmids to be transfected into mammalian cells. One *E. coli* colony containing the plasmid of interest was picked from an appropriate selection plate and inoculated into 20 ml LB, supplemented with the correct antibiotic, in a 50ml polypropylene tube. The culture was incubated at 37°C overnight, while shaking at 250rpm in a YIH DER model LM-530 shaking incubator.

The following morning the culture was centrifuged for 10min at 3000rpm in a Beckman model TJ-6 centrifuge. The supernatant was discarded and the pellet was resuspended gently in 1.25ml resuspension solution (Wizard® Purefection Plasmid DNA purification kit, Promega Corp. Madison Wisconsin, U.S.A). Two millilitres of cell lysis solution was added and the contents were mixed by gentle inversion of the tube which was subsequently incubated at room temperature for 5 minutes. Two millilitres of neutralisation solution was added to the tube and the contents were once again mixed by gentle inversion and incubated at room temperature for 5 minutes. The bacterial lysate was centrifuged at 3000rpm for 30 min and the supernatant transferred to a 15ml polypropylene tube. Two hundred and fifty microlitres of endotoxin removal resin was added to the tube and mixed thoroughly. This was followed by a 10 min incubation at room temperature, vortexing the mixture periodically for approximately 5 seconds using a Snijders model 34524 press-to-mix vortex (Snijders Scientific, Tilburg, Holland). The tube was then placed onto a MagniSil™ Magnetic Separation Unit and the solution was allowed to clear for approximately 30 sec. The tube was kept on the magnet and the supernatant was transferred to a new 15ml polypropylene tube.

One millilitre of 5M guanidine thiocyanate was added to the supernatant-containing tube and then mixed vigorously (to allow binding of the DNA to the magnetic particles). To this, 0.75ml Magnesil™ Paramagnetic particles was added, mixed thoroughly and then incubated at room temperature for 2min. The tube was placed onto the Magnisil™ Magnetic Separation Unit and the solution was allowed to clear for 30sec. The supernatant was discarded and after removing the tube from the magnet, the particles were washed by adding 1ml 4/40 wash solution. The particles were completely resuspended in the wash solution by vortexing using a Snijders

model 34524 press-to-mix vortex for at least 10sec. The wash solution helps remove extraneous proteins, such as nucleases, from the DNA. The tube was once again placed on the Magnisil™ Magnetic Separation Unit and the solution allowed to clear for 30 seconds. The supernatant was discarded and the particles were washed twice more with the 4/40 wash solution. Following the final wash, the tube was placed on the Magnisil™ Magnetic Separation Unit and the solution allowed to clear. The supernatant was discarded and after the tube was removed from the magnet, 1.2ml double distilled H_2O (ddH_2O) was added to the particles and mixed vigorously. The tube was incubated for 1min at room temperature and then returned to the Magnisil™ Magnetic Separation Unit. The solution was allowed to clear and the supernatant containing the DNA was carefully transferred to a new 15ml polypropylene tube. The volume of supernatant was measured and the DNA precipitated by adding 0.5 volumes of 7.5M ammonium acetate, per measured volume and 2.5 volumes of 96% ethanol to the combined volume of the supernatant and ammonium acetate. The solution was mixed well by inversion of the tube. This was followed by centrifugation at 14000 rpm for 15 min in a Beckman Microfuge Lite. The supernatant was removed and the DNA pellet washed with 70% ethanol before centrifuging at 14000 rpm followed by removal of the supernatant. The pellet was then air-dried for 5-10min to remove all the residual ethanol, after which the DNA was resuspended in 100µl ddH_2O. Subsequently the DNA concentration was determined by electrophoretically separating an aliquot of DNA adjacent to a DNA marker standard in a 1% agarose gel and visually assessing the concentration. [2]

2 All products used in this purification procedure were supplied by the manufacturer (Promega Corp. Madison Wisconsin, U.S.A)

2.3.3 3 Yeast genomic DNA purification

Yeast cells containing the DNA of interest were inoculated into 1ml synthetic dropout (SD) medium containing the appropriate dropout supplement (BD Bioscience, Clontech, Paulo Alto, CA, U.S.A) and incubated overnight at 30°C shaking at 250rpm in a shaking incubator. The following morning, 4ml YPDA (a blend of yeast extract, peptone, and dextrose supplemented with adenine) was added to the culture which was incubated for an additional 4 hours at 30°C. Thereafter, 1.5ml of the culture was transferred into a 2ml Eppendorf microfuge tube, which was centrifuged at 14000rpm for 30sec in a Beckman Microfuge Lite. The supernatant was discarded and to the pellet was added 200µl yeast lysis buffer, 200µl PCI and 0.3g sterile 450-600µm glass beads. The yeast cells were milled by vortexing this mixture for 2.5min using a Snijders model 34524 press-to-mix vortex, followed by centrifugation at 14000rpm for 5min at room temperature Beckman Microfuge Lite (Beckman Instruments Inc., CA, USA) for phase separation. The aqueous phase was transferred to a new, sterile 1.5ml microfuge tube.

Subsequently the DNA was precipitated by adding 20µl of 3M NaAc (pH 6.0) and 500µl 95% ethanol, after which the mixture was incubated at -20°C for 30 min. Following incubation, the mixture was centrifuged at 14000rpm for 15 min at room temperature in a Beckman Microfuge Lite (Beckman Instruments Inc., CA, USA). The supernatant was discarded and the pellet washed twice with 1ml 95% ethanol, before being air-dried and resuspended in an appropriate volume of ddH_2O.

2.4 GEL ELECTROPHORESIS

2.4.1 Agarose gel electrophoresis

Agarose gel electrophoresis was used either to visualise PCR-amplified fragments or plasmid preparations for verification of their presence and expected size (section 2.2.3).

2.4.1.1 Agarose gel electrophoresis for the visualisation of PCR-amplified products

In order to verify that the PCR amplifications were successful, the amplification productswere electrophoretically separated as follows: 8µl PCR product was mixed with 1µl bromophenol blue loading dye. Each sample was then loaded into separate wells of a 1-2% (depending on the size of the amplified fragment) horizontal agarose

gel of 7x9x1 cm dimensions, containing 1µg/ml ethidium bromide and 1xTBE buffer. A molecular size marker of either bacteriophage λ DNA digested with PstI (λPst) (Promega, Madison WI, USA) or a 100bp ladder (Promega, Madison WI, USA) was co-electrophoresed with all the PCR amplified products. Electrophoresis was performed at 10V/cm for 20min in 1xSB running buffer. Following electrophoresis, the DNA fragments were visualised on a long wave 3UV trans-illuminator (UVP, Inc. Upland, CA, U.S.A) and photographs were obtained using an ITC Polaroid camera and Sony video-graphic printer (Sony Corporation, Shinagawa-ku, Tokyo,Japan).

2.4.1.2 Agarose gel electrophoresis for the visualisation of plasmids isolated from E. coli

One to five microlitres of plasmid isolated from *E. coli* was mixed with 1µl of bromophenol blue loading dye and electrophoresed on a 1% horizontal agarose gel of 7x9x1cm dimensions, containing 1µg/ml ethidium bromide and 1xSB buffer. The λPst size marker was co-electrophoresed with all the purified plasmids. Electrophoresis occurred at 6V/cm for 30-45min in 1xSB buffer. Following electrophoresis, plasmids were visualised on a long wave 3UV trans-illuminator (UVP, Inc. Upland, CA, U.S.A) and photographs were obtained using an ITC Polaroid camera and Sony video-graphic printer (Sony Corporation, Shinagawa-ku, Tokyo, Japan).

2.5 5 Restriction enzyme digestion for cloning

2.5.1 Restriction digests for cloning inserts into pGBKT7 for Y2H analysis

To clone the PCR-generated Cx45 COOH-terminal fragment into the pGBKT7 vector (Figure 2.2), for Y2H analysis, both the insert and vector were sequentially double-digested with *Nde*I and *Eco*RI (Promega, Madison WI, USA). The digests were prepared in a 100µl reaction volume as follows: 50µl insert DNA (100ng/µl) or 20µl pGBKT7 vector DNA was mixed with 5µl *Nde*I (10u/µl), 10µl restriction enzyme buffer D (Promega, Madison WI, USA) and the appropriate volume of ddH_2O to make volume up to 100ul (Insert, 35µl; vector, 65µl). The mixtures were incubated at 37°C for 3h.

Following this, the samples were purified using the GFX® DNA purification kit (AmershamPharmacia Biotech, New Jersey, USA), as discussed in section 2.3.2,

with the only exception being that instead of gel electrophoresis and subsequent excision of DNA from the gel for purification, the samples were purified directly.

The samples were subsequently eluted from the GFX^{TM} column in 50µl ddH_2O and mixed with 5µl *Eco*RI (12u/µl), 10µl restriction buffer H (Promega, Madison WI, USA) and 35µl ddH_2O. Subsequently, the samples were incubated at 37°C for 3 hours, after which they were again purified using the GFX^{TM} DNA purification kit (AmershamPharmacia Biotech, New Jersey, USA). Double-digested pGBKT7 was subsequently treated with calf intestinal alkaline phosphatase (CIP) (section 2.6.3) to prevent the vector from annealing to itself, while double-digested insert was used directly in ligation reactions.

2.5.2 Restriction digests for cloning inserts into pM and pVP-16 for M2H analysis

In order to clone the PCR-generated fragments (section 2.6.2) into the pM and pVP-16 vectors (Figure 2.4 and Figure 2.5, respectively), for M2H analysis, both the insert and vector were sequentially double-digested with appropriate 5' and 3' restriction enzymes (Promega, Madison WI, USA). The digests were prepared in a 100µl reaction volume as follows: 50µl insert DNA or 20µl appropriate vector DNA (pM for Cx45 domain insert, pVP-16 for putative ligand insert) was mixed with 5µl restriction enzyme, 10µl restriction enzyme buffer (Promega, Madison WI, USA) and the appropriate volume of ddH_2O (insert, 35µl; vector, 65µl). The mixtures were incubated at 37°C for 3h. Following this, the samples were purified using the GFX^{TM} DNA purification kit (AmershamPharmacia Biotech, New Jersey, USA). The samples were then eluted in 50µl ddH_2O and mixed with 5µl *Sal*I (test enzyme[3]), 10µl restriction buffer D (Promega, Madison WI, USA) and 35µl ddH_2O. Subsequently, the samples were incubated at 37°C for 3 hours, after which they were again purified using the GFX^{TM} DNA purification kit (AmershamPharmacia Biotech, New Jersey, USA). Double-digested vectors were then treated with calf intestinal alkaline phosphatase (CIP) (Section 2.6.3) prior to being used in ligation reactions, while

3 Test enzyme is used to detect whether the plasmid or the DNA fragment of interest has additional unexpected restriction sites, the presence of which jeopardise subsequent experiments. This enzyme should not linearise the DNA fragment at all

double-digested insert was used directly in ligation reactions. For cloning of prey insert into pVP16, the same protocol was followed as shown above.

2.6 GENERATION OF Y2H AND M2H CONSTRUCTS

2.6.1 2.6.1 Y2H constructs

After the restriction enzyme digestion of the PCR amplified Cx45 COOH-terminal fragment, it was cloned into the pGBKT7 bait-vector (Figure 2.3) and, after verification of the integrity of the sequence and conservation of the GAL4 DNA-BD reading frame by automated sequencing, transformed (section 2.10.2) into the *S. cerevisiae* strain AH109. This construct was used to screen a CLONTECH MATCHMAKER pre-transformed adult human cardiac cDNA library, comprising adult cardiac cDNAs cloned into the pGADT7-Rec (Figure 2.3) prey-vector and transformed into the *S. cerevisiae* strain Y187 (section 2.10.2).

2.6.2 M2H constructs

Subsequent to the Y2H analysis, the *Cx45* bait-insert was cloned into the pM GAL4-DNA binding domain vector, while putative Cx45-interacting clones were cloned into the pVP16 GAL-activation domain vector (Figure 2.5). The integrity of the sequence and conservation of the GAL4 DNA-BD and GAL4-activation domain reading frame was verified by automated sequencing.

2.6.3 Alkaline phosphatase treatment of vector

To prevent the vector to be used in Y2H and M2H cloning re-circularising by self-ligation, following double restriction enzyme digestion (section 2.5.1), the ends of the linearised plasmid was CIP (calf intestine phosphatase)-treated to remove the 5' phosphate groups. This was accomplished by mixing 50µl of the digested vector with 1µl CIP (1u/µl) (Promega, Madison WI, USA), 10ul CIP buffer (Promega, Madison WI, USA) and 38µl ddH_2O. The sample was incubated at 37°C for 30 min, after which another 2µl CIP was added and the mixture incubated for a further 30min. Following this, 2µl 0.5M EDTA was added and the sample was incubated at 65°C for 20 minutes to inactivate the enzyme. The vector was subsequently purified using the GFX^{TM} DNA purification kit (AmershamPharmacia Biotech, New Jersey, USA) (section 2.3.2).

2.6.4 DNA ligation

DNA ligations were performed in order to generate the Y2H bait constructs to be used in Y2H analysis and M2H bait and prey constructs for M2H analysis. In general, 2µl of the double-digested insert (section 2.5.1) was added to 1µl of CIP-treated, double-digested vector. To this mixture, 5µl 2x T4 DNA ligase buffer (Promega, Madison WI, USA), 5U T4 DNA ligase and ddH_2O, to a final volume of 10µl, was added. The sample was then incubated for 16 hours at 4°C. Following incubation, 5µl of the sample was transformed into the bacterial strain DH5α (section 2.10.1) and plated onto LB agar plates containing the appropriate antibiotic. After incubation of the plates, successful ligation reactions were confirmed by bacterial colony PCRs (section 2.2.3.). Control ligations were also run for at different insert-to-vector ratios to assess optimal ligation aliquots.

2.7 BACTERIAL STRAINS, YEAST STRAINS AND CELL LINES[4]

2.7.1 Bacterial strains

To facilitate the selection and purification of Y2H constructs, ligation reactions (section 2.6.4) were transformed into the *E. coli* DH5α strain. Transformed bacterial colonies were selected on the basis of their ability to grow on LB agar plates containing selection antibiotics (Appendix I), and recombinant plasmids identified by colony PCR (section 2.2.3). When selecting for recombinant bait vector pGBKT7, kanamycin was used as a selection antibiotic, while ampicillin was used when selecting for recombinant prey vector pGADT7-Rec, pM and pVP16.

4 Genotypes of bacterial strains, yeast strains and cell lines used are in Appendix I.

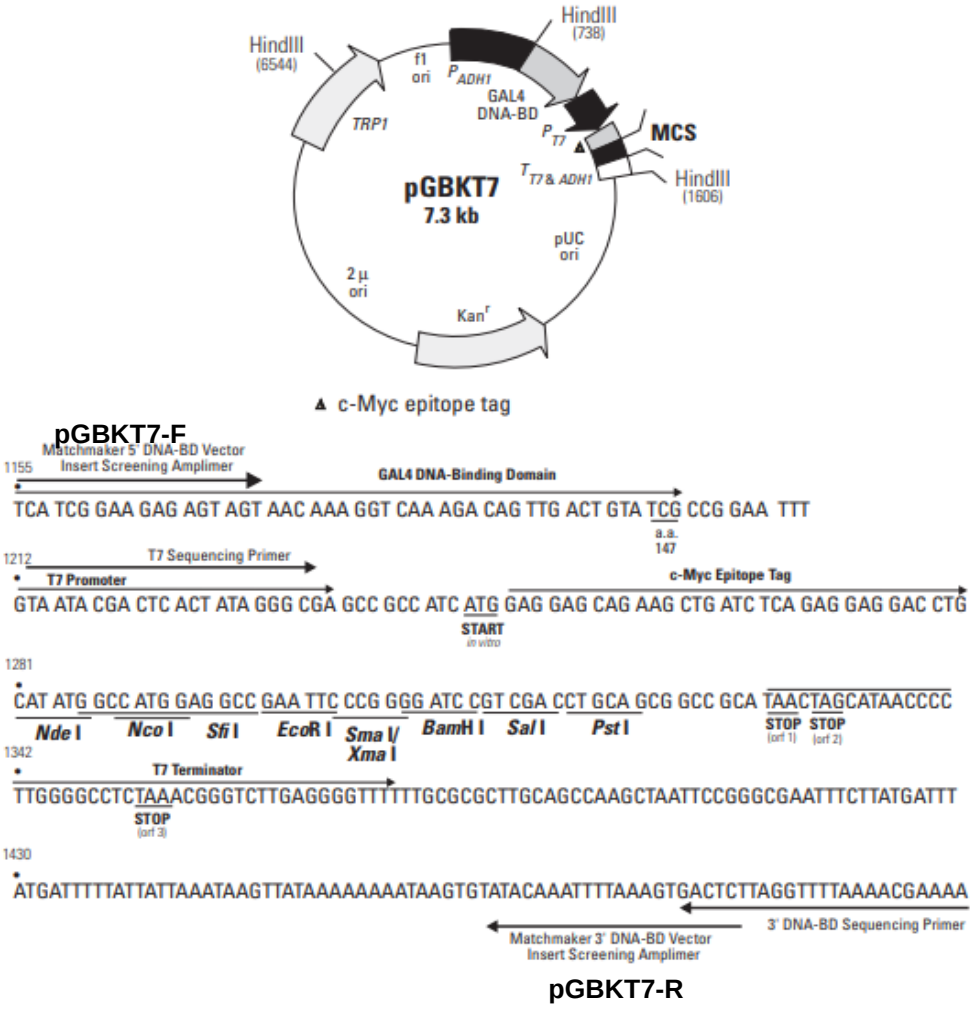

Figure 2.2 Restriction map and multiple cloning site (MCS) of pGBKT7 Y2H bait vector. a).

The positions of the kanamycin resistance gene (*kan*), TRP1 and GAL4-BD coding sequences, f1 bacteriophage and pUC plasmid origins of replication, the truncated *S. cerevisiae* ADH1 promotor sequence (P_{ADH1}), the T7 RNA polymerase promoter, the T7 and c-Myc epitope tag are indicated on the map. b) Nucleotide sequence of the pGBKT7 MCS. The positions of all unique restriction enzyme recognition sequences, stop codons in the T7 terminator sequence, the GAL4-BD coding sequence, the T7 promoter sequence, c-Myc epitope tag and the positions of pGBKT7-F and pGBKT7-R screening primers and sequencing primers are indicated on the sequence. (Taken from Clontech MATCHMAKER vectors handbook).

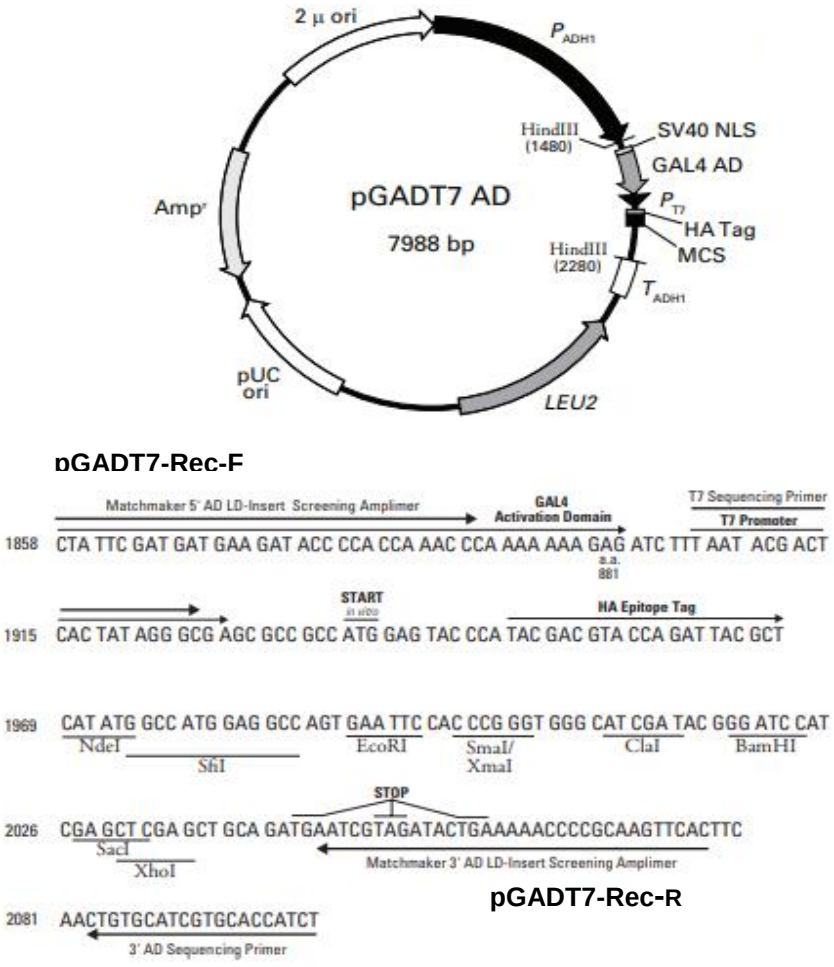

Figure 2.3 Restriction map and multiple cloning site (MCS) of pGADT7-Rec Y2H prey vector. a)

The positions of unique restriction sites are indicated in bold. The position of the ampicillin resistance gene (*Amp*^{r}), LEU2 and GAL4-AD coding sequences, and pBR322 plasmid origins, the *S.cerevisiae* ADH1 promoter, *S.cerevisiae* ADH1 termination sequence, Lox sites (Lox 1 and Lox 2), the Heamagglutinin (HA) epitope tag and the MCS are indicated on the map. b) Nucleotide sequence of the pGADT7-Rec MCS. The positions of all unique restriction sites, stop codons, the position of the final codon (881) of GAL4-AD coding sequence, the positions of the pGADT7-Rec-F and pGADT7-Rec-R primers and the HA epitope tags are all indicated in the map. (Taken from Clontech MATCHMAKER vectors handbook).

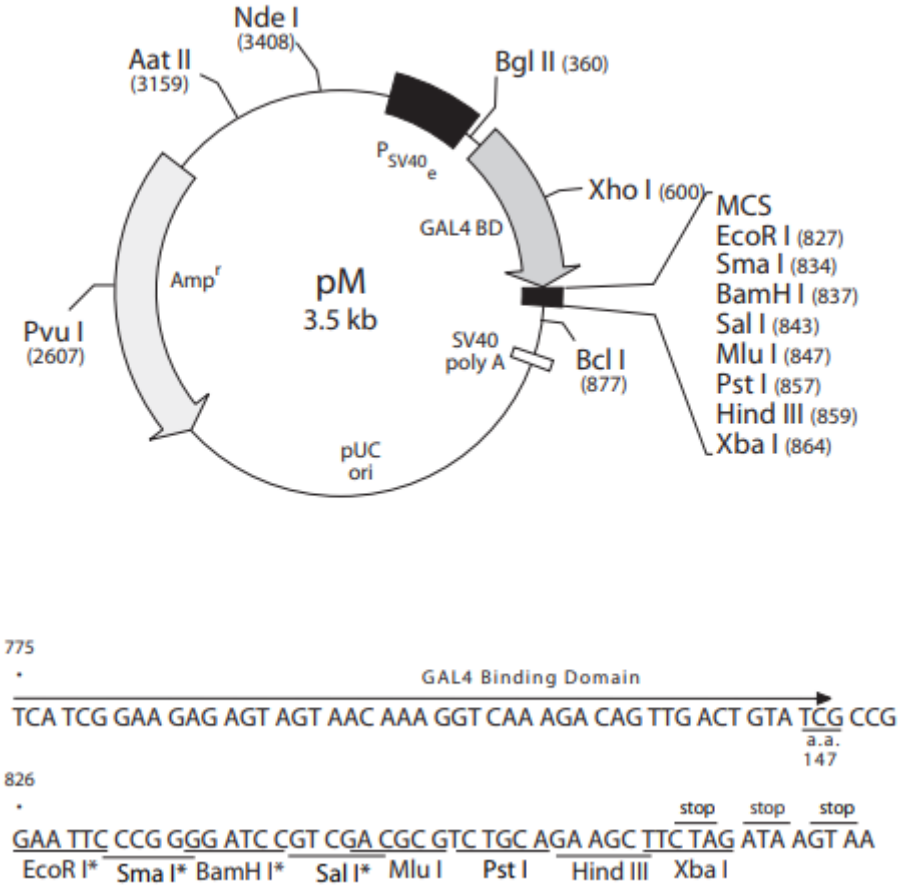

Figure 2.4 Restriction map and multiple cloning site (MCS) of pM M2H GAL4 BD vector. a)

The positions of unique restriction sites are indicated in bold. The position of the ampicillin resistance gene (*Amp*^{r}), GAL4-BD coding sequences, the SV40 promoter and SV40 polyA transcription termination sequence and the MCS are indicated on the map. b) Nucleotide sequence of the pM MCS. The positions of all unique restriction sites, stop codons, the position of the GAL4-BD coding sequence and the position of the pM sequencing primer are all indicated in the map. (Taken from Clontech MATCHMAKER Two-Hybrid Assay Kit User Manual).

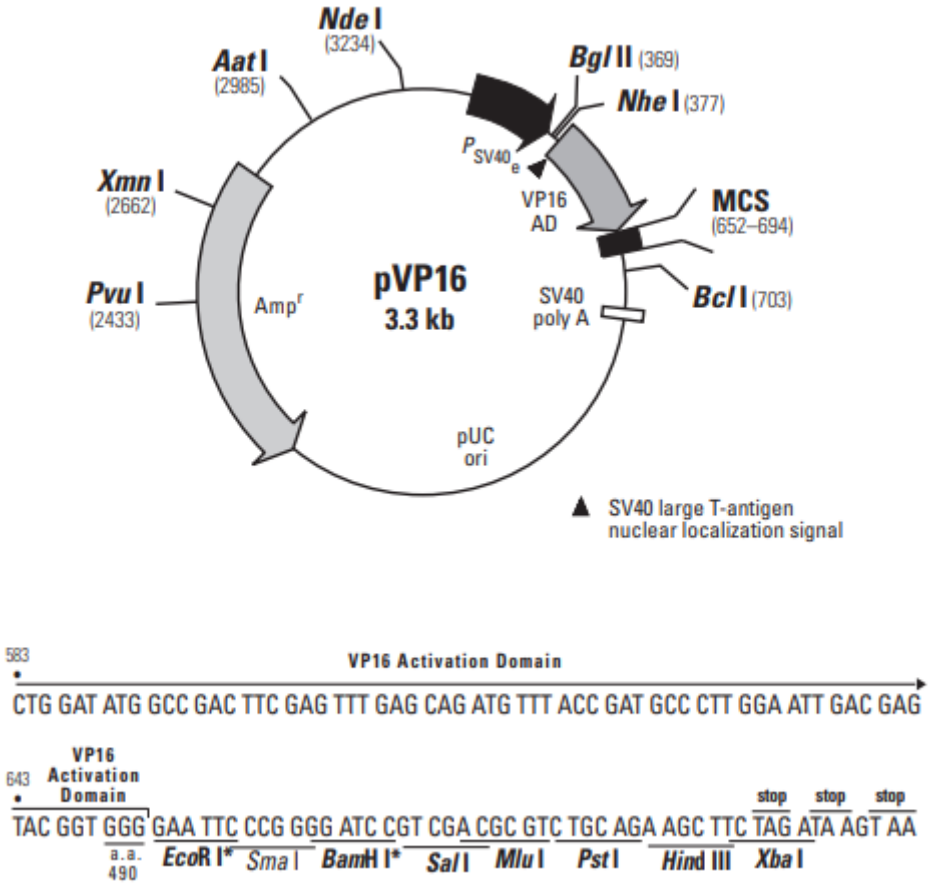

Figure 2.5 Restriction map and multiple cloning site (MCS) of pVP M2H GAL4-AD vector.

The positions of unique restriction sites are indicated in bold. The position of the ampicillin resistance gene (*Amp*^{r}), GAL4-AD coding sequences, the SV40 promoter and SV40 poly A transcription termination sequence and the MCS are indicated on the map. b) Nucleotide sequence of the pM MCS. The positions of all unique restriction sites, stop codons, the position GAL4-AD coding sequence and the position of the pVP16-F and pVP16-R primers are indicated on the map. (Taken from Clontech MATCHMAKER Two-Hybrid Assay Kit User Manual).

2.7.2 Yeast strains

The pGBKT7 bait construct was transformed into the *S. cerevisiae* strain AH109, while all the prey clones present in the pre-transformed CLONTECH cDNA library used in the Y2H analysis had been transformed into the *S. cerevisiae* strain Y187 by the supplier (BD Bioscience, Clontech, Paulo Alto, CA, U.S.A).

2.7.3 Cell lines

The pM and pVP-16 constructs were co-transfected into a human cardiac (H9C2) cell line for M2H analysis together with the pG5SEAP vector, which is a reporter vector that contains the secreted alkaline phosphatase (SEAP) reporter gene downstream and under the control of a GAL4-responsive element (Figure 2.6).

2.8 GENERATION OF *E. coli* DH5α COMPETENT CELLS

- An aliquot of *E. coli* DH5α frozen (-70°C) glycerol stock was inoculated into 10ml LB-media. The culture was then incubated overnight at 37°C in a YIH DER model LM-530 shaking incubator (SCILAB instrument CO. Ltd, Taipei, Taiwan) at approximately 200rpm. Following incubation, a 1ml aliquot of this culture was inoculated into a 2l Erlenmeyer flask containing 200ml LB media. This culture was then incubated at room temperature for 24 hours, while shaking at 200rpm, to mid log phase (OD_{600nm}=0.6) on a Labcon orbital shaker (Labcon Pty, Ltd, Maraisburg, RSA). At this point, the culture was decanted into 4x 50ml polypropylene tubes and centrifuged at 3000rpm for 15 min at 4°C in a Multitex centrifuge (MSE instruments, England). The supernatant was removed and 8ml of ice-cold CAP buffer used to resuspend the pellet. The cells were re-pelleted by centrifugation at 3000rpm for 15 min at 4°C in a Multitex centrifuge (MSE instruments, England). The supernatant was discarded and the pellet was resuspended in 4ml of ice-cold CAP buffer. The suspended cells were subsequently transferred into 1.5ml microfuge tubes in 500µl aliquots and snap frozen by immersion in liquid nitrogen. The cells were then stored at -70°C until they were needed.

2.9 CULTURING OF THE H9C2 CELL LINE

2.9.1 Culture of H9C2 cells from frozen stocks

2.9.1.1 Thawing the cells

Frozen H9C2 cells, a kind gift from Prof Janet Hapgood, Dept Biochemistry, University of Stellenbosch, were thawed rapidly by immersing the vial containing the frozen stock in a 37°C waterbath (Memmert®, Schwabach, Germany) for 10min. Once the cells were thawed, the outside of the vial was immediately sterilized with 70% ethanol.

2.9.1.2 Removing DMSO from stocks and culturing cells

As the frozen stocks contained DMSO, it was necessary to remove the DMSO for maximum viability of the cells upon plating, as follows. One millilitre of growth medium (GeneJuice) (Appendix I), pre-warmed to 37°C, was added to the thawed stock and mixed by gentle pipetting. The mixture was transferred to a 12ml Greiner tube (Greiner Bio-one, Frickenhausen, Germany) and another 5ml growth medium was added. The cells were then pelleted by centrifugation at 10 000rpm for 1min using a Sorval® GLC-4 General Laboratory centrifuge (Separations Scientific, Johannesburg, South Africa) followed by removal of the supernatant. The pellet was resuspended in another 5ml growth medium and the cells were once again centrifuged at 10 000rpm for 1 min using a Sorval® GLC-4 General Laboratory centrifuge. Following this, the cells were resuspended in 10ml growth medium and transferred into a T25 culture flask. The flask was gently swirled in order to distribute the cells evenly over the growth surface of the flask. The flask was then incubated at 37°C in a Farma termosteri-cycle 5% carbon dioxide humidified incubator (Farma International, Miami, Florida, U.S.A).

2.9.2 Subculturing of H9C2 cells

Cell cultures were subcultured every 2-4 days when they reached approximately 80%-90% confluency. Briefly, the growth medium was removed from the flask as the cells were washed with sterile phosphate buffered saline (PBS) containing no calcium or magnesium (Appendix I). To this, 2ml of trypsin (Highveld Biological, Lyndhurst, South Africa) was added to facilitate the detachment of the cells from the growth surface of the flask. After 3min, 5ml growth medium was added and the cells were gently resuspended. The cells from one flask were then transferred into 4 flasks each containing 10ml of growth medium. This procedure was conducted by Mrs Lundi Korkie and would like to extend my appreciation for her assistance.

2.10 TRANSFORMATION AND TRANSFECTION OF PLASMIDS INTO PROKARYOTIC AND EUKARYOTIC CELLS

2.10.1 Bacterial plasmid transformation

Prior to the transformation, an aliquot of competent *E. coli* DH5α was removed from the -70°C freezer and allowed to thaw in ice for 20-30 min. Once the cells had thawed, 1µl plasmid DNA or 3-5µl of the ligation reaction (section 2.6.4) was added. This mixture was then incubated on ice for 20-30 min after which were placed in a

Lasec 102 circulating water-bath (Lasec Laboratory and Scientific Company Pty Ltd, Cape Town, R.S.A) at 42°C for exactly 45s. The sample was then removed from the water-bath and left at room temperature for 2min. Next, 1ml of LB media was added to the mixture and the sample was incubated for 1h at 37°C, while shaking at 200rpm in a YIH DER model LM-530 shaking incubator shaking (SCILAB instrument CO. Ltd, Taipei, Taiwan). Following this incubation step, 200µl of the sample was plated onto LB agar plate containing the appropriate selection antibiotic (Appendix I). The remaining transformation reaction mixture was centrifuged at 14000rpm for 2min in a Beckman Microfuge Lite, the supernatant was discarded and the pellet resuspended in 200µl LB media in order to concentrate the transformation mixture. This was then also plated onto the appropriate LB-agar plate. The plates were then incubated, inverted, for 16h at 37°C in a model 329 stationary CO_2 incubator (Former Scientific, Marieta, Ohio, U.S.A).

2.10.2 Yeast Plasmid transformation

The yeast strain to be transformed was streaked from frozen stocks onto YPDA agar plate. These plates were then incubated at 30°C for 2-3 days in a Sanyo MIR262 stationary ventilated incubator (Sanyo, Electronic Company Ltd, Ora-Gun, Japan). Following incubation, a scraped yeast colony representing a volume of 20-50µl were picked and resuspended in 1ml sterile ddH_2O in a sterile 2ml tube. The cells were then re-pelleted by centrifugation at 13000rpm for 30sec in a Beckman Microfuge Lite. The supernatant was removed and the pellet was resuspended in 1ml 100 mM lithium acetate (LiAc) and incubated for 5 min at 30°C in a MIR262 stationary ventilated incubator. The cells were again pelleted by centrifugation at 13000 rpm for 20s in a Beckman Microfuge Lite and all the LiAc was removed. Next, 240µl of 50% polyethylene glycol (PEG), 36µl 1M LiAc, 25µl of 2mg/ml heat-denatured and snap-cooled sonicated herring sperm DNA (Promega, Madison WI, USA), 10-20µl recombinant pGBKT7-*Cx45* and ddH_2O were added to a final volume of 350µl. The sample was then mixed by vortexing using a Snijders model 34524 press-to-mix vortex (Snijders Scientific, Tilburg, Holland) for at least 1 min and incubated at 42°C for 20-30 min in a Lasec 102 circulating water-bath (Lasec Laboratory and Scientific Company Pty Ltd, Cape Town, R.S.A). Following incubation, the cells were pelleted by centrifugation at 13000rpm in a Beckman Microfuge Lite (Beckman Instruments Inc, CA, U.S.A) and all the supernatant was removed. The cells were resuspended in 250µl sterile Millipore ddH_2O. One hundred and fifty microlitres of this sample was plated onto the appropriate selection plate and incubated inverted at 30°C for 2-5

days in a Sanyo MIR262 stationary ventilated incubator (Sanyo, Electronic Company Ltd, Ora-Gun, Japan).

2.10.3 Transfection of H9C2 cells

Forty-eight hours before transfecting the cells, approximately 1-3 x 10^4 cells (determined from the haemocytometer) per well were plated in complete growth media in a 24-well tissue culture plate and incubated at 37°C in a 5% Farma-thermosteri-cycle carbon dioxide humidified incubator (Farma, international, Miami, Florida, U.S.A). Two days later, the cells were visualised under a Nikon TMS light microscope (Nikon, Tokyo, Japan) to determine the level of confluence. Cells were only transfected once they reached approximately 80% confluence. For each transfection performed, 100µl of serum-free medium was aliquoted into a sterile 1.5ml eppendorf tube. Three microlitres GeneJuice® (EMD Biosciences, Darmstadt, Germany) was added to each tube. This mixture was thoroughly vortexed using a Snijders model 34524 press-to-mix vortex and incubated at room temperature for 5 minutes. A total of 1µg of the four plasmids combined (pM-Cx45, pVP16-putative ligand, pSV-β-galactosidase and pG5SEAP reporter vector [Figure 2.6]) (table 2.8) was added to the mixture and mixed gently by pipetting. The GeneJuice/DNA/medium was incubated at room temperature for 15min. The entire volume of the mixture was then added drop-wise to the cells in the growth medium. The culture plates were gently rocked back and forth in order to evenly distribute the drops across the surface of the plate. The cells were incubated at 37°C, 5% carbon dioxide humidified incubator (Farma, international, Miami, Florida) for 48 hours. The cells were transferred to eppendorf tubes, subsequently pelleted by centrifugation at 13000rpm in a Beckman Microfuge Lite and 1ml of the supernatant transferred into a sterile eppendorf tube. The supernatants were stored at -20°C until needed for subsequent assays (section 2.13). This procedure was conducted by Mrs Lundi Korkie and would like to extend my appreciation for her assistance.

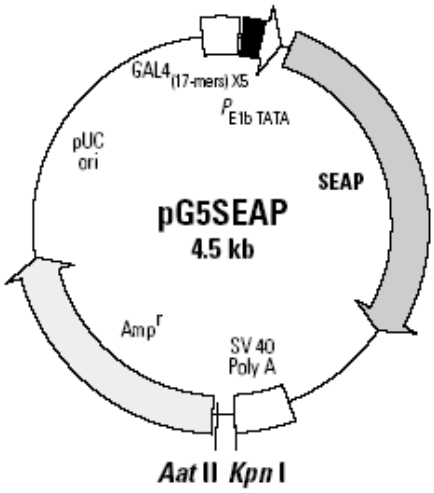

Figure 2.6 Map of pG5SEAP reporter vector.

This vector contains 5 GAL4 binding sites and an adenovirus E1b minimal promoter sequence upstream of the secreted alkaline phosphatase (SEAP), as indicated on the map.

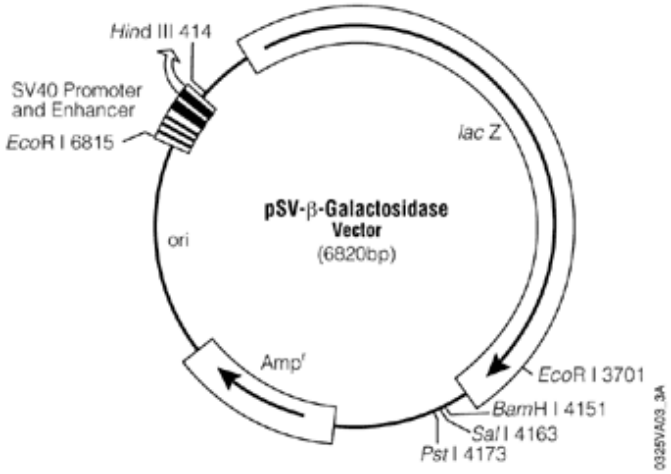

Figure 2.7 Map of pSV- pSV-β-galactosidase vector.

This vector contains the SV40 promoter and enhancer which drive transcription of the bacterial *lac*Z gene, which in turn, is translated into the β-galactosidase enzyme.

2.11 ASSESMENT OF Y2H CONSTRUCTS

2.11.1 Phenotypic assessment of *S. cerevisiae* strains

Prior to being transformed, each of the *S. cerevisiae* strains (See appendix I for genotype) used in the Y2H analysis was assessed phenotypically. This involved

plating strains AH109 and Y187 onto agar plates lacking essential amino acids, ie., agar plates SD^{-Ade}, SD^{-Trp}, SD^{-His}, SD^{-Leu} and SD^{-Ura}. Concurrently, *S. cerevisiae* AH109 and Y187 transformed with recombinant pGBKT7 and pTD1.1 plasmids were assessed for the autoactivation of the endogenous reporter genes of the GAL4 system, by growing them on all of the above-mentioned media.

2.11.1 Toxicity tests of transformed cells

In order to proceed with the Y2H assay, it was important to establish whether the *Cx45*-bait construct had any markedly toxic effect on its host *S. cerevisiae* strain, AH109. To achieve this, a growth curve of AH109 transformed with the pGBKT7-bait construct was generated and subsequently compared to a growth curve of AH109 yeast transformed with non-recombinant pGBKT7. These two growth curves were set up concurrently and under the same experimental conditions.

The two growth curves were generated by growing each of the transformed yeast strains to stationary phase in SD^{-Trp} in a 50ml polypropylene tube at 30°C in a YIH DER model LM-530 shaking incubator shaking at 200rpm. Following this incubation, a 1:10 dilution of each primary culture was made in SD^{-Trp} and incubated for an additional 24h in a 50ml polypropylene tube at 30°C in a YIH DER model LM-530 shaking incubator shaking at 200rpm. Every 2 hours, over a period of 8 hours during this incubation, a 1ml aliquot of the culture was taken and its OD_{600nm} was measured. An overnight (24h) reading was also taken. A linearised graph of the log of these OD_{600nm} readings versus time was constructed and the slopes of the graphs generated for the recombinant and non-recombinant transformants were compared.

2.11.2 Testing the mating efficiency

In order to determine the effect that the *Cx45*-bait construct had on the mating efficiency of AH109, small scale matings were performed. In these mating experiments, the *S. cerevisiae* AH109 transformed with pGBKT7-*Cx45*-bait construct was mated with the prey host strain, *S. cerevisiae* Y187 transformed with the non-recombinant prey vector pGADT7-rec (Clontech). Concurrently, control matings were also performed in which the *S. cerevisiae* AH109 transformed with non-recombinant pGBKT7 or the control pGBKT7-53 vector was mated with the prey host strain, *S. cerevisiae* Y187 transformed with the non-recombinant prey vector pGADT7-rec.

The experimental procedures were as follows:

Each of the yeast strains used in the mating efficiency experiments was plated onto the appropriate nutritional selection plates (AH109 pGBKT7-Cx45, AH109 pGBKT7 and AH109 pGBKT7-53 on SD^{-Trp} plates; Y187 pGADT7-rec and Y187 pTD.1.1 on SD^{-L} plates). These plates were incubated for 2-5 days at 30˚Cin a Sanyo MIR262 stationary ventilated incubator (Sanyo, Electronic Company Ltd, Ora-Gun, Japan). A single colony from these agar plates was used for each the test mating experiments; which was performed in 1ml YDPA media in a 2ml microfuge tube. The matings were incubated overnight at 30°C, shaking at 200rpm, in a YIH DER model LM-530 shaking incubator (SCILAB instrument CO. Ltd, Taipei, Taiwan). Following the overnight incubation, serial dilutions (1:10; 1:100; 1:1000 and 1:10000) of the mating cultures were plated onto SD^{-Leu}, SD^{-Trp} and $SD^{-Leu-Trp}$ agar plates and incubated for 4-5 days at 30° in a Sanyo MIR262 stationary ventilated incubator (Sanyo, Electronic Company Ltd, Ora-Gun, Japan). After the incubation period, the colonies on each plate were counted and used to calculate the mating efficiency using the formulae below:

$$\frac{\text{Colony forming unit (cfu) X 100ul/ml}}{\text{Volume plated (ul) X dilution factor}} = \text{Number of viable cfu/ml}$$

$$\text{Then, } \frac{\text{Number of viable cfu/ml of diploids } (SD^{-Leu,-Trp})}{\text{Number of viable cfu/ml of limiting partner}} \times 100 = \%\ \text{mating effiency}$$

Where, limiting partner has lower cfu count on either SD^{-Leu}, or SD^{-Trp}

2.12 Y2H ANALYSIS

2.12.1 The adult human cardiac cDNA library

A pre-transformed human MATCHMAKER heart cDNA Library (BD Bioscience, Clontech, Paulo Alto, CA, U.S.A) consisting of *S. cerevisiae* Y187 transformed with a normal, adult heart cDNA library constructed in pGADT7-Rec, was used in the Y2H library assay. This library was constructed from a pool of 3 Caucasian males, 1 aged 33 years, the other two aged 55 years. The library was *Xho*I-(dT)15 primed and

contains approximately $1.15x10^7$ independent clones cloned into the pGADT7-Rec through *EcoR*I and *Xho*I sites. The average insert size for this library is 2.0kb with a range of between 0.5 and 3.0kb (Clontech™ Matchmaker™ vector handbook) or (www.clontech.com).

2.12.2 Establishment of bait culture

A colony of *S. cerevisiae* AH109 transformed with the Cx45-bait construct was streaked out onto SD^{-Trp} plates. Four of the resultant yeast colonies were inoculated into four separate 500ml Erlenmeyer flasks, each containing 50ml SD^{-Trp} media. The reason for producing four bait cultures was to facilitate the pooling of the initial cultures, thereby allowing the generation of a final bait culture with a titre of at least $1x10^{10}$, i.e. 100-fold excess of bait to prey to facilitate high mating efficiency. The four initial cultures were incubated at 30°C overnight, while shaking at 200rpm in a YIH DER model LM-530 shaking incubator. Following overnight incubation, the cultures were transferred into individual 50ml polypropylene tubes and the cells pelleted by centrifugation at 3000rpm for 10min at room temperature in a Beckman Microfuge Lite. The supernatants were discarded and the four pellets were resuspended together in 50ml SD^{-Trp} medium following which the suspension was transferred to a single 500ml Erlenmeyer flask and the culture was incubated for a further 16h at 30˚Cin a YIH DER model LM-530 shaking incubator, shaking at 200 rpm. After incubation, the titre of the bait culture was estimated by measuring the OD_{600nm} of a 1ml aliquot of the bait culture. This estimation was subsequently confirmed by means of a haemocytometric cell count.

The bait culture was centrifuged at 3000rpm at room temperature for 10min in a Beckman Microfuge Lite to pellet the cells, the supernatant was removed and the pellet resuspended in ml SD^{-Trp} medium. An appropriate number of 10µl aliquots of this culture were removed for control mating experiments.

2.12.3 Haemocytometric cell count

Haemocytometric cell count using a Neubauer haemocytometer was performed to determine the titre of bait culture used in the library mating experiment. Prior to aliquoting the sample onto the haemocytometer, a glass coverslip was placed over the counting surface. Approximately 50µl of a 1 in 10 dilution of bait culture was then pippeted into one of the wells. This allowed for the area under the coverslip to be filled with the sample through capillary action. The counting chamber was

subsequently placed on a microscope stage and the counting area was brought into focus under low magnification. The number of cells per millilitre was determined using the following formula:

number of cells/ml = number of cells x dilution factor x 10^4 (a constant used because the depth of the haemocytometer is 0.1mm)

2.12.4 Library mating

A 1ml aliquot of the pre-transformed adult human cardiac cDNA library was removed from the -70°C freezer and thawed at room temperature. Once thawed, the library aliquot was vortexed using a Snijders model 34524 press-to-mix vortex and 10µl aliquoted into a sterile 1.5µl microfuge tube for library titering. The pGBKT7-Cx45 transformed AH109 pellet was then resuspended in 45ml 2x YPDA media supplemented with 10µg/ml kanamycin (Kan) in a 2L Erlenmeyer flask). Subsequently, the remaining 990µl of the library culture was added to this Erlenmeyer flask. This mating culture was incubated at 30°C overnight, while shaking at 200rpm in a YIH DER model LM-530 shaking incubator.

After the overnight incubation, the entire mating culture was transferred into a sterile 50ml polypropylene centrifuge tube and the cells pelleted by centrifugation in at 3000rpm for 5min in a Multex centrifuge, and the supernatant subsequently removed. The Erlenmeyer flask in which the library mating was performed was rinsed twice with 40ml 2x YPDA containing 10µg/ml Kan. Each time the flask was rinsed, the 2x YPDA medium was used to resuspend the cell pellet and the cells then re-pelleted by centrifugation at 3000rpm for 10min at room temperature in a Multex centrifuge. Following the final centrifugation step, the supernatant was removed and the pellet resuspended in 15ml 0.5x YPDA containing 10µg/ml Kan.

Serial dilutions of 100µl aliquots (1:10; 1:100; 1:1000; and 1:10000) of this cell-suspension were plated onto 90mm SD^{-L}, SD^{-W} and SD^{-L-W} agar plates in order to determine mating efficiency. Two hundred and 50 microlitres aliquots of the rest of the culture was plated onto each of 59 140mm TDO (media lacking leucine, trytophan and histidine) plates (250µl culture/plate for14.9ml culture = 59 plates). The TDO plates were incubated, inverted, at 30°C for 2 weeks in a Sanyo MIR262 stationary ventilated incubator (Sanyo, Electronic Company Ltd, Ora-Gun, Japan).

2.12.5 Establishing a library titre

The serial dilutions of the mating culture plated onto the 90mm SD^{-Leu}, SD^{-Trp} and $SD^{-Leu/Trp-}$ agar plates were inverted and incubated in a Sanyo MIR262 stationary ventilated incubator for 4 days. Colony counts were performed on the SD^{-Leu}, SD^{-Trp} and $SD^{-Leu-Trp}$ plates after the 4 day incubation in order to calculate the mating efficiency of the library mating and the number of library plasmids screened.

2.12.6 Control matings

Control matings were set up concurrently with library matings in order to determine whether the recombinant Cx45 construct (transformed into *S. cerevisiae* AH109) had any negative effect on the ability of the transformed AH109 strain to mate with the library strain (Y187). A 10µl aliquot of the bait culture and a single test prey- (*S. cerevisiae* strain Y187 transformed with pTD 1.1 control vector) colony were co-inoculated in 1ml 0.5x YPDA containing 10µg/ml kanamycin in a 2ml centrifuge tube. This culture was subsequently incubated for 24h at 30°C in a DER model LM-530 shaking incubator, shaking at 200 rpm. Following incubation, serial dilutions (1:10; 1:100; 1:1000; 1:10000) were plated onto SD^{-Lue}, SD^{-Trp} and $SD^{-Leu-Trp}$ agar plates and incubated for 4 days in a Sanyo MIR262 stationary ventilated incubator. Following this, colony counts were done and the mating efficiency was calculated.

2.12.7 Detection of activation of nutritional reporter genes

2.12.7.1 Selection of transformant yeast colonies

Yeast transformed with the bait construct to be used in Y2H analysis was plated onto SD^{-Leu}, SD^{-Trp} and $SD^{-Leu-Trp}$ agar plates. Following incubation of these plates for 4-6 days in a Sanyo MIR262 stationary ventilated incubator at 30˚C, transformant yeast colonies were picked and used in small and large scale bait cultures and library matings.

2.12.7.2 Selection of diploid yeast colonies containing putative interactor peptides

In order to identify yeast colonies in which an interaction between the bait- and prey-fusion peptides had taken place, yeast colonies were plated onto TDO (lacking leucine, histidine, tryptophan) plates as well as QDO (media lacking leucine, histidine, tryptophan and adenine) plates. Growth of the yeast cells on TDO plates signified the transcriptional activation of the *HIS3*, nutritional reporter gene, while

growth on the QDO plates indicated that both the *HIS3* and *ADE2*, nutritional reporter genes had been transcriptionally activated. The activation of these genes in these diploid yeast cells is indicative of an interaction between the bait and prey peptides.

Briefly, the library mating culture was plated directly onto 58 140mm TDO agar plates and incubated in a Sanyo MIR262 stationary ventilated incubator for 2 weeks at 30˚C. The growth of these colonies on the TDO plates was monitored every 2 days and colonies were picked and restreaked onto TDO and QDO plates in order to test for the activation of *HIS3* and *ADE2* nutritional reporter genes. These plates were incubated for 3-6 days at 30°C in a Sanyo MIR262 stationary ventilated incubator.

2.12.8 Detection of activation of colourimetric reporter genes

X-α-Galactosidase assay

X-α-galactosidase assays were performed in order to test for the activation of the *MEL1* reporter gene by the specific interaction between specific bait and prey peptides. Briefly, yeast colonies in which the *HIS3* and *ADE2* reporter genes have been activated, as determined by their growth on QDO agar plates, were replicated from QDO plates onto Hybond N^+ nylon membranes. These membranes were subsequently placed colony-side up onto a QDO plate impregnated with 20mg/ml X-α-Gal solution (BD Biosciences, Clontech, Palo Alto, CA, U.S.A). The plates were subsequently incubated at 30°C in a Sanyo MIR262 stationary ventilated incubator for three to five days. Following incubation, the intensity of the blue colour of yeast colonies that had activated the *MEL1* reporter gene was assessed.

2.12.9 Rescuing prey plasmids from diploid colonies.

In order to identify the interactor proteins, each individual prey needed to be isolated from the diploid colonies. To this end, plasmid DNA was isolated from each of the diploid yeast cells following the protocol described in section 2.3.1 and transformed into *E. coli* strain DH5α as described in section 2.10.1. The transformants were plated onto LB^{amp} plates which only allows for the growth of transformants containing the prey constructs. These prey constructs were subsequently transformed into the yeast strain Y187.

2.12.10 Interaction specificity test

To test whether the interactions detected by Y2H analysis, through the activation of nutritional and colourimetric reporter genes, were specific interactions between the pGBKT7-*Cx45*-bait and a particular prey peptide, interaction specificity tests were used. Y187 colonies expressing the specific prey peptide were individually mated with the yeast strain AH109, transformed with the pGBKT7-*Cx45*-bait construct, AH109 transformed with non-recombinant pGBKT7, AH109 transformed with the pGBKT7-53 control bait-plasmid, encoding murine p53, supplied by the manufacturer (BD Biosciences, Clontech, Palo Alto, CA, U.S.A) and AH109 transformed with a heterologous bait, encoding the brain expressed protein reelin (a kind gift from Dr Craig Kinnear). After the resulting diploid clones were selected, these clones were streaked onto TDO and QDO selection plates to test for the activation of nutritional reporter genes, thereby testing whether the prey-peptides were able to interact with these heterologous baits as well as with the pGBKT7-*Cx45*-bait (Figure 2.8).

Clones that interacted specifically with the pGBKT7-*Cx45*-bait, as determined by the interaction specificity tests, were considered putative true interactors. The inserts of these putative interactors were then sequenced to determine their identities.

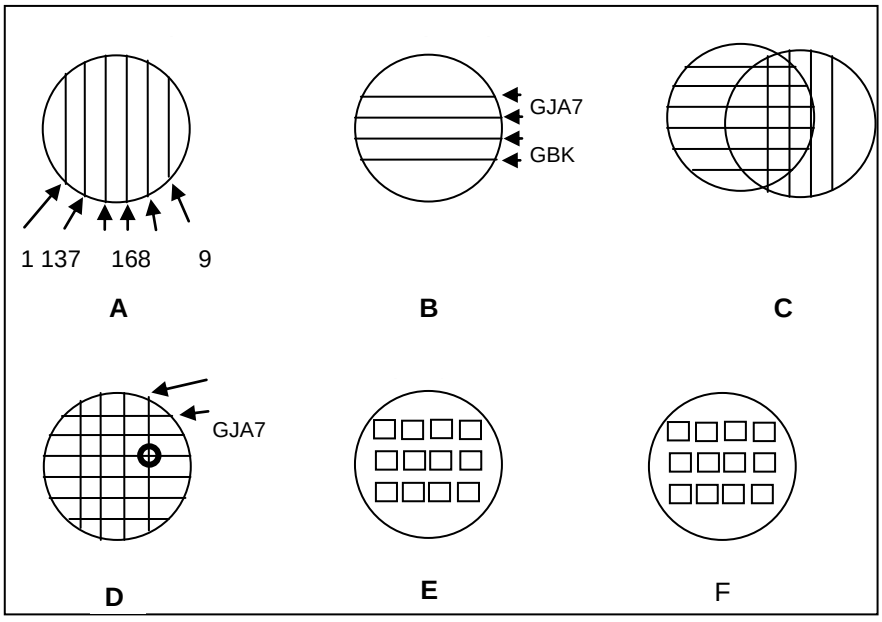

Figure 2.8. Diagrammatic representation of the heterologous bait mating.

The baits and preys were streaked in parallel lines on 140mm –leu [A] and –trp plates [B] respectively. [C] illustrates the mating of bait and prey, perpendicularly to

each other. Baits and preys were allowed to mate on a YPDA plate overnight at 30^0C [D] before an aliquot of the cross over region between bait and prey was streaked onto a –leu/-trp plate [E]. Following incubation at 30^0C for 4 days an aliquot of yeast growth on this plate was streaked on TDO and QDO plates respectively [F]. These plates were incubated at 30^0C for 4 days then a further 3 days. On these days the yeast growth on each plate was scored (Reproduced from A. Ramburan, 2005 – report).

2.13 M2H analysis

The M2H analysis was performed using the Matchmaker™ Mammalian Assay Kit 2 (BD. Biosciences, Palo Alto, U.S.A.). This kit includes the pM, pVP16 and pG5SEAP vectors (figs. 2.4, 2.5 and 2.6, respectively). The H9C2 cells used for the M2H analysis were cultured and transfected as described in sections 2.9.1 and 2.10.3 respectively. Expression of the secreted alkaline phosphatase (SEAP) reporter gene (*SEAP*) on the pG5SEAP reporter vector (Figure 2.6) occurs when there is an interaction between the fusion proteins generated by the pM and pVP16 constructs that were co-transfected with the reporter vector. Whether or not the *SEAP* reporter gene was activated and the strength of ligand binding was determined using the Great EscAPe™ chemiluminescent Detection Kit (BD Biosciences, Clontech, Palo Alto, CA, U.S.A) by measuring the SEAP activity in the culture medium using a chemiluminescent substrate.

2.13.1 Secreted alkaline phosphatase (SEAP) reporter gene assay

Fifteen microlitres of each culture medium supernatant from transfected H9C2 cells to be assayed was aliquoted into 4 separate wells of a white opaque 96-well flat-bottom microtitre plate (PerkinElmer Life And Analytical Sciences, Inc Boston, MA, U.S.A.). To this, 45µl of 1X dilution buffer (BD Biosciences, Clontech, Palo Alto, CA, U.S.A) was added and the plate incubated at 65°C for 30 min in a water-bath (Memmert ®, Schwabach, Germany). Following the incubation, the plate was left on ice for 3min to cool down the samples. The samples were then allowed to equilibrate to room temperature before 60µl assay buffer (BD Biosciences, Clontech, Palo Alto, CA, U.S.A) was added to each well.

The chemiluminescent substrate (CSPD) was then prepared by making a 1:20 dilution of the CSPD (BD Biosciences, Clontech, Palo Alto, CA, U.S.A) in

chemiluminescent enhancer (BD Biosciences, Clontech, Palo Alto, CA, U.S.A). The diluted substrate was then added to each well and the plate was incubated for 10 min at room temperature. The SEAP activity was then determined by reading the chemiluminescent signal every 10 minutes for a period of 2 ½ hours using a Bio-Tek® Synergy HT plate luminometer (Winooski, Vermont, U.S.A.).

Several control assays were included as comparisons for each experiment as shown in table 2.8. The reading obtained for the untransfected control represents the background SEAP signal of the H9C2 cells used in the experiments, while the basal control reading corresponds to basal level of SEAP activity in the experiments resulting from non-recombinant pM and pVP16 transfection. The GAL4 DNA-B control and the VP16 AD controls shown in table 2.8 were included in order to determine whether the Cx45 construct or each of the putative ligands used in the experiments function autonomously as *SEAP* reporter gene transcriptional activators. Positive control assays were also included in the experiment. The pM3-VP16 positive control plasmid (table 2.8) encodes a fusion of the GAL4 DNA-binding domain and VP16 activation domain and therefore gives very strong SEAP expression when co-transfected with pG5SEAP. The co-transfection of the individual pM53, pVP16T and pG5SEAP was also included in the experiment as another positive control. The pM53 expresses a fusion of the GAL4 DNA binding domain to the mouse p53 antigen, while the pVP16T expresses a fusion of the VP16 activation domain to the Simian Virus 40 large T-antigen which is known to interact with p53 and therefore produces strong SEAP expression. An additional, control vector, pSV-β-Galactosidase, was included in all transfections the assay in order to monitor the transfection efficiencies of the mammalian cells.

2.14 Automated DNA sequencing

Automated DNA sequencing of the cloned inserts was performed at the Core Sequencing Facility of the Department of Genetics at the University of Stellenbosch, RSA on an ABI Prism™ 377 or an ABI Prism™ 3100 automated sequencer (P.E. Applied Biosystems, Forster City, CA, U.S.A). The *Cx45*-bait construct was sequenced using the both of the primers designed to amplify the COOH-terminal domain fragment. While the cloned prey inserts from the Y2H screen were sequenced, the vector specific primers were used especially to assess that the preys were in the correct reading frame. The M2H constructs on the other hand were

sequenced using the forward prey specific and the vector specific primers, also to ensure that the correct reading frame was maintained.

Table 2.8 Transfections of tests and controls to be used in the SEAP and β-galactosidase assay of M2H analysis of putative Cx45-ligands

Transfection (5:5:1:1)	GAL4 DB-plasmid (µl)	VP16 Activation plasmid(µl)	Promoter(µl) (SEAP)	Promoter(µl) (pSV-β-gal)
Experiment 1	pM-Cx45 (2.2)	pVP16-MYO (1.9)	pG5SEAP (2.3)	pSV-β-gal (2.3)
Experiment 2	pM-Cx45 (2.2)	pVP16-OBS (2.5)	pG5SEAP (2.3)	pSV-β-gal (2.3)
Experiment 3	pM-Cx45 (2.2)	pVP16-CD63 (2.9)	pG5SEAP (2.3)	pSV-β-gal (2.3)
Experiment 4	pM-Cx45 (2.2)	pVP16-COX (2.2)	pG5SEAP (2.3)	pSV- β-gal (2.3)
Experiment 5	pM-Cx45 (2.2)	pVP16-TX2 (1.8)	pG5SEAP (2.3)	pSV-β-gal (2.3)
Experiment 6	pM-Cx45 (2.2)	pVP16-NADH (2.6)	pG5SEAP (2.3)	pSV-β-gal (2.3)
Experiment 7	pM-Cx45 (2.2)	pVP16-SCF (2.7)	pG5SEAP (2.3)	pSV-β-gal (2.3)
Untransfected control	None	None	None	None
GeneJuice control	None	None	None	None
Basal Control	pM (1.5)	pVP16 (2.8)	pG5SEAP (2.3)	pSV-β-gal (2.3)
GAL4 DNA-B control	pM-Cx45 (2.2)	pVP16 (2.8)	pG5SEAP (2.3)	pSV-β-gal (2.3)
VP16 AD control (1)	pM (1.5)	pVP16-MYO (1.9)	pG5SEAP (2.3)	pSV-β-gal (2.3)
VP16 AD control (2)	pM (1.5)	pVP16-OBS (2.5)	pG5SEAP (2.3)	pSV-β-gal (2.3)
VP16 AD control (3)	pM (1.5)	pVP16-CD63 (2.9)	pG5SEAP (2.3)	pSV-β-gal (2.3)
VP16 AD control (4)	pM (1.5)	pVP16-COX (2.2)	pG5SEAP (2.3)	pSV-β-gal (2.3)

Transfection (5:5:1:1)	GAL4 DB-plasmid (µl)	VP16 Activation plasmid(µl)	Promoter(µl) (SEAP)	Promoter(µl) (pSV-β-gal)
VP16 AD control (5)	pM (1.5)	pVP16-TX2 (1.8)	pG5SEAP(2.3)	pSV-β-gal(2.3)
VP16 AD control (6)	pM (1.5)	pVP16-NADH (2.6)	pG5SEAP (2.3)	pSV-β-gal (2.3)
VP16 AD control (7)	pM (1.5)	pVP16-SCF (2.7)	pG5SEAP (2.3)	pSV-β-gal (2.3)
Positive control (1)	pM3-VP16 (2.8)	None	pG5SEAP (2.3)	pSV-β-gal (2.3)
Positive control (2)	pM53 (1.8)	pVP16-T (0.9)	pG5SEAP (2.3)	pSV-β-gal(2.3)

The ratio of pM:pVP16:pReporter:pSV-β-gal used in the transfections was 5:5:1:1

2.15 ANALYSIS OF Cx45 BAIT AND PUTATIVE LIGANDS

2.15.1 Sequence homology searches

Sequence analyses were done using the ChromasPro computer program (Techelysium Pty Ltd, Helensvale, Queensland, Australia) to verify the sequence integrity of the *Cx45*-bait fragment generated by PCR-amplification (section 2.2.2), as well as to identify Y2H putative interactor prey clones isolated during Y2H library screening. The nucleotide sequence of the fragment encoding the Cx45 COOH-terminal domain as determined by automated sequencing was compared to the Cx45 cDNA and mRNA sequences obtained from the Genbank database (www.ncbi.nlm.nih.gov/Entrez). The sequences obtained for the Y2H prey constructs, through automated sequencing, were BLAST-searched against the GenBank database using both BLASTP and BLASTN (www.ncbi.nlm.nih.gov/Entrez) in order to assign identity to them (section 2.15). The BLASTP programme was used to determine the relationship of the translated ORF query sequence against protein sequences of different proteins in the database, while the BLASTN programme was to compare the nucleotides of query DNA sequence with sequences in the database. The BLASTP and BLASTN results of each prey were then compared to assess whether they identified the same protein. This comparison was also useful in assessing whether the protein identified was translated in the correct reading frame.

2.15.2 Prioritisation of identified putative ligands as PFHBII candidate genes

After their identification, all putative Cx45 preys were assessed for the possibility of being PFHBII causative genes. All genes which mapped to the locus PFHBII are considered disease-causing candidate genes because of their chromosomal location. However, some are functionally more attractive candidates, particularly if they exhibit additional features, such as expression in the heart, association with heart function and physiology, involvement in cardiac disease (particularly conduction disturbances) and cell-cell communication. Genes that fulfilled most of these criteria were prioritised for the further verification studies. Prioritisation of these ligands was most importantly to assess the functional specificities of the different cardiac Cxs in cardiac function, by comparing the ligands of Cx45 with known ligands of Cx43 as well as ligands of Cx40 which were identified by R. Keyser, 2007 (MSc Thesis Univerisity of Stellenbosch).

PART II: WHOLE EXOME SEQUENCING

2.16 STUDY PARTICIPANTS

PFHBII has been described in one family only (Fig 2.9) (Brink and Torrington, 1977). Clinical records and family history of 24 members of the PFHBII family were previously collected and filed for a long-term study. These individuals were examined and described in the original PFHBII study (Brink and Torrington, 1977), and the clinical data was collected as part of an ongoing study (Fernandez et al., 2004, Yako et al., 2007). Affected and unaffected individuals that were entered into the current study are shown in Table 2.9.

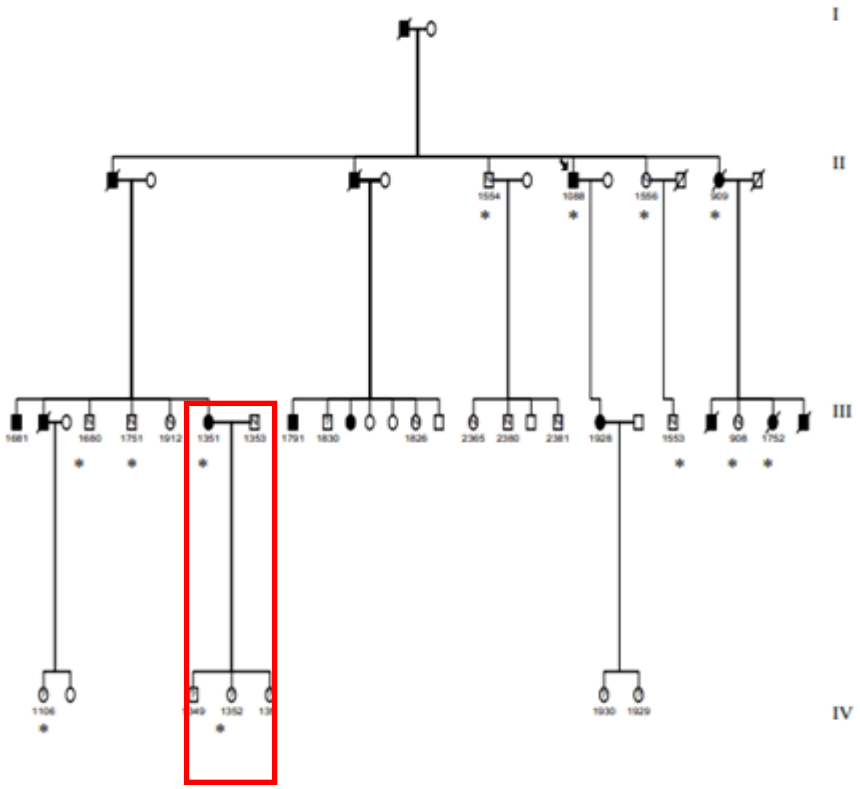

Figure 2.9: A four-generation pedigree of the PFHBII-affected family.

The roman figures represent the four generations of the family, squares indicate males; circles indicate females. Open symbols indicate individuals of unknown clinical status; N indicates unaffected individuals; solid symbols indicate PFHBII-affected subjects; diagonal lines indicate deceased individuals; question marks indicate individuals of unknown clinical status; arrow shows the proband. The numbers represent identification numbers of family members and those that were analysed by Yako et al., 2007, (both affected and unaffected) are indicated by

asterisks. The family members analysed in the current study are marked by the red box also detailed below in figure 2.10.

Family trees, or a preliminary pedigree structure of individuals entered into the study, were traced by Sr Althea Goosen, if the family had a history of the FHC. In addition, a detailed history and clinical records of the probands and their relatives, where possible, were also obtained by Sr Goosen to establish the frequency of sudden deaths and disease-related deaths. Probands with clinical features and a history of PFBH II, or any individuals who demonstrated PFHB II-like symptoms upon examination, were continuously identified, informed of the PFHB II mutation screening project, and given the opportunity to participate if they so wished.

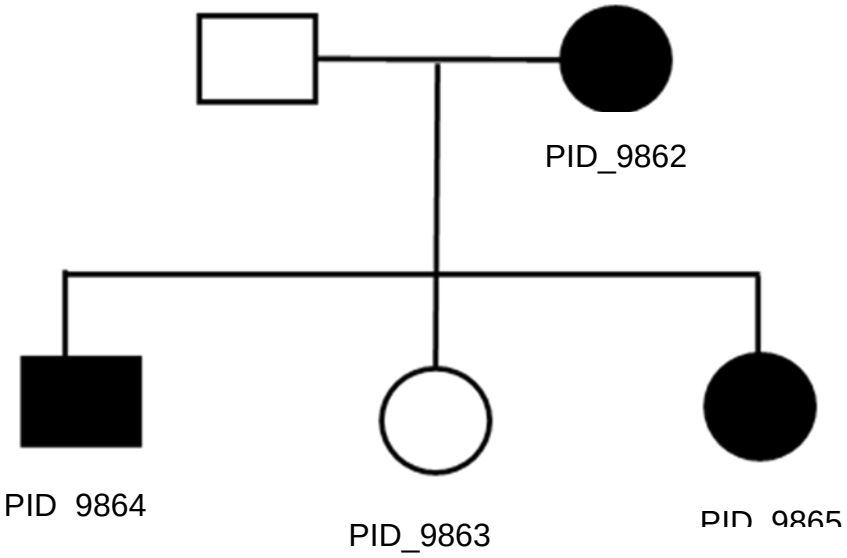

Figure 2.10: PFHB II family members analysed in the current study.

Solid circle = affected female, solid square = affected male, open circle = unaffected female, open square unaffected male.

Table 2.9: List of PFHB II patients sent for whole exome sequencing.

Patient ID	Sex	Date of birth	Clinical Diagnosis
PID_9862	F	20.07.1962	PFHB II
PID_9864	M	13.07.1979	PFHB II
PID_9863	F	16.04.1988	PFHB II
PID_9865	F	04.07.1981	Healthy daughter of PID_9862

ID = Identity; F = Female; M = Male; PFHBII = Progressive familial heart block type 2.

2.17 WHOLE EXOME SEQUENCING

2.17.1 DNA PURIFICATION

2.17.1. Extraction of nuclei from whole blood

Blood from three 5ml EDTA tubes per patient was transferred into a 50ml Falcon tube. The tube was then filled to 20 ml with ice-cold lysis buffer (appendix I). After gently inverting the tubes a few times, the sample was incubated on ice for 5-10 min. The sample was then centrifuged at 2500-3000 rpm at room temperature in a Beckman model TJ-6 centrifuge (Scotland, UK). The supernatant was discarded and the pellet was resuspended in 20ml, ice-cold lysis buffer, followed by another round of incubation and centrifugation. The supernatant was discarded and the pellet resuspended in DNA extraction buffer (appendix I), after which the nuclei were either immediately used for DNA extraction, or stored at -70°C until DNA was required.

2.17.2. Extraction of DNA from nuclei

To the freshly prepared or thawed nuclei, 100ml of proteinase K (10µg/ml) was added and the mixture was incubated overnight at 37°C. After this step, 2ml distilled water, 500ml 3M sodium-acetate (appendix I) and 25ml phenol/chloroform (appendix I) were added to the sample. The tubes were subsequently inverted and mixed gently for 10 min on a Voss rotator (Voss of Maldon, England) at 4°C. The mixture was then transferred to a glass Corex tube so that the aqueous phase could be clearly distinguished from the organic phase, followed by centrifugation in a Sorvall RC-5B refrigerated super-speed centrifuge (rotor SS 34, Dupont Instruments) at 8000 rpm for 10 min at 4°C.

The upper aqueous phase, containing the DNA, was transferred to a clean Corex tube using a sterile plastic pasteur pipette, while taking care not to disturb the interface or the organic phase. Approximately 25ml chloroform/octanol (appendix I) was added to the aqueous phase after which the tube was closed with a polypropylene stopper and gently inverted for 10 min. This mixture was centrifuged at 4°C, followed by the removal of the upper aqueous phase as described earlier. The DNA was then ethanol precipitated by adding two volumes of ice-cold 96% ethanol and inverting gently until DNA strands appeared as a white precipitate.

The DNA strands were removed using a yellow-tipped Gilson pipette and placed in a clean, 1.5ml Eppendorf microfuge tube. One millilitre 70% ethanol was then added to the DNA and the mixture centrifuged in a Beckman microfuge for 3 min at 13000 rpm. The ethanol was carefully decanted and the 70% ethanol wash repeated one more time in order to remove any excess salts. After careful removal of most of the ethanol, the DNA pellet was air-dried for 30-60 min at room temperature by inverting the Eppendorf microfuge tube on Carlton paper. Two hundred microlitres Tris-EDTA (appendix I) buffer was added and the DNA was resuspended, initially by stationary incubation at 37°C overnight and subsequently by gentle mixing in a Voss rotator at 4°C for a further 3 days. This was followed by stationary incubation at 4°C until the DNA had been fully resuspended.

After 1-2 weeks, when the DNA had completely resuspended in the buffer, the optical density (OD) of the DNA was determined in a Milton Roy series 120i spectrophotometer (USA) at 260nm (OD_{260}). The DNA concentration, in mg/ml, was determined by diluting 10ml of DNA in 500ml of TE and multiplying the measured OD_{260} by a factor of 2.5, while the purity of the DNA was monitored by the OD_{260}/OD_{280} ratio, which should be approximately 1.8 for pure DNA.

2.17.3. Exome capture and sequencing

Library preparation for sequencing was carried out using the Ion AmpliSeq™ Exome RDY Kit and the Ion Xpress™ Barcode Adaptors 1–16 Kit (Life Technologies, Carlsbad, California, United States). The DNA template for sequencing was prepared on the Ion Chef system using the Ion PI™ Hi-Q™ Chef Kit and the Ion PI™ Chip Kit v3. Sequencing was carried out on the Ion Proton™ (Thermo Fisher, Carlsbad, California, United States) at the Central Analytical Facility (CAF) at Stellenbosch University, Stellenbosch, South Africa.

2.17.4. Read mapping, variant detection and functional annotation

Sequences were aligned to the human reference genome, hg19 using TMA (version 4.4.11-1) in the ion-analysis workflow on the Torrent Suite (version 4.4.3). Base quality score recalibration, indel realignment and variant calling were performed using the variantCaller (version 4.4.3.3) plugin on the Torrent Suite and variant annotation was performed. Variant prioritization was performed using TAPER™, a custom-designed, in-house method and variants in a homozygous recessive state or

compound heterozygous state were prioritized as potential candidate variants. In brief, TAPER^{TM} 1) submits VCF files to an online variant caller, 2) removes all synonymous and non-frameshift variants, 3) removes all variants with a frequency of greater than 1% if present in the 1000 Genomes Project or Exome Sequencing Project 6500, 4) removes all variants with negative GERP+++ scores, 5) removes all variants with FATHMM scores greater than 0.1, 6) removes X and Y chromosome variants (if the pedigree does not indicate sex-linked inheritance) and lastly 7) identifies associated disorders for prioritised genes. Only variants associated with cardiomyopathies as well as those linked to Cx 45 ligands identified in this study were investigated for potentially disease causing variants in PFHB II cases.

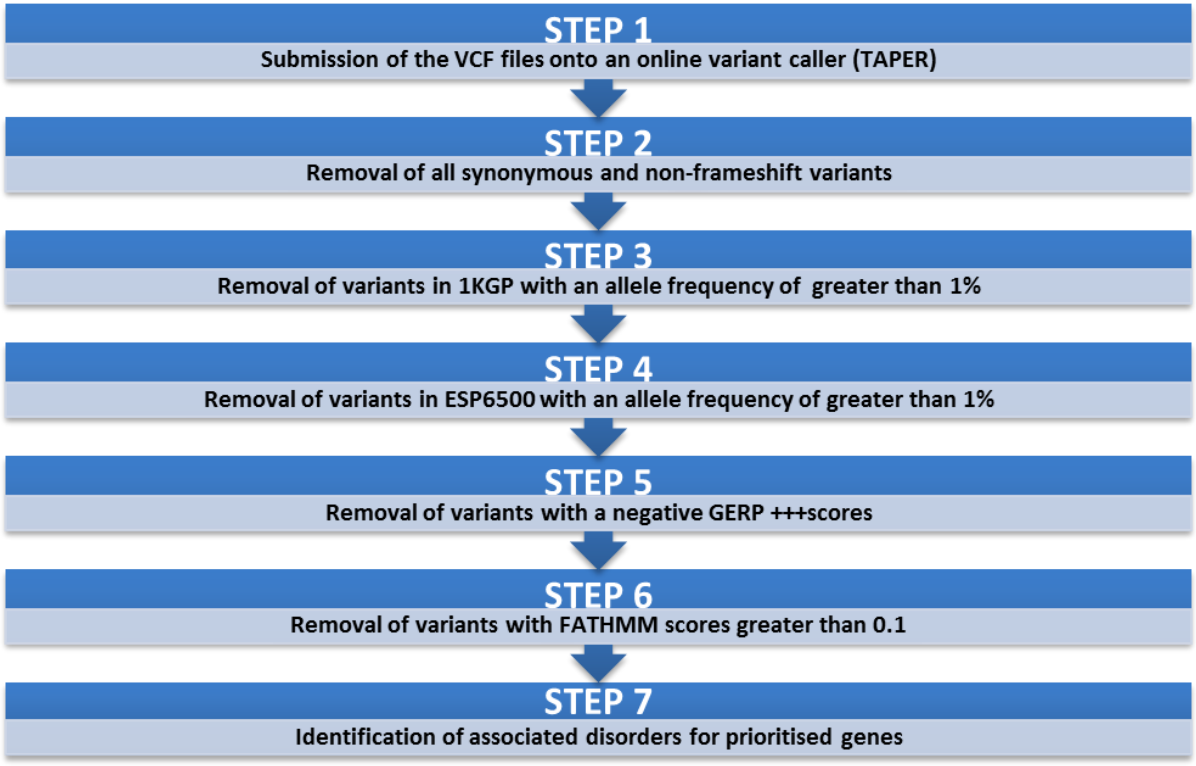

Figure 2.11: Overview of filtering process used to determine potential disease-causing variants.

These filtering steps were used to predict which of the identified variants might be disease-causing. SNVs = Single nucleotide variants; 1KGP = 1000 Genomes Project; ESP = Exome Sequencing Project; FATHMM = Functional analysis through hidden Markov models; GERP = Genome evolutionary rate profile, TAPER = Tool for Automated selection and Prioritization for Efficient Retrieval of sequence variants.

2.18 IN SILICO VARIANT PREDICTIONS

In the current study, MutationTaster2 (MT2; http://www. mutationtaster.org/), PolyPhen-2 (PP-2; http://genetics.bwh. harvard.edu/pph2/) and Sorting Tolerant From Intolerant (SIFT; http://sift.jcvi.org/) were used to predict the functional and structural consequences of each of the variants of interest. These specific tools were chosen since they are commonly used, and their efficacy has been proven (Adzhubei *et al*., 2010; Gnad *et al*, 2013; Ng and Henikoff, 2003; Venselaar et al., 2010). Several studies have used these four tools to predict the effects of amino acid exchanges on protein structure and function. Most have reported a very useful improvement in their understanding of biological pathways in which these proteins are situated, and thus a more effective design of downstream laboratory-based experiments, based on the results of these tools (Alipoor *et al*., 2016; Hassan *et al*., 2016; de Voer *et al*., 2016; Atik *et al*., 2015; Costa *et al*., 2016; Akhoundi *et al*., 2016; Stoll *et al*., 2016; Kinnersley *et al*., 2016).

2.18.1 MutationTaster2

MT2 rapidly and effectively evaluates the potential of DNA variations to cause disease by using reputable analysis tools and combining information from several biomedical databases. It takes into account splice-site changes, alterations that can influence mRNA expression, evolutionary conservation and loss of protein features. A Bayes classifier is used to predict the diseasecausing potential of each variant (Schwarz *et al.*, 2010) by calculating the probability of variants to be rare disease causing mutations or innocuous polymorphisms based on characteristics of each variant and the results of all applied tests. In order to make these predictions, the occurrence of all individual features for known disease causing mutations or common polymorphisms are studied in a large set of >100 000 known disease mutations from HGMD Professional and >6 million harmless SNPs and Indel polymorphisms from the 1KGP (Schwarz *et al*., 2014) .

2.18.2 PolyPhen-2

PP-2 uses a collection of structure- and sequence-based automatically-selected predictive features to compare properties of a mutant allele to that of a wild-type allele. It (1) determines how probable the two alleles are to inhabit the specific site of interest; (2) how different the mutated protein is from the wild-type protein; and (3) if the altered allele originated at a hypermutable site (Schmidt *et al*. 2008). These

features are used to determine the functional importance of the alteration using a Bayes classifier (Adzhubei *et al*., 2010). PP-2 has been trained and tested using two pairs of datasets: HumDiv and HumVar. HumDiv consists of 6 321 differences between human proteins and closely related mammalian homologs assumed to be non-damaging, and 3 155 alleles in UniProt classified as influencing protein function and stability and causing Mendelian diseases. HumVar contains all mutations from UniProt classified as disease-causing and ~9 000 non-synonymous non-diseasecausing SNPs.

A comparative study found PP-2 to be superior to two other predictive tools Gnad *et al*., 2013; , Bromberg *et al*., 2008; Yue *et al*., 2006). HumVar is usually less accurate in its predictions due to the inclusion of mildly deleterious alleles in its dataset. However, HumVar is more appropriate for diagnosing Mendelian diseases, while HumDiv is used for dense mapping of regions identified via GWAS, to evaluate rare alleles and to analyze natural selection (Adzhubei *et al*., 2010) PP-2 is the most prominent prediction tool currently available that uses sequence as well as structural protein information to make predictions (Adzhubei *et al*., 2010).

2.18.3 SIFT

SIFT predicts whether protein function is affected by amino acid variations based on the extent of amino acid conservation in closely related protein families (Ng and Henikoff, 2002). It interrogates protein databases to create a dataset of protein sequences functionally related to a protein of interest. An alignment built from these homologous sequences is used to determine the likelihood for each of the 20 amino acids to exist at a position of interest. The probability of the most common amino acid is used to normalize these probabilities, which is referred to as the SIFT scores (Altschul *et al*., 1997) Positions associated with low levels of conservation tolerate most alterations, while conserved positions do not. The confidence with which these predictions are made is indicated by conservation values of 0 (all amino acids can fill position) to log220 (only 1 amino acid is observed) (Ng and Henikoff, 2002). SIFT does not use protein structure to evaluate the consequence of an amino acid alteration.

A comparative study between PP-2, MT2 and SIFT found that MT2 is the most accurate and sensitive of these tools, while HumVar of PP-2 is the most specific.

These tools are each clearly quite effective. However, individually, any of them can lead to mislabeled variants and thus result in either false negative or false positive identification of potentially disease-causing variants. By using a combination of all these tools, we aimed to mitigate this.

CHAPTER THREE: RESULTS

3.1 IDENTIFICATION OF CX45 COOH-TERMINAL LIGANDS BY YEAST TWO-HYBRID (Y2H) ANALYSIS

3.1.1 Construction of DNA binding-domain target fusion protein (the bait fragment)

The Cx45 COOH-terminal encoding domain was successfully amplified by PCR using custom designed primers (section 2.1.1.1). The size of product obtained corresponded to the expected size (approximately 450bp) of the COOH-terminal encoding domain of Cx45 (www.ncbi.org.gov) as shown below in figure 3.1.

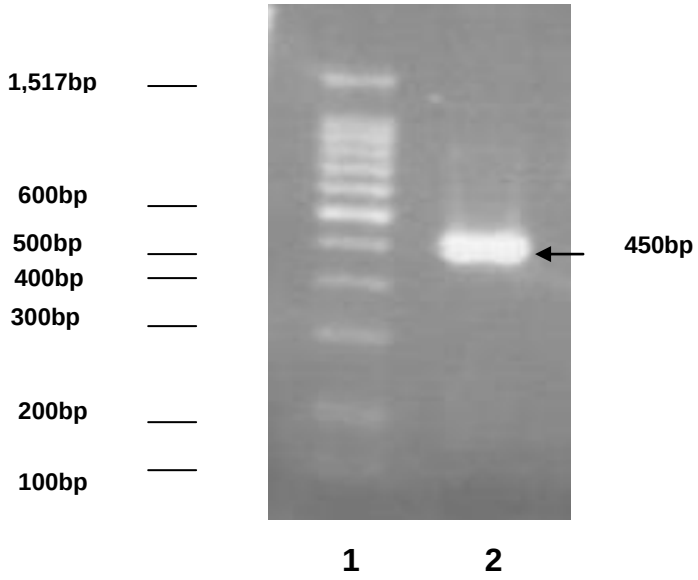

Figure 3.1 PCR-amplified product of the Cx45 COOH-terminal encoding.

PCR-amplified product of the Cx45 COOH-terminal encoding to be used as bait, electrophoretically separated on a 2% agarose gel. Lane 1- 100 bp ladder, lane 2- Cx45 COOH-terminal encoding PCR product.

Colony PCR reactions (section 2.2.3) performed to assess successful cloning of the Cx45 COOH-terminal encoding fragment into pGBKT7 revealed that only two colonies out of a total of 100 potential recombinants assessed contained the recombinant Cx45-pGBKT7 plasmid representing a 2% success rate, based on the size of the products viewed (figure 3.2).

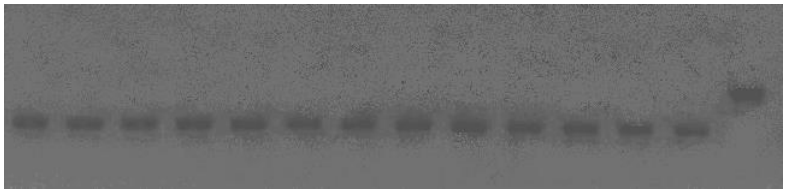

Figure 3.2 A representative sample of colony PCR products electrophoretically separated on a 0.5% agarose gel.

Lanes 1 to 13, non-recombinant bait vector (pGBKT7) (7,5 kilobases [Kb]); lane 14, recombinant Cx45-pGBKT7.

Restriction enzyme analyses of the two recombinant plasmids detected by colony PCR, verified the incorporation of the Cx45-bait fragment into pGBKT7. As expected, the recombinant plasmid, Cx45-pGBKT7, was linearised by both *EcoR*I and *Nde*I but not by the test enzyme *Sfi*I (figure 3.3).

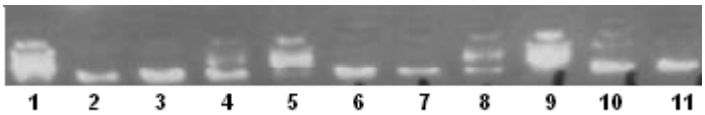

Figure 3.3 Linearised recombinant plasmids analysed in duplicate after restriction enzyme digestions.

Lanes 1 to 8 = recombinant plasmids; lanes 1, 5 and 9 = undigested; lanes 2 and 6 = digested with *EcoR*I*;* lanes 3 and 7, = digested with *Nde*I; lanes 4 and 8 = digested with *Sfi*I; lanes 9, 10 and 11= non-recombinant plasmids; sample in lane 9 = undigested; lanes 10 and 11 = digested with *EcoR*I and *Nde*I*,* respectively.

3.1.2 Integrity of bait construct

Automated sequencing of the insert contained in one of the two recombinant plasmids identified (figure 3.3) confirmed full correct sequence of Cx45 COOH-terminal domain and integrity and conservation of the GAL4 DNA-BD reading frame (Appendix V for sequence homology alignment).

3.1.3 Phenotype assessment of *Saccharomyces cerevisiae* strains

Tests based on nutritional selection markers (Ade, Trp, His, Leu, Ura) confirmed the correct phenotype of transformed and untransformed *S. cerevisiae* strains AH109

and Y187. Thus, untransformed strains AH109 and Y187 failed to grow on SD^{-Ade}, SD^{-Trp}, SD^{-His}, SD^{-Leu} but grew on SD^{-Ura}, implying their viability for transformation and subsequent Y2H analysis (table 3.1). Additionally, these nutritional selection tests confirmed the inability of the recombinant Cx45-pGBKT7 bait vector to autoactivate the endogenous reporter genes of the Y2H system. Thus, transformed *S. cerevisiae* AH109 (Cx45-pGBKT7) failed to grow on SD^{-Ade}, SD^{-His} and SD^{-Leu} but grew on both SD^{-Trp} and SD^{-Ura} while *S. cerevisiae* Y187 (pTD1.1) grew only SD^{-Leu} and SD^{-Ura} (table 3.1).

Table 3.1 Phenotypic assessment of S. cerevisiae colonies for the non-activation of Y2H endogenous reporter genes

Strain	SD^{-Ade}	SD^{-Trp}	SD^{-His}	SD^{-Leu}	SD^{-Ura}
S. cerevisiae AH109	-	-	-	-	+
S. cerevisiae Y187	-	-	-	-	+
S. cerevisiae AH109 (Cx45-pGBKT7)	-	+	-	-	+
S. cerevisiae Y187 (pTD1.1)	-	-	-	+	+

- , No growth observed, +, growth observed, SD^{-Ade} = Single dropout medium (adenine-deficient); SD^{-Trp}= tryptophan deficient, SD^{-His}= histidine deficient; SD^{-Leu}= leucine deficient; SD^{-Ura}= uracil deficient, Cx45-pGBKT7 = bait control, pTD1.1 = prey control.

3.1.4 Expression of Cx45-pGBKT7 bait construct

3.1.4.1 Toxicity test

Growth rates derived from concurrently generated curves for transformed *S. cerevisiae* AH109 (Cx45-pGBKT7), transformed *S. cerevisiae* AH109 (non-recombinant pGBKT7) and untransformed AH109 (figure 3.3) showed the Cx45-COOH terminal fragment to be slightly toxic to its host strain *S. cerevisiae* AH109, considering that the growth rate of untransformed *S. cerevisiae* AH109 was slightly higher. However since, *S. cerevisiae* AH109 transformed with the Cx45-pGBKT7 bait

construct grew at the same rate as *S. cerevisiae* AH109 transformed with the non-recombinant pGBKT7 plasmid, Cx45 was not excluded as bait for the Y2H screen (figure 3.4).

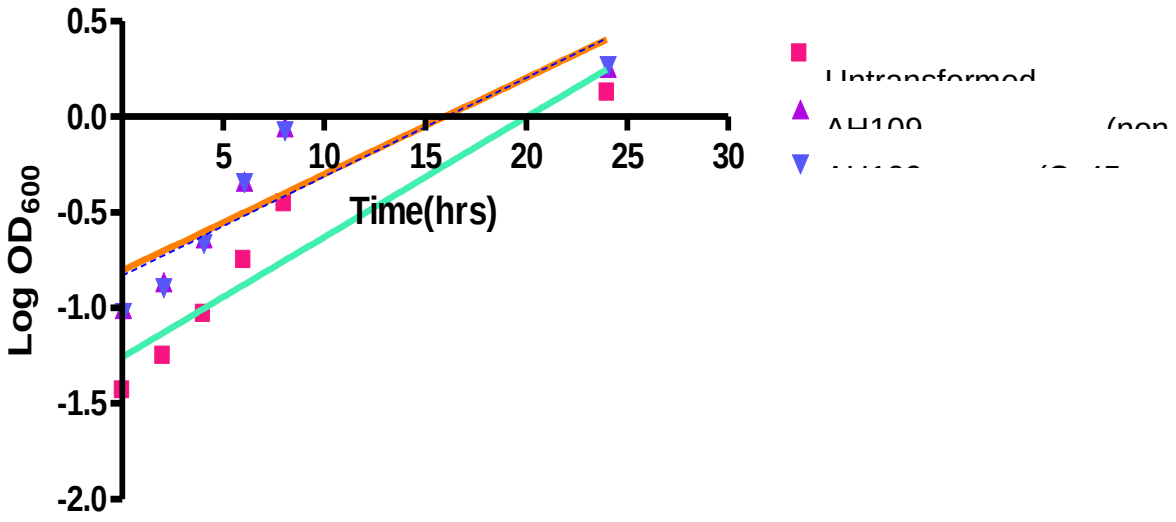

Figure 3.4 Comparative growth rates of *S. cerevisiae* AH109, *S. cerevisiae* AH109 (pGBKT7), *S. cerevisiae* AH109 (Cx45-pGBKT7).

Growth rate, as determined from the slopes of the respective curves, of *S. cerevisiae* AH109 transformed with Cx45-pGBKT7 construct, in comparison to that of *S. cerevisiae* AH109 with the non-recombinant pGBKT7 plasmid (pink and dotted blue lines), as well as untransformed *S. cerevisiae* AH109 (aqua line).

3.1.4.2 Mating efficiency test

Comparative small scale matings of *S. cerevisiae* AH109 transformed with the Cx45-pGBKT7 bait construct and *S. cerevisiae* Y187 transformed with pTD1.1 (prey control vector) revealed that the mating efficiency[5] was well above the threshold of 2% (table 3.3) making Cx45 a viable bait for the Y2H screen.

[5] Mating efficiency determined from the formula in section 2.11

Table 3.2 Total number of colonies per growth medium

Growth Medium	SD^{-Trp}			SD^{-Leu}			$SD^{-Leu/-Trp}$		
Dilution factor	10^{-1}	10^{-2}	10^{-3}	10^{-1}	10^{-2}	10^{-3}	10^{-1}	10^{-2}	10^{-3}
(CONTROL MATING) Y187 (pTD1.1) x AH109(pGBKT7)	TNC	TNC	1088	TNC	TNC	2096	TNC	23	7
(TEST MATING) Y187 (pTD1.1) x AH109 (Cx45-pGBKT7)	TNC	1536	151	TNC	TNC	595	TNC	76	15

-*TNC= Too numerous to count;* SD = single dropout medium; SD^{-Trp} = Tryptophan deficient, SD^{-Leu} = Leucine deficient; $SD^{-Leu/-Trp}$ = Leucine and tryptophan deficient.

Table 3.3 Mating efficiency determined from colony forming units of S. cerevisiae grown on SD-Trp, SD-Leu and SD-Leu,Trp

Mating	Mating efficiency (%)
(CONTROL MATING) Y187 (pTD1.1) x AH109(pGBKT7)	2.6
(TEST MATING) Y187 (pTD1.1) x AH109 (Cx45-pGBKT7)	4.9

3.1.5 Y2H analysis to identify ligands of Cx45 COOH-terminal domain

3.1.5.1 Y2H screen

The initial selection of putative Cx45 ligands on TDO growth medium, 371 clones containing ligands were obtained which were later reduced to 154 on QDO growth medium (table 3.4). Some of these clones from the latter selection presented white colonies while others presented pink colonies, the latter indicating poorer adenine expression. In spite of this, the pink colonies were selected mainly for comparative purposes.

Table 3.4 Total number of colonies obtained from the Y2H screen

Growth medium	Selection marker	# of *S. cerevisiae* colonies obtained
TDO	TRP1, LEU2, HIS3	371
QDO	TRP1, LEU2, HIS3, ADE2	154

Table 3.5 Growth scores of 154 sequentially identified colonies.

Growth scores of 154 sequentially identified colonies of putative ligands from the library screened by the (MEL1) α-galactosidase assay as well as their growth scores on TDO and QDO plates

Clone #	TDO (R&S)	QDO (R&S)	Colony phenotype[a] QDO (Ade)	QDO (α-gal)
1	4	4	white	2
4	4	4	white	3
5	4	4	white	3
8	4	3	pink	-
9	4	3	pink	3
12	4	3	pink	4
13	4	2	pink	3
21	4	3	pale pink	3
25	4	3	pale pink	1
27	4	3	pale pink	2
33	4	3	pink	-
35	4	4	white	2
38	4	3	pink	-
47	4	3	pink	2
49	4	2	pink	-
51	4	3	pink	-
52	4	2	pink	4
53	4	3	pink	2
55	4	3	pink	2
59	4	4	pink	3

Clone #	TDO (R&S)	QDO (R&S)	Colony phenotype[a] QDO (Ade)	QDO (α-gal)
60	4	3	pink	1
61	4	2	pink	-
65	4	4	white	3
66	4	2	pink	1
67	4	4	pink	1
69	4	3	pink	-
70	4	4	white	2
71	4	4	pink	1
72	4	4	pink	1
74	4	2	pink	-
78	4	3	pink	-
79	4	3	pink	-
80	4	3	pink	-
81	4	3	pink	-
83	4	3	pink	-
84	4	4	white	-
85	4	4	white	1
87	4	3	pink	1
88	4	4	pink	1
91	4	3	white	1
93	4	4	pink	3
97	4	4	pink	1
98	4	3	pink	1
99	4	3	white	1
102	4	3	pink	2
103	4	3	white	3
105	4	3	pink	1
106	4	3	white	3
108	4	2	white	3
114	4	3	white	3
115	4	4	pink	3
116	4	4	pink	3
119	4	3	pink	1
120	4	4	pink	3
124	4	3	pink	-

Clone #	TDO (R&S)	QDO (R&S)	Colony phenotype[a] QDO (Ade)	QDO (α-gal)
125	4	3	pink	3
127	4	3	white	3
128	4	4	pink	-
130	4	2	white	4
131	4	3	white	3
133	4	4	pink	3
136	4	4	pink	1
138	4	3	white	3
139	4	4	white	1
146	4	3	white	2
147	4	3	white	4
148	4	3	pink	2
149	4	3	pink	1
150	4	3	pink	1
151	4	4	pink	3
152	4	4	pink	2
154	4	4	white	4
155	4	3	white	3
157	4	4	pink	3
161	4	3	pink	1
167	4	3	white	3
168	4	4	white	2
173	4	3	white	2
174	4	4	white	3
175	4	4	white	1
179	4	4	pink	-
180	4	3	pink	3
181	4	3	pink	3
182	4	4	pink	3
183	4	4	white	2
185	4	4	pink	2
188	4	3	white	3
189	4	3	white	4
199	4	3	pink	3
201	4	3	pink	1

Clone #	TDO (R&S)	QDO (R&S)	Colony phenotype[a] QDO (Ade)	QDO (α-gal)
202	4	3	white	-
203	4	4	pink	3
207	4	2	white	-
208	4	2	pink	1
211	4	4	pink	1
214	4	4	pink	-
218	4	3	white	2
220	4	2	white	2
225	4	3	white	2
226	4	4	pink	4
227	4	3	white	1
232	4	3	pink	-
233	4	3	white	3
234	4	3	white	4
235	4	3	pink	-
236	4	2	white	3
237	4	3	white	3
238	4	2	white	2
242	4	4	white	-
245	4	3	pink	1
249	4	3	pink	2
250	4	4	pink	3
252	4	2	white	1
253	4	3	white	-
254	4	2	white	3
256	4	3	pink	3
266	4	3	white	1
267	4	2	white	2
271	4	4	white	3
272	4	4	white	4
273	4	4	white	4
277	4	4	white	2
279	4	4	white	2
280	4	3	white	2
282	4	4	white	-

Clone #	TDO (R&S)	QDO (R&S)	Colony phenotype[a] QDO (Ade)	QDO (α-gal)
285	4	4	white	2
286	4	4	white	3
289	4	4	white	3
301	4	4	pink	2
304	4	4	white	1
306	4	4	white	1
314	4	3	white	3
315	4	3	white	3
316	4	3	white	2
318	4	3	white	3
328	4	4	pink	2
330	4	4	white	2
331	4	4	pink	2
332	4	3	pink	2
336	4	3	white	3
340	4	3	white	3
342	4	3	white	1
343	4	2	pink	2
346	4	3	white	2
347	4	3	white	1
348	4	3	white	4
349	4	4	white	2
352	4	3	white	3
354	4	2	white	4
359	4	3	white	3
362	4	2	white	3
364	4	2	white	2
371	4	3	white	2

Clones in black were excluded from further testing; those highlighted in red were included in the subsequent specificity test (heterologous bait mating). Scores of 4, 3, 2, 1 on TDO and QDO denote the robustness and size (R&S) of colony, indicating strength of bait/prey interaction, (4) most robust (1) least robust; white colonies, strong adenine producers; pink colonies, weak adenine producers. On QDO-X-α-galactosidase, scores of 4, 3, 2, 1 indicate the intensity of the blue colour presented by each colony; (4) dark blue, (1) light blue, (-) indicate no blue colour observed. [a]

phenotype of *S. cerevisiae* on QDO. Cells highlighted in purple = primary interactors; cells highlighted in blue = secondary interactors.

Table 3.6 Heterologous bait mating of prey clones tested against Cx45-pGBKT7, pGBKT7, pGBKT7-53 and Reeler –pGBKT7

		DAY4				DAY7			
Clone #	α-gal	Cx45	pGBKT7	pGBK-53	Reeler	Cx45	pGBKT7	pGBK-53	Reeler
1	2	4	-	-	-	4	-	-	-
4	3	3	3	4	4	-	4	4	4
5	3	4	4	4	4	4	4	1	-
6	3	4	4	4	3	3	-	1	-
12	4	4	4	4	4	2	-	-	4
21	3	4	4	4	3	4	1	1	-
27	2	4	4	4	3	2	1	2	-
33	3	4	3	4	2	3	-	1	-
35	2	4	2	4	4	3	-	-	-
52	4	4	2	4	4	4	-	-	3
55	2	3	1	4	3	3	-	-	-
60	1	3	3	4	3	4	-	4	4
65	2	4	4	4	3	3	1	1	-
70	2	4	3	4	3	1	2	4	-
85	1	4	2	4	4	-	-	4	4
87	1	3	2	4	3	-	-	4	-
88	1	3	2	4	3	-	-	4	4
93	3	4	2	4	3	4	-	-	-
97	1	4	3	4	2	-	-	4	4
98	1	4	2	4	4	4	-	4	4
99	1	4	3	4	2	1	1	4	-
102	2	3	1	4	2	-	-	-	1
103	3	3	1	4	4	4	-	-	-
106	3	3	1	4	1	-	-	-	-
108	3	3	1	4	1	-	-	-	-
114	3	2	2	4	2	-	-	-	-
115	3	4	3	4	4	-	-	-	-
116	3	4	4	4	3	3	-	-	-

		DAY4				DAY7			
Clone #	α-gal	Cx45	pGBKT7	pGBK-53	Reeler	Cx45	pGBKT7	pGBK-53	Reeler
120	3	4	1	4	2	4	-	1	-
125	3	4	2	4	3	-	-	-	-
127	3	3	1	4	2	-	-	-	-
130	4	3	1	4	2	-	-	-	-
133	3	4	4	4	3	3	2	1	
136	2	2	3	4	3	2	1	3	-
138	3	2	1	4	3	3	-	-	-
139	1	2	3	4	3	-	4	4	-
146	2	4	4	4	2	3	-	4	2
147	4	3	1	4	1	-	-	-	-
148	2	3	2	4	3	-	4	4	4
150	2	4	3	4	2	2	-	4	-
154	4	4	4	4	4	4	3	2	3
157	4	4	4	4	4	4	3	2	3
167	3	3	1	4	4	2	-	-	-
168	2	2	1	4	2	-	-	-	-
173	2	4	3	4	4	4	4	4	4
175	1	3	3	4	2	1	-	4	-
180	3	4	2	4	4	3	-	-	-
181	3	3	2	4	3	-	-	-	-
185	2	3	1	4	1	-	-	-	-
188	3	2	4	3	-	-	-	-	
189	4	2	1	4	3	-	-	-	-
203	3	4	3	4	4	4	-	-	-
211	1	3	1	4	2	-	-	-	-
218	2	3	1	4	3	4	-	-	-
225	2	3	1	4	1	-	-	-	-
226	4	4	4	4	3	4	-	-	-
233	3	1	-	2	-	-	-	-	-
234	4	1	1	4	2	-	-	-	-
236	3	3	3	4	2	-	-	-	-
237	3	3	1	4	2	-	-	-	-
238	2	3	2	4	2	2	-	4	1

		DAY4				DAY7			
Clone #	α-gal	**Cx45**	**pGBKT7**	**pGBK-53**	**Reeler**	**Cx45**	**pGBKT7**	**pGBK-53**	**Reeler**
245	1	4	3	4	3	3	-	4	-
249	2	3	3	4	3	-	-	3	2
254	3	2	1	4	1	-	-	-	-
256	3	4	3	4	4	2	-	-	4
267	2	3	2	4	3	-	-	-	-
273	1	3	3	4	3	2	-	3	-
279	2	4	2	4	3	-	-	-	-
280	3	3	1	4	4	-	-	-	4
288	2	3	1	4	1	-	-	-	
289	3	4	4	4	3	3	-	-	-
301	2	4	4	4	3	3	-	4	-
306	1	3	3	4	3	2	-	3	-
314	3	1	1	4	2	-	-	-	-
315	3	3	1	4	4	3	-	-	-
316	2	3	3	4	3	1	-	4	4
318	3	1	1	4	2	-	-	-	-
328	2	4	3	4	3	3	-	-	-
330	2	3	1	3	1	-	-	-	-
331	2	4	1	4	3	3	-	-	-
332	2	1	1	4	2	-	-	-	-
336	3	2	1	4	2	-	-	-	-
342	1	4	3	4	2	3	-	4	-
344	4	3	2	4	2	-	-	-	-
346	2	1	1	4	1	-	-	-	-
347	1	3	3	4	2	1	-	4	-
349	2	1	1	4	2	-	-	-	-
352	3	4	2	4	3	-	-	-	4
359	3	3	2	4	2	-	-	1	-
364	2	2	2	3	2	-	-	-	-

(-) Negative indicates no *S. cerevisiae* growth while a score of 1 to 4 indicates robustness and size of colony, in increasing order of growth. Preys highlighted in purple were selected for sequencing.

3.1.5.2 Detection of activation of colourimetric *MEL1* reporter gene (X-α-Galactosidase assay)

The blue colour presented by some colonies indicated the activation of the *MEL1* reporter gene of the GAL4 reporter system. Thus, the intensity of the blue colour and robustness (tables 3.5 and 3.6) of the colonies obtained from the X-α-galactosidase (X- α-Gal) assay gave an indication of the strength strength of the interaction between Cx45 and its possible ligands. Colonies with scores of 4 and 3 were grouped as primary Cx45 interactors, while those with scores of 2 were grouped as secondary interactors. Fifty-eight (scoring 1 or 0) of these colonies were excluded from further analysis, as they did not produce any blue colour, suggesting their inability to activate the *MEL1* reporter gene (table 3.6).

3.1.5.3 Interaction test

Ninety-six preys of the original 154 colonies (table 3.6) from the QDO-X-α-galactosidase assay were screened for specificity of their interaction with Cx45, by the heterologous bait mating assay. These preys showed varying degrees of interaction; preys such as clones 154 and 173 interacted with all four heterologous baits, others like clones 102 and 218 interacted only with brain expressed reelin, while preys such as clones 189 and 346 showed no interaction. Out of all the preys screened in this round, only nineteen showed a relatively specific interaction with Cx45. These also included preys with a slight interaction with pGBKT7-53. However, this was not totally unexpected as pGBKT7-53 has a tendency to interact with most preys (BD biosciences Clonetech user manual, 2005) (table 3.7).

Table 3.7 Total number and growth scores of colonies of putative ligands from the α-galactosidase assay

	Primary interactors		**Secondary interactors**		
Growth score	4	3	2	1	0
Total # of colonies	15	49	35	32	26

3.1.6 Sequence homology searches

After conducting a battery of screening assays (sections 2.12.7 and 2.12.8), twenty-five (clones 1, 6, **21**, 33, 35, 52, 55, **102**, 103, 116, 120, 130, 138, **139**, **154**, **157**, 167, 180, 289, 218, 226, **234**, 315, 328, and 331) putative preys of Cx45 were selected for sequencing (table 3.8). These preys consisted of the nineteen Cx45 specific preys as well as another six randomly chosen clones (**21, 102, 139, 154, 157, and 234**) from the heterologous bait mating assay, for comparative purposes. Satisfactory sequencing results were obtained for most of the inserts. However, after several rounds of plasmid extraction, purification and sequencing, four clones continuously produced sequences of poor quality and were therefore excluded from further experiments. The genes harboured in each of the remaining twenty-one were then identified, by conducting sequence homology alignments - comparing their sequences with those in the Genbank databases (www.ncbi.org/BLAST) (The sequence alignments on which the identification of clones was based are shown in Appendix V). This allowed the identification of the following encoded proteins: - phosphodiesterase 4D interacting protein (myomegalin), cytochrome C oxidase subunit I, thioredoxin 2 precursor, solute carrier family member 25, HtrA serine peptidase 3, Alu subfamily SB1 sequence, ubiquitin specific protease 42, hypothetical protein FLJ14981, NADH dehydrogenase subunit 4, *Homo sapiens* CD63 antigen, obscurin-RhoGEF (also known as myosin light chain kinase) and SCF apoptosis response protein 1. Ultimately, seven of these ligands were prioritised as putative ligands of Cx45, based on their subcellular localisation, potential interaction with Cxs in general, as well their relevance to cardiac function (Table 3.9).

As shown in table 3.9, the majority of the putative ligands represented mitochondrial proteins (10), while the rest represented cytoplasmic (3), extracellular (1) and nuclear proteins (3). Some of the ligands such as, mitochondrial cytochrome C oxidase subunit 1 were represented by more than one clone, suggesting the possible authenticity of their interaction. Chromosomal localisation of the encoded proteins also determined the inclusion of a particular protein as a candidate causative gene for PFHBII. However, none of the identified ligands were found to be situated inthe PFHBII locus. Initially myomegalin was viewed as a particularly interesting functional candidate as it is located on chromosome 1q12.1, but it was excluded as the putative causative gene for PFHBII (1q32.2 – 32.2) because it lay outside the defined interval (figure 3.5). Nevertheless it was prioritised as a putative Cx45 ligand based on its subcellular localisation and biological relevance to cardiac function.

Table 3.8 Blast-search data obtained using NCBI alignments

Prey #	In-frame ORF protein hit (BLASTP)	Accession # (E-value)	Genomic hit (BLASTN)	Accession # (E-value)
1	Phosphodiesterase 4D interacting protein isoform 4 (Myomegalin)	NP_001002810 (0.0)	*Homo sapiens* phosphodiesterase 4D interacting protein, transcript variant 4, mRNA	NM_001002810 (0.0)
6	Cytochrome C oxidase subunit I	YP_214942.1 (2e-97)	*Homo sapiens* isolate IND23 mitochondrion	DQ246833.1 (0.0)
21	Cytochrome C oxidase subunit I	AAP89662.1 (9e-133)	*Homo sapiens* mitochondrial DNA	AP008389.1 (0.0)
35	Thioredoxin 2 precursor	NP_036605.2 (3e-90)	*Homo sapiens* thioredoxin 2	NM_012473.3 (0.0)
55	Solute carrier family 25 (mitochondrion)	AAH63643.1 (8e-85)	*Homo sapiens* solute carrier family 25, adenine nucleotide translocator member 4	BC063643.1 (0.0)
103	Cytochrome C oxidase subunit I	AAP89662.1 (3e-99)	*Homo sapiens* isolate B15mitocondrion	AY713995.1 (0.0)
116	Cytochrome C oxidase subunit I	AAU02594.1 (1e-65)	*Homo sapiens* isolate IND23 mitochondrion	DQ246833.1 (0.0)
120	HtrA serine peptidase 3 [*Homo sapiens*]	AAH34390.1 (2e-101)	*Homo sapiens* HtrA serine peptidase 3	BC034390.1 (0.0)
33	Cytochrome C oxidase subunit I	YP_214942.1 (2e-97)	*Homo sapiens* isolate IND23 mitochondrion	DQ246833.1 (0.0)
130	No significant hit	-	*Homo sapiens* clone SCb-41A3	AC005826. (0.0)
138	Cytochrome C oxidase subunit I	AAP91157.1 (5e-126)	*Homo sapiens* isolate IND18 mitochondrion	DQ246828.1 (0.0)
139	Cytochrome C oxidase subunit I	AAU13071.1 (3e-140)	*Homo sapiens* isolate IND18 mitochondrion	DQ246828.1 (0.0)
157	Alu subfamily SB1 sequence	P39189 (3e-26)	*Homo sapiens* BAC clone RP11-124A7 from 4, complete sequence	AC095043.3 (9e-198)
167	Ubiquitin specific protease 42	EAL23715.1 (1e-30)	*Homo sapiens* ubiquitin specific peptide	NM_032172.1 (2e-109)
328	R31167_1, partial protein [*Homo sapiens*] (hypothetical protein FLJ14981)	AAD24592.1 (1e-158)	*Homo sapiens* MPN domain containing protein	AC027793.9 (2e-07)
180	NADH dehydrogenase subunit 4	AAP48162.1 (5e-48)	*Homo sapiens* isolate C180 mitochondrion	AY713999.1 (0.0)
234	CD63 antigen [*Homo sapiens*]	NP_001771.1 (7e-42)	Homo sapiens CD63 antigen (melanoma)	NM_001780.3 (0.0)

Prey #	In-frame ORF protein hit (BLASTP)	Accession # (E-value)	Genomic hit (BLASTN)	Accession # (E-value)
289	NADH dehydrogenase subunit 4	AAO67017.1 (5e-48)	*Homo sapiens* isolate C180 mitochondrion	AAO67017.1 (5e-48)
218	hypothetical protein FLJ14981	NP_080806.2 (3e-137)	full-length cDNA clone CS0DI076YF	CR610197.1 (0.0)
315	Obscurin, cytoskeletal calmodulin binding protein	CAH71673.1 (1e-35)	Homo sapiens obscurin, cytoskeleton	NM_052843.2 (3e-157)
331	SCF apoptosis response protein 1	NP_060948.2 (5e-93)	*Homo sapiens* chromosome 20 open reading frame 35	NM_018478.2 (0.0)
93	Ubiquitin specific protease 42	NP_115548.1 (1e-31)	*Homo sapiens* mRNA for ubiquitin	AJ601395.1 (7e-108)

- E-values denote the degree of homology between the reference sequence and the query sequence; values less than zero (0) mark high degree of homology

Table 3.9 Putative ligands prioritised according to function, subcellular localisation and chromosomal location

In-frame Protein hit	Primary function	Subcellular localisation	Chromosomal location	Clone #	Total # of preys identified as containing the same clone
Phosphodiesterase 4D interacting protein (myomegalin)	**Required for protein transport from the ER to the golgi complex. Thought to be present on vesicles operational between the ER and the golgi complex.**	**Cytoplasmic**	**1q12.1**	**1**	**1**
Thioredoxin 2 precursor	**Anti-apoptosis and regulation of mitochondrial membrane potential, suggested to be involved in the resistance of anti-tumour agents, also possesses a dithiol-reducing activity**	**Mitochondrial inner membrane**	**22q13.1**	**35**	**1**
Solute carrier family 25 (mitochondrial carrier; adenine nucleotide translocator),	**Catalyses the exchange of ADP and ATP across the mitochondrial inner membrane**	**Mitochondrial inner membrane**	**5q31**	**55**	**1**

In-frame Protein hit	Primary function	Subcellular localisation	Chromosomal location	Clone #	Total # of preys identified as containing the same clone
member 4*					
HtrA serine peptidase 3*	Protease that regulates the availability of insulin-growth factors (Igfs) by cleaving Igf-binding proteins. This protein is a secreted enzyme that is proposed to regulate the availability of (Igfs) by cleaving IGF-binding proteins. It has also been suggested to be a regulator of cell growth.	Extracellular	4q16.1	120	1
Aldehyde dehydrogenase 7 family, member A1*	Aldehyde metabolism	Unknown	9q21.13	130	1
Homo sapiens CD63 antigen (melanoma)	Member of tetraspanin family. Mediates signal transduction events in the regulation of cell development, activation, growth and motility. Associated with Hermansky-Pudlak syndrome and tumour progression	Plasma membrane	12q12-q13	234	1
Ubiquitin specific protease 42*	Unknown	Nucleus	7p22.1	167, 93	2
Obscurin-RhoGEF also known as myosin light chain kinase	Contains 68 Ig domains, 2 fibronectin domains, 1 calcium/calmodulin-binding domain, 1 RhoGEF domain with an associated PH domain, and 2 serine-threonine kinase domains. Belongs to the family of giant sacormeric	Cytoplasm	1q42.13	315	1

In-frame Protein hit	Primary function	Subcellular localisation	Chromosomal location	Clone #	Total # of preys identified as containing the same clone
	signaling proteins that includes titin and nebulin, and may have a role in the organization of myofibrils during assembly and may mediate interactions between the sarcoplasmic reticulum and myofibrils				
SCF apoptosis response protein 1	Protein-binding, transport	Cytoplasm	20q13.12	331	1
NADH dehydrogenase subunit 4	Electron carrier activity	Mitochondrial matrix	5q11.1	180, 289	2
Cytochrome C oxidase subunit I	Mitochondrial electron transport	Mitochondrial inner membrane	16q22-qter	139, 138, 116, 103, 33, 21,6	6
Hypothetical protein LOC68047*	Transcription activity	Nucleus	19p13.3	318, 328	2

- Proteins highlighted in blue are mitochondrial, proteins of other subcellular localisation are in red, green is unknown *

  Proteins excluded from verification analyses

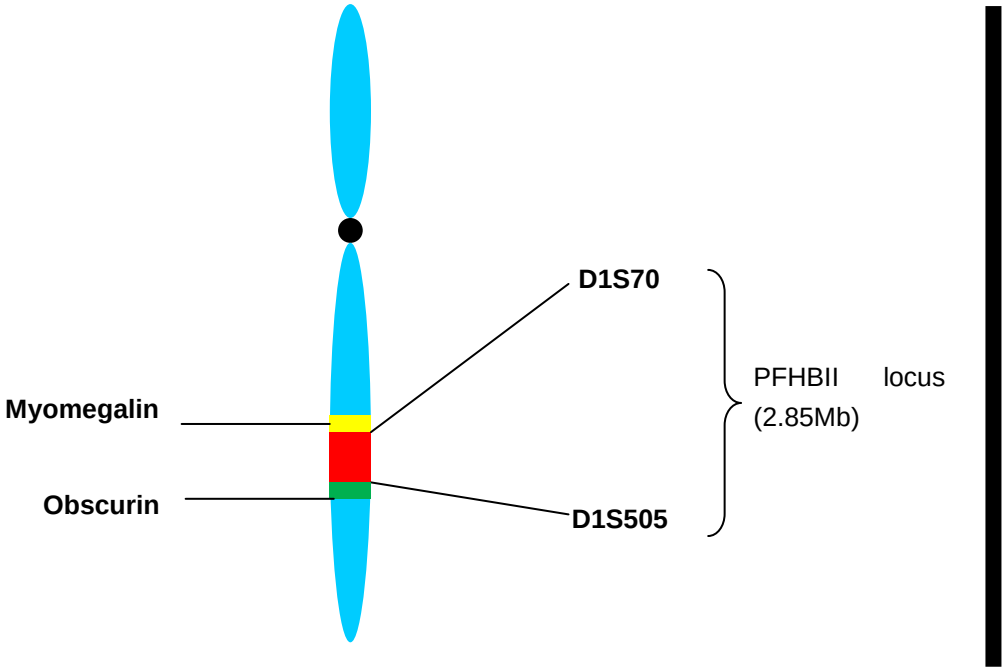

Figure 3.5 Chromosomal location of myomegalin (1q12.1) and obscurin (1q42.1)

3.2 MAMMALIAN TWO-HYBRID (M2H) ANALYSIS

3.2.1 Generation of M2H constructs

The M2H constructs generated consisted DNA fragments encoding the seven prioritised preys identified from Y2H (Myomegalin, CD63-antigen, SCF-apoptosis response protein 1, NADH dehydrogenase subunit IV, Thioredoxin 2, Obscurin and Cytochrome C oxidase subunit) as well as the Cx45 COOH-terminal domain. The constructed Cx45 bait-insert was successfully cloned into the pM GAL4-DNA binding domain vector, while inserts encoding the putative Cx45-ligands (PCR products of which are presented in figure 3.6) were cloned into the pVP16 GAL-activation domain vector. The integrity of the sequences and conservation of the GAL4 DNA-BD and GAL-activation domain reading frame was verified by automated sequencing (sequence traces in Appendix V).

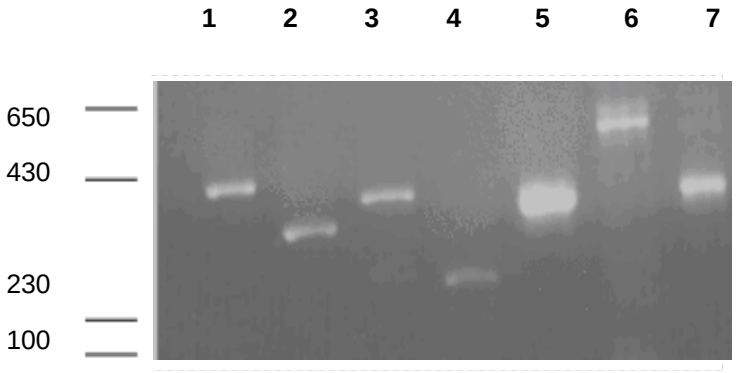

Figure 3.6 PCR amplification of inserts encoding putative Cx45 ligands electrophoretically separated on a 1% agarose gel.

Sharp bands represent approximate sizes of PCR products of prioritised Cx45 ligands. Lane 1, Myomegalin (400bp); lane 2, CD63-antigen (300bp); lane 3, SCF-apoptosis response protein 1 (350bp); lane 4, NADH dehydrogenase subunit IV (250bp); lane 5, Thioredoxin 2 (430bp); lane 6, Obscurin (650bp); lane 7 Cytochrome C oxidase subunit I (420bp).

3.2.2 Secreted alkaline phosphate (SEAP) assay

The SEAP data was inconclusive as the enzyme activity for two of the negative controls (lanes 19 and 20) and the basal control (lane 18) was higher than that for the positive control (lane 16) (fig 3.7). The beta-galactosidase assays indicated that the transfection efficiency of H9C2 cells was poor (data not shown). Thus it was impossible to draw conclusions from the M2H assays and time constraints prevented optimisation of the technique.

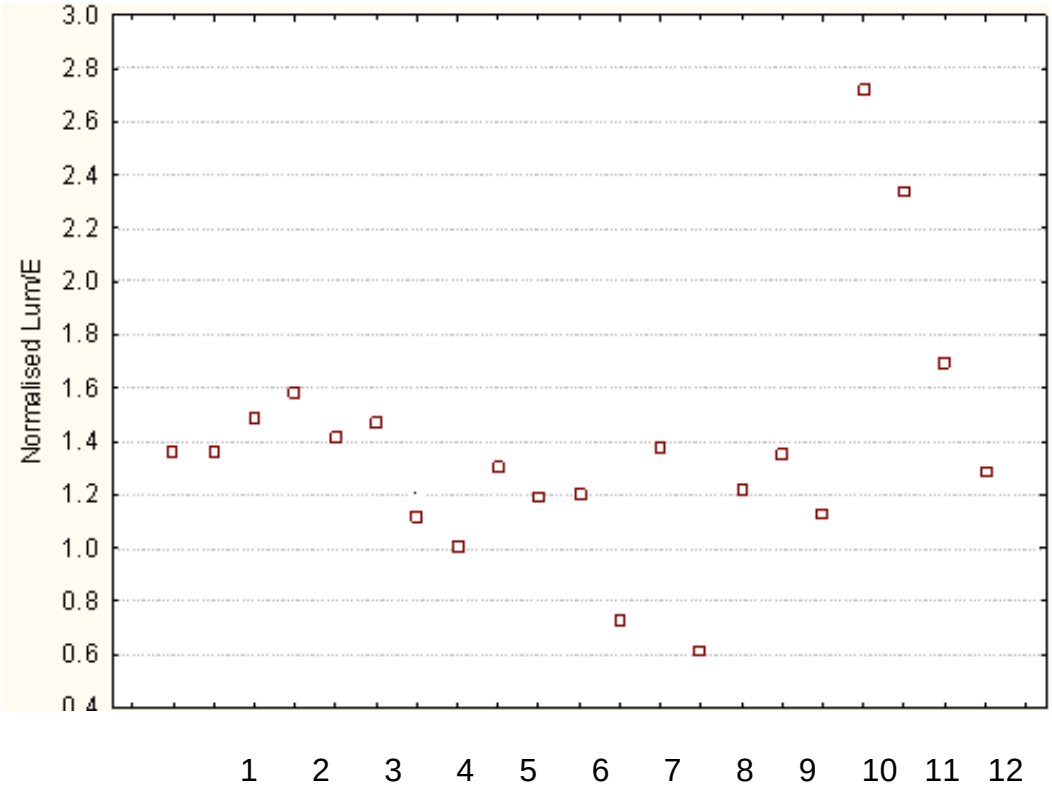

Figure 3.7 Box plot of secreted alkaline phosphate (SEAP) activity normalised to β-galactosidase activity of co-transfected H9C2 human cardiac cells.

The SEAP activity of each experiment was compared to its corresponding control assay as well as the basal control (lane 15) SEAP activity levels using ANOVA. Lane 1 (myomegalin); lane 2 (myomegalin control); lane 3 (obscurin); lane 4 (obscurin control); lane 5 (CD63-antigen); lane 6 CD-63 (antigen control); lane 7 (cytochrome C oxidase subunit 1); lane 8 (cytochrome C oxidase subunit 1 control); lane 9 (thioredoxin 2); lane 10 (thioredoxin 2 control); lane 11 (NADH dehydrogenase subunit 4); lane 12 (NADH dehydrogenase subunit 4 control); lane 13 (SCF apoptosis response protein 1); lane 14 (SCF apoptosis response protein 1 control); each sample and its control are adjacent to each other; lane 15 (negative control – gene juice); lane 16 (positive control – pM3-VP16); lane 17 (pM53 and pVP16-T); lane 18 (basal control); lane 19 (pM-Cx45 and pVP16); lane 20 (SEAP vector); lane 21 (β-gal vector).

3.3 WHOLE EXOME SEQUENCING

WES was used to identify putative PFHBII-causing variants in four PFHBII patients. The total amount of variants identified in each patient ranged between 36 000 and 39 000 (Table 3.9).

After filtration a total of 1258 variants for PID_9862, 1290 for PID_9864, 1324 for PID_9863 and 1240 for PID_9865 were identified as possibly disease-causing. After removing all variants homozygous in either of the parents, only one variant of the remaining variants was located in a functionally relevant gene according to OMIM and NCBI (Table 3.10). The gene associated with this variant was obscurin due to its clinical linkage to dilated cardiomyopathy, of the clinical traits of PFHB II and only this one was investigated further.

Table 3.10: Variants identified in thePFHB II patients after WES.

	PID_9862	PID_9864	PID_9863	PID_9865
Total variants	37668	37263	38520	36653
All synomous and non-frameshifts removed	27348	27026	28029	26482
Remove all variants with a frequency >1 % in 1KGP	26687	26375	27358	25862
Remove all variants with a frequency >1 % in ESP6500	26649	26337	27321	25824
Remove all variants with negative GERP +++ scores	1467	1432	1463	1413
Remove all variants with positive FATHMM scores	293	294	297	299
Novel variants	103	132	117	109
Variants with rs numbers	288	287	291	295

1KGP = 1000 Genomes Project; ESP = Exome Sequencing Project; GERP = Genomic Revolutionary rare profiling; FATHMM = Functional Analysis Through Hidden Markov Models; rs = Reference single nucleotide polymorphism

Table 3.11: Potentially disease causing variant identified in functionally relevant genes in PFHB II patients

Patient	Gene	Heterozygous variants	rs ID
PID_9862	OBSCN	c.2721_2722CA:p.A908T c.2997_2998CA:p.A1000T	rs386640006
PID_9864	OBSCN	c.2721_2722CA:p.A908T c.2997_2998CA:p.A1000T	rs386640006
PID_9865	OBSCN	c.2721_2722CA:p.A908T c.2997_2998CA:p.A1000T	rs386640006

rs IDs: Reference single nucleotide polymorphism cluster identities; OBSCN = obscurin

A potentially disease-causing variant situated in PFHB II-causing genes was identified in three of the investigated patients (Table 3.10), which was found to be heterozygous.

3.4 IN SILICO VARIANT PREDICTIONS

SIFT, MutationTaster2 (MT2) and PolyPhen-2 (PP-2) were used to predict the probability that each identified sequence variant is disease-causing. None of the metrics from the prediction tools used in this study could be obtained for the variant identified in the study, strenghthening the possibility of it being a disease-causing variant.

CHAPTER FOUR: DISCUSSION AND CONCLUSION

4.1 IDENTIFICATION OF CX45 COOH-TERMINAL TAIL LIGANDS BY YEAST TWO-HYBRID (Y2H)

Protein-protein interactions have gained a great deal of attention since most biological functions are regulated by protein interactions and several techniques, such as co-immunoprecipitation, surface plasmon resonance, cytokine-receptor-based interaction trap, Y2H and M2H analyses, for identifying different ligands of chosen proteins have been developed (Fields and Song, 1989; Vasavada *et al*., 1991, Schuk, 1997, Eyckerman *et al*., 2001). The technology has evolved greatly over the years, to also include array-based Y2H whose advantage has been shown to the direct identification of interacting protein pairs without further downstream experiments (Mehla *et a*l., 2015).

4.1.1 Construction of DNA binding target fusion protein choice of bait fragment

Among the different domains of Cx45, the cytoplasmic COOH-terminal domain (150 amino acids) was chosen as the bait fragment because the major differences in amino acid sequence among the different Cxs occur in this domain (figures 1.1 and 4.1), which suggests functional specificity, and because it is known to participate in protein-protein interactions (Goodenough *et al*., 1996; Evans and Martin, 2002). Another domain of the Cx45 protein which could have been used as bait was the cytoplasmic loop, as it is also a region which shows less amino acid sequence homology among the Cx isoforms (Causier, Davies, 2001 and Oyamada *et al*., 2005, 2013), and again may facilitate specific functions. Despite the absence of any reports of its involvement in protein-protein interactions, it may have yielded novel and biologically relevant interactors and could be considered in subsequent screens. The full length Cx45 was not used as bait because the transmembrane domains could possibly have prevented the Cx45-GAL4-DNA-BD proteins from translocating to the nucleus where interaction with GAL4-AD-prey fusion occurs thereby driving transcription of reporter genes occurs in the Y2H technique (Causier, Davies, 2001, Oyamada *et al*., 2005, 2013).

```
Cx40      MGDWSFLGNFLEEVHKHSTVVGKVWLTVLFIFRMLVLGTAAESSWGDEQADFRCDTIQPG    60
Cx43      MGDWSALGKLLDKVQAYSTAGGKVWLSVLFIFRILLLGTAVESAWGDEQSAFRCNTQQPG    60
Cx45    -MSWSFLTRLLEEIHNHSTFVGKIWLTVLIVFRIVLTAVGGESIYYDEQSKFVCNTEQPG      59
Cx40          CQNVCYDQAFPISHIRYWVLQIIFVSTPSLVYMGHAMHTVRMQEK-----------R 106
```

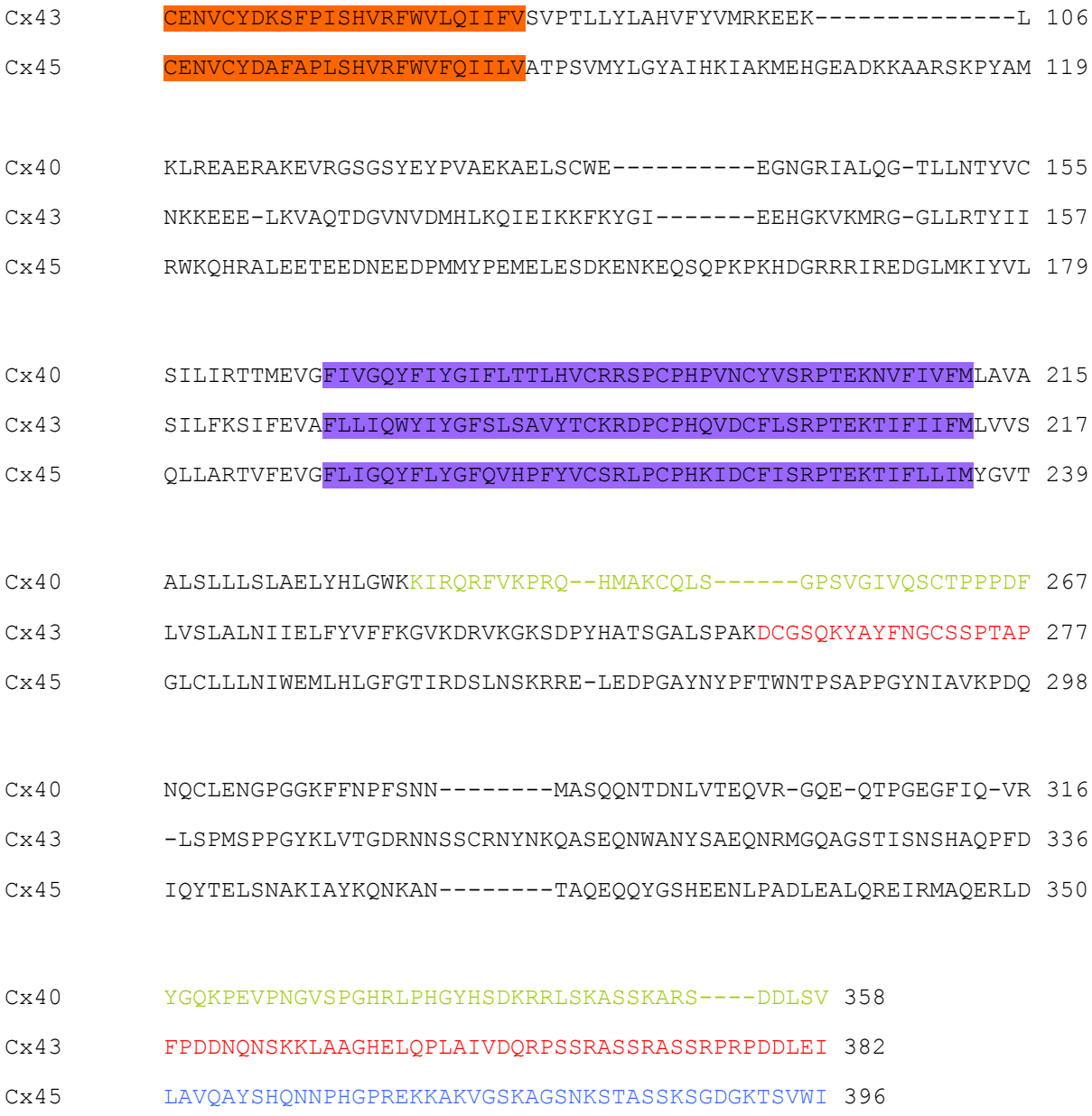

Figure 4.1 Alignments of human connexins

Cx40 (226 to 357 aa), Cx43 (255 to 382 aa) and Cx45 (245 to 396 aa) polypeptides highlighting variations in amino acid sequences among their COOH-termini (in coloured font) as well as regions of high homology; NH_2-termini (highlighted in pink) and extracellular loops 1 and 2 (highlighted in orange and purple, respectively). Multiple sequence alignments were performed by use of the ClustalW BLAST programme.

4.1.2 Phenotype assessment of *S. cerevisiae* strains

It has been reported that bait proteins sometimes interfere with mating if they are highly homologous to proteins involved in yeast mating (Schultz *et al.,* 1995). However, the mating efficiency of *S. cerevisiae* AH109 transformed with the Cx45-pGBKT7 bait construct and *S. cerevisiae* Y187 transformed with pTD1.1 (4.9% shown in table 3.3) was high enough to rule out toxicity due to the presence of the Cx45-bait construct.

4.1.3 cDNA-cardiac library screen

Since the cDNA-cardiac library was constructed from males who died of accident trauma (BD Bioscience, Clontech, Paulo Alto, CA, U.S.A), it is possible that some biologically relevant protein interactions were not screened for, as some proteins may have not been expressed at time the RNA was extracted. However, the proteins identified in this study (table 3.6) give an indication of the possible interactions of Cx45 with other proteins and enabled us to make an initial assessment of the range of specific and overlapping roles played by the selected Cxs.

4.1.4 Clones excluded from or included in M2H analysis

Clones excluded from further verification studies by M2H analysis included sequenced prey clones encoding proteins likely to be expressed at locations where an interaction with a Cx would be unlikely, such as the nucleus and the extracellular matrix (table 3.4). Initially in this study, mitochondrial proteins, such as NADH dehydrogenase subunit 4, cytochrome C oxidase and thioredoxin 2, would have been omitted as putative candidate ligands of Cx45, on the rationale that these mitochondrial proteins form part of a list of known false positives (which includes ribosomal proteins, cytochrome oxidase, mitochondrial proteins, proteasome subunits, ferritin, tRNA synthase, Zn finger proteins, vimentin) that are frequently found in a Y2H screen, independent of the bait used (van Criekinge, Beyaert, 1999 and Lievens *et al*., 2009). However, they were thereafter prioritised based on findings from a recent study by Boengler and colleagues (2005) who presented evidence for the presence of Cx43 in the mitochondrial matrix, near the inner membrane, suggesting another as yet unidentified role for Cxs other than cell-cell communication.

In addition to identifying the ligands, sequence homology and BLAST searches allowed the determination of likely subcellular localisations, constituent domains and

the biological relevance of the putative ligands; all features significant in the prioritisation of the ligands. Furthermore, the number of clones identified as the same protein was assumed to be suggestive of the importance of the interaction, as in the case of cytochrome C oxidase (table 3.9).

It was also intriguing to note that out of the six randomly chosen clones sequenced for comparative purposes; four (clone 21, 102, 139 and 234), showed significant interaction. In fact, all four had a strong interaction with Cx45, and a slight interaction with other preys. Clones 154 and 157, both strongly interacting with all four preys in the specificity assay (table 3.7) gave insignificant BLAST results, which further warranted their exclusion as Cx45 interactors.

4.1.5 Proteins prioritised as possible Cx45 ligands

The candidature of each of the seven prioritised putative ligands of Cx45 will be discussed, with a focus on the arrangement of the constituent domains, their possible relevance in Cx interactions and their potential involvement in cardiac function. These putative ligands of the Cx45 COOH-terminal domain ranged from mitochondrial to cytoplasmic proteins (Table 3.9) and were identified as thioredoxin 2, NADH dehydrogenase subunit IV, cytochrome C oxidase subunit I, SCF apoptosis response factor 1, *Homo sapiens* CD63 antigen, phosphodiesterase 4D interacting protein (also known as myomegalin) and obscurin-RhoGEF (also known as myosin light chain kinase). It is interesting to note that through whole exome sequencing (WES), obscurin was identified as a potential PFHB II causative gene.

A. Thioredoxin 2 (TRX2)

Thioredoxin 2, a mitochondrial inner membrane protein which belongs to the thioredoxin family, is a member of a class of small multifunctional 12kDa proteins present in both prokaryotes and eukaryotes. They control cellular redox states and protect the cell against oxidative damage. Thioredoxins are characterised by the redox active site Trp-Cys-Gly-Pro-Cys. Mammalian TRX2, a potential ligand of Cx45, is encoded by a nuclear gene but is directed to the mitochondrion by an NH_2-terminal mitochondrial presequence (Smeets *et al*., 2005, Lee *et al*., 2013). Spyrou and co-workers showed that recombinant rat liver TRX2 possessed dithiol-reducing activity. In the presence of thioredoxin reductase and NADPH, TRX2 reduced the interchain disulfide bridges of insulin, a well-known thioredoxin test substrate

(Spryrou *et al*., 1997). Based on the interaction of TRX2 and the disulfide bridges of insulin, it is tempting to speculate that Cx45 interacts with TRX2, as connexons are joined by disulfide bonds. However, since only the COOH-terminal domain of the *Cx* sequence was used as bait, and although this interaction may occur *in vivo*, it cannot underlie the bait:prey interaction in Y2H, as no disulphide bonds were present in the bait.

Nonetheless, Damdimopoulos and colleagues (2002, Huang *et al*., 2015) showed that human embryonic kidney cells over-expressing TRX2 were resistant to cell death caused by etoposide, a topoisomerase II poison, and more sensitive to rotenone, an inhibitor of complex I of the mitochondrial respiratory chain. Over-expression of TRX2 in this cell system also seemed to increase the mitochondrial membrane potential. Furthermore, treatment with oligomycin (an inhibitor of ATP synthase) reversed the effect of rotenone and decreased the membrane potential, suggesting that TRX2 interferes with the activity of ATP synthase. Consequently, Damdimopoulos *et al*. (2002, Huang *et al*., 2015) concluded that TRX2 interacts with specific components of the mitochondrial respiratory chain and plays a role in the regulation of the mitochondrial membrane potential.

Thus, TRX2, as an electron carrier involved in regulating membrane potential, can be suggested to interact with the COOH-terminal domain of Cx45. Although the mechanism through which this interaction occurs and relevance thereof are not clear, it is possible that the two proteins work closely in regulating energy potential in cells, particularly cardiac cells.

B. NADH dehydrogenase subunit IV (NADH IV)

NADH dehydrogenase subunit IV (NADH 1V) is one of seven transmembrane subunit components of the NADH ubiquinone oxidoreductase (NQO) complex I (Shoffner and Wallace, 1995, Arizmendi *et al*., 1992; Wallace *et al*., 1994) located in the mitochondrial outer membrane. This reductase complex I accepts electrons from NADH, transfers them to ubiquinone (coenzyme Q10) and uses the energy released to pump protons out across the mitochondrial inner membrane. NADH dehydrogenase subunit IV is thought to be the part of hydrophobic component of complex I (Powis and Montfort, 2001).

The function of the putative interaction between NADH dehydrogenase subunit IV and Cx45 is not understood. However, findings from a study presented by Boengler

and colleagues in 2005, where they found traces of Cx43 in the mitochondrial matrix near the inner membrane can be extrapolated to suggest another function of Cx45, apart from cell-cell communication. It is also not clear how the Cx isoform is imported into the mitochondrial matrix but it could be speculated to be through the action of translocases which present cytosolic proteins to mitochrondrial receptors and transport them further into the mitochondrial matrix though a series ATP-dependant reactions as shown in figure 4.2 (Mokranjac and Neupert, 2005).

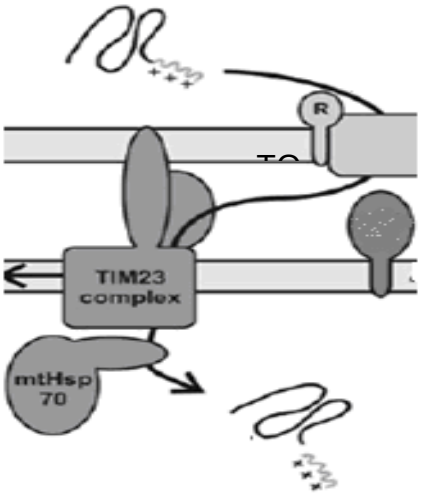

Figure 4.2 Proposed mechanism of protein import into the mitochondrion.

Receptors within the membrane-integrated TIM23 (translocase of the inner membrane) complex recognise the precursor proteins as they appear at the outlet of the TOM (translocase of the outer membrane) complex which then delivers them to the translocation channel. The motor part of the complex then takes the presequence as it enters the matrix face of the translocation channel to the mitochondrial heat shock protein (mtHsp70) via through a series of ATP-dependant reactions after which the protein is released into the mitochondrial matrix (adapted from Mokranjac and Neupert, 2005).

The p49/STRAP (or SRFBP1) proteins was also identified as a cofactor of serum response factor that contributes to the regulation of SRF target genes in the heart (Zhang et al., 2008).

C. Cytochrome C oxidase subunit I

Cytochrome C oxidase subunit I is one of three mitochondrial DNA-encoded subunits of respiratory complex IV, located within the mitochondrial inner membrane. Complex IV is the third and final set of enzymes of the electron transport chain of mitochondrial oxidative phosphorylation. It collects electrons from reduced cytochrome C oxidase and transfers them to oxygen to create water. The energy released is used to transport protons across the mitochondrial inner membrane. Complex IV is composed of 13 polypeptides. Subunits I, II, and III are encoded by mtDNA**,** while subunits IV, Va, Vb, VIa, VIb, VIc, VIIa, VIIb, VIIc, and VIII are nuclear-encoded (Kadenbach *et al.*, 1983; Shoffner and Wallace, 1995).

Proton translocation in Complex IV involves four electrons to reduce oxygen and four protons taken up from the matrix side of the mitochondrial membrane for the formation of water. Four more protons are vertically translocated from the matrix to the cytosolic side of the membrane. Evidence is accumulating that proton translocation is linked to electron transfer at the binuclear oxygen binding site, which has been extended to suggest that proton translocation is associated with proximal ligand exchange between tyrosine and histidine on cytochrome a3 (Rousseau *et al.*, 1993).

Cytochrome C oxidase has been associated with the development of cardiovascular disease. Wisloff and colleagues (2005) hypothesised that artificial selection of rats based on low and high intrinsic exercise capacity would yield models that also differed for cardiovascular disease risk. Indeed, after eleven generations, rats with low aerobic capacity scored higher on cardiovascular risk. The decrease in aerobic capacity was associated with decreases in the amounts of transcription factors required for mitochondrial biogenesis and in the amounts of oxidative enzymes in skeletal muscle. Wisloff et al. (2005) found that the amounts of peroxisome proliferative activated receptor, gamma (PPARG) coactivator-1-alpha, ubiquinol-cytochrome C oxidoreductase core 2 subunit, cytochrome C oxidase subunit I, uncoupling protein-2, and ATP synthase H+-transporting mitochondrial F1 complex were markedly reduced in the low capacity runner rats in comparison with the high capacity runners. The decline in these proteins was consistent with the hypothesis that reduced aerobic metabolism plays a causal role in the development of the differences between the low capacity runner and high capacity runner rats. It was thus concluded that impairment of mitochondrial function, as a result of sequence variants in genes encoding proteins that regulate pathway that facilitate mitochondrial processes, may be associated with reduced fitness in cardiovascular and metabolic disease (Wisloff et al. 2005). It can therefore be proposed that Cx45,

as one of the prominent cardiac Cx isoforms, is involved as a ligand in processes in which cytochrome C oxidase functions.

D. SCF (stem cell factor) apoptosis response protein 1

The SCF apoptosis response protein 1 is a cytoplasmic protein which is mainly composed of the dysbindin domain, which binds to alpha- and beta-dystrobrevins, components of the dystrophin-associated protein complex in both muscle and non-muscle cells. Dysbindin itself is a component of the biogenesis of lysosome-related organelles complex 1. SCF apoptosis response protein 1 is involved in migration, adhesion, proliferation and survival of germ cells by prtecting them from apoptosis. It is also central in blood-forming tissue where Cx43 and Cx45 were found to also play a regulatory role in blood coagulation (Rosendaal and Krenacs, 2000; Cancelas *et al.,* 2000). SCF apoptosis response protein 1 has been associated with Hermansky-Pudlak syndrome (HPS), a genetically heterogeneous disorder characterised by oculocutaneous albinism, prolonged bleeding and pulmonary fibrosis due to abnormal vesicle trafficking to lysosomes and related organelles, such as melanosomes and platelet dense granules (Hoffman and Valencia, 2004). The involvement of SCF apoptosis in migration and adhesion and its putative association with Cx45 suggest a role of Cx45 in exporting molecules from the cell, working as part of a multiprotein complex.

E. CD63-antigen

The CD63-antigen is a glycoprotein expressed strongly during early stages of tumour progression. It has four transmembrane domains and three N-glycosylation sites and has been associated with membrane structures (Metzelaar *et al*., 1998) and Hermansky-Pudlak syndrome (HPS), as has SCF apoptosis response protein 1.

Nishibori and colleagues (1993) used immunofluorescence with anti-CD63 and anti-granulophysin antibodies to demonstrate deficiency of these proteins in HPS and was the first to report a protein present in platelet dense granules, lysosomes, and melanocytes, but deficient in a patient with HPS. Clarification as to whether deficiency in CD63 is the primary defect in HPS still needs to be determined in patients with this disorder. That the primary defect resides in the CD63 gene was made unlikely by the demonstration by Fukai *et al.* (1995) that the HPS gene maps to chromosome 10, not chromosome 12, where CD63 lies.

Gwynn et al. (1996) found that the cDNA encoding mouse CD63 detects two closely-related sequences that map to different regions of the mouse genome. One locus maps to mouse chromosome 10, in a region that shares synteny with chromosome 12, where human CD63 maps. The second locus maps to mouse chromosome 18 in a region that bears no homology to known human CD63-related genes. No platelet storage pool deficiency disorder has been mapped to these regions of either mouse chromosome 18 or human chromosome 12. The association between Cx45 and CD63 is illusive, but it may be speculated to be linked to the CD63-antigen in the same fashion that SCF apoptosis response protein 1 interacts with this Cx isoform, ie., as part of a multicellualr complex. It is intriguing to discover that Cx45 has a possible association with two different proteins involved in the same disorder which could be due to the specificity of the function of this Cx isoform.

F. Phosphodiesterase 4D interacting protein also known as myomegalin

Myomegalin is a protein which interacts with 3, 5 cyclic adenosine monophosphate (cAMP) phosphodiesterase (Verde *et al*. 2000). Phosphodiesterases, myomegalin interactors, generally regulate the local concentration of cAMP within cells, ultimately activating the cAMP-dependent protein kinase (PKA) which signals cellular compartmentalisation (Huston *et al*., 2006). The interaction of Cx45 with myomegalin suggests a possible role of myomegalin as a scaffolding protein in the phosphorylation of Cx45 by cAMP dependant kinase.

It is interesting to note that phosphodiesterase inhibitors have been linked to heart failure and cardiac arrhythmias in mice. Additionally, phosphodiesterase knock-out mice have been reported to present dilated hearts with normal muscle structure, a clinical feature present in DCM patients (as reviewed by Lehnart *et al.*, 2005). It is also possible that Cx45, along with myomegalin, plays a role in the development of cardiac disorders particularly due to the involvement of myomegalin in cAMP regulation, an important step in ATP generation. Myomegalin was also found to be involved in the phosphorylation of cardiac myosin binding protein C (Uys *et al.*, 2011).

G. Obscurin

Obscurin is an interesting candidate as it was first identified as a Cx 45 ligand through Y2H studies and later shown through WES to be a potential causative gene

for PFBH II. Obscurin has been somewhat neglected as a potential player in the development of cardiomyopathies, largely because its functional role is far from clear. The development of WES enabled researchers to look into the function of this protein as well as the various roles it plays in the development of inherited cardiomyopathies.

The obscurin gene, expressed in both both cardiac and skeletal muscles, is located on chromosome 1.42q13 and spans more than 150 kb and contains over 80 exons that encode a protein of approximately 720 kDa (Bowman *et al*. 2007; Fukuzawa *et al.* 2008; Kontrogianni-Konstantopoulos *et al*. 2006; Shriver *et al*. 2015). The encoded protein contains 68 Ig domains, two fibronectin domains, one calcium/calmodulin-binding domain, one Rho guanine nucleotide exchange factor (GEF) domain with an associated PH domain, and two serine-threonine kinase domains. This protein belongs to the family of giant sarcomeric signaling proteins that includes titin and nebulin, and it is speculated that these proteins may have a role in the organisation of myofibrils during assembly and may mediate interactions between the sarcoplasmic reticulum (SR) and myofibrils. Obscurin surrounds the myofibrils at the level of Z-disk and M-band, where it is suitably positioned to participate in their assembly and integration with the elements of the SR. In fact, studies by Kontrogianni-Konstantopoulos *et al.* (2006, 2014) showed obscurin to indeed play a role in the assembly and organisation of the sarcomeres and sarcoplasmic reticulum. The importance of its COOH-domain was also discovered in this study. Obscurin is also suggested to serve as a kinase anchor protein. It could play a role in the phosphorylation of Cx45 by cAMP dependant kinase, which normally requires a scaffolding protein such as obscurin (Wei *et al*., 2004).

Obscurin has been found to interact with various ligands suggesting diversity in its functional role. Within the sarcomere at the level of the M-band, mammalian obscurins interact with titin, myomesin, ankyrin-B, Ras homolog gene family, member A (RhoA), and slow skeletal myosin binding protein C variant 1 (sMyBP-Cv1) (Perry *et al*. 2013). In C. elegans at the M-band, UNC-89 interacts with copine domain protein atypical-1 (CPNA-1), UNC-15 (paramyosin), small CTD-phosphatase-like-1 (SCPL-1), four and a half LIM domains protein 9 (LIM9/FHL), maternal effect lethal 26 (MEL-26), and Rho1 (Gieseler *et al*. 2016; Qadota *et al*. 2008; Warner *et al*. 2013; Wilson *et al*. 2012) and Drosophila obscurins interact with Ball and multiple Ankyrin repeats single KH domain (MASK) at the M-band

(Katzemich *et al*. 2015). In addition, mammalian obscurins interact with the NH2-terminus of titin and Ran-binding protein 9 (RanBP9) at Z-discs (Bowman et al. 2008), small ankyrin- 1 at the SR (Kontrogianni-Konstantopoulos *et al*. 2003), and ankyrin-B at costameres (Randazzo *et al*. 2013). At the ID of mammalian cardiac muscle, obscurin polypeptides interact with N-cadherin and Na+/K+ ATPase (Hu and Kontrogianni- Konstantopoulos, 2013).

Other ligands of mammalian obscurins include calmodulin and calcium/calmodulin-dependent protein kinase I (CaMKII), both of which promiscuously localize throughout myocytes; consequently, the location and function of the interaction between obscurins and these proteins remain elusive. Calmodulin interacts with the IQ motif of obscurins, which localizes to M-bands of developing and adult heart and skeletal muscles, as well as to the sarcolemma and neuromuscular junction of skeletal muscles (Carlsson et al. 2008).

The obscurin variants found so far seem to be distributed throughout the molecule (figure 4.3), mostly with no apparent connection to any functional domain. Arimura *et al*. (2007) have proposed that the R4344Q mutation affects binding of obscurin to Z-line titin (domains Z9-Z10), and Marston *et al*. (2015) noted obscurin haploinsufficiency but did not measure any functional properties. The best clues to the physiological function of obscurin are provided by the obscurin knockout mouse model (Lange *et al*. 2009); however, the effects of knockout have only been fully studied in skeletal muscle rather than in cardiac muscle and no cardiac defect was reported. In skeletal muscle, absence of obscurin results in disorganisation of microtubules at the sarcolemma and delocalisation of dystrophin at costameres. More striking abnormalities appear with intense exercise, including fibre damage, atrophy and degeneration which revert when exercise is stopped (Randazzo *et al*. 2017). It was proposed that the absence of obscurin causes the failure of the muscle sarcolemma to support the mechanical stress of intensive chronic contraction. In the heart, this may be manifested as development of a hypo-contractile heart under stress which could trigger DCM.

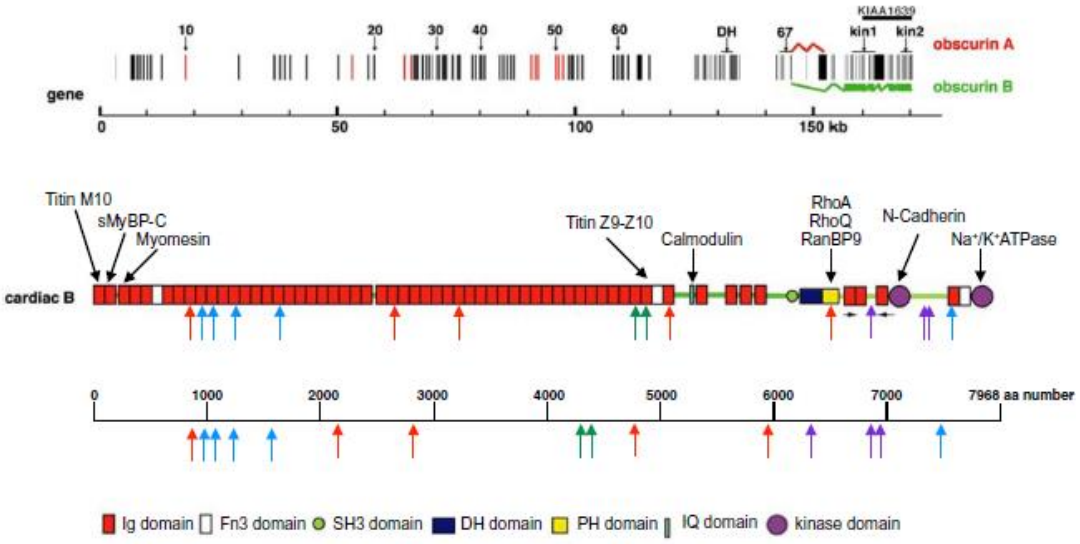

Figure 4.3: Obscurin structure and cardiomyopathy-associated mutations.

Top gene structure, showing the exons and alternative splicing that yields obscurin A or B. Middle schematic domain structure of obscurin B. Adapted from Marston (2017).

4.1.6 Limitations of the Y2H method

Despite the isolation and identification of putative ligands of Cx40 in the present study, some caveats of the methodology must be considered. Since in Y2H analysis, combinations of protein-protein interactions are assayed, the possibility of identifying artefactual partners exists. It is also possible that both proteins (bait and prey), although able to interact in the Y2H assay, are never in close proximity to each other within the cell. The two proteins could be expressed in different cell types, or even when found in the same cell they could be localised in different subcellular compartments. Moreover, interacting proteins can be expressed at different time points in the cell cycle (Greener and Perkel, 2005), giving a false impression of interactions occurring in physiological systems. For this reason, further assays were undertaken in an attempt to strengthen the candidature of the selected ligands.

4.2 MAMMALIAN TWO-HYBRID (M2H) ANALYSIS

M2H was the method chosen to verify the putative interactions between the Cx bait and selected preys. However, in the present study, the high SEAP activity in the negative controls (figure 3.7) is inexplicable and has made it impossible to derive any statistical correlations between the regions encoding the Cx45 COOH-terminal

domain and identified putative ligands. The higher SEAP activity in the controls can be speculated to be due to cellular endogenous phosphate or experimental error. Another contributory factor could be the cell line used. A cardiac myocyte cell line (H9C2) was used, as the aim was to mimic the *in vivo* cardiac milieu as far as possible. However, these cells proved difficult to transfect, a problem that was encountered by other workers in the group. Thus further studies were therefore needed, either to optimise transfections with this line, or to investigate use of another cell line. It may also be necessary to conduct further assays such as co-immunoprecipitation and surface plasmon resonance, among others, in order to verify the authenticity of protein interactions identified (Phizicky and Fields, 1995; Wu and Brand, 1994; Wilson and Hastings, 1998). However, due to time constraints we were unable to conduct these verifications.

As highlighted in the previous section, the M2H method also does not offer all the answers to protein interactions as it is also reliant on interactions occurring in nucleus and on GAL4 domains.

4.3 A SPECULATIVE MODEL OF CX45 PROTEIN-PROTEIN INTERACTIONS AND FUNCTIONAL SPECIFICITIES IN RELATION TO CX40 AND CX43

Based on the prioritised Cx45 ligands, described above, it can be speculated that this isoform participates in a number of physiological processes, ranging from energy transport in cells to blood coagulation. Just like Cx43 (Wei *et al*., 2004), it can function as a member of a multi-protein network in energy production required in cardiac function (section 1.1.5.1). Its proposed interaction with proteins such as myomegalin and obscurin further supports this assumption, as these proteins serve as scaffolding or anchoring proteins for kinases. Additionally, it can be deduced that these interactions, although not specific, play a role in the gating of Cx45 channels.

It is also interesting to note the distribution of Cx 45 throughout the heart. Its prominence in the atrioventricular node and the Purkinje Fibres suggests an association with the development of PFHB II whose other clinical characteristic is complete heart block at an atrioventricular nodal level. The Purkinje Fibres, influenced by the electrical discharge from the SA node could also be affected by Cx 45 protein interactions and can contribute to the development of cardiac diseases

such as PFHB II. The newly found association of Cx 45 with obscurin is worth investigating further.

As the above findings are based on Cx43 studies, it is possible that the two isoforms, Cx43 and Cx45, have overlapping roles. Co-localisation of Cx43 with blood coagulation factors such as SCF apoptosis response protein 1, and the newly proposed association of SCF apoptosis response protein 1 with Cx45 in the present study, also suggests that these two cardiac Cxs have similar cellular functions. The association of both SCF apoptosis response protein 1 and CD63-antigen in HPS also suggests that the two proteins share functional roles, especially since they both interact with Cx45 (Nishibori *et al*.; 1993; Hoffman and Valencia, 2004).

Based on the organisation of the constituent domains of the mitochondrial proteins prioritised (thioredoxin 2, NADH dehydrogenase subunit 4 and cytochrome C oxidase), it can be speculated that these ligands interact with Cx45 in a similar manner. Connexin 45 possibly recognises the transmembrane domain (present in all three identified mitochondrial proteins) to adhere to the target protein, and by fusing its COOH-terminus with the NH_2-terminus of the mitochondrial protein, it is transported into the mitochondrial matrix (Wilcox *et al.*, 2005). Additionally, since these mitochondrial proteins play a major role in energy production via the electron transport chain, and that energy production is an integral part in cardiac function, it can be speculated that Cx45 as part of the gap junction channel co-facilitates the electron transport with these ligands. Although the mechanism through which these protein interactions affect cardiac function is unknown, it also tempting to assume that they may contribute to the aetiology of some cardiac disorders.

It is also evident that Cxs have specific functions, as assessed in a study by R. Keyser (Identification of ligands of cardiac Cx40 and their possible association with the development of the cardiac conduction disorders, progressive familial heart block type I and type II [PFHBI and PFHBII]), where ligands of the COOH-terminal domain of cardiac Cx40 were identified. In fact, Cx40 was found to interact mostly with cytoplasmic proteins. However, the possibility of shared functions between the two cardiac Cxs (Cx40 and Cx45) can not be totally excluded, as Cx40 was found have an interaction with NADH dehydrogenase subunit 6 (R. Keyser, 2007, MSc Thesis – University of Stellenbosch Keyser, 2007). NADH dehydrogenase subunit 6 is part of

the NADH dehydrogenase complex which also consists of NADH dehydrogenase subunit 4 (figure 4.2), a putative ligand of Cx45 (unpublished data - Nxumalo, 2018).

4.4 PFHBII POTENTIAL CANDIDATE GENES – THE SEARCH CONTINUES

Another facet of this study was to investigate if the identified ligands play a role in the development of PFHBII. In spite of the reports linking mutations in genes that encode ion channels (Benson, 2004), energy metabolism proteins (Blair *et al*., 2001) and cardiac structural proteins to the development of cardiac conduction disorders, none of the ligands identified in this study showed a possible association with either of these disorders through chromosomal position.

BLAST-searches indicated that the ligands (which included energy metabolism proteins such NADH dehydrogenase subunit IV, cytochrome C oxidase subunit I and thioredoxin II and cardiac structural proteins – myomegalin and obscurin) did not lie in the locus ofPFHBII. It is possible that mutations in other proteins that interact closely with these ligands are involved as cause of this disorder. It is possible that future cascade studies may identify them.

Interestinglythe PFHBI gene was identified in a collaboration between our group and two groups in Germany (Corfield personal communication- 2007). Of significance is the fact that the candidate gene was indirectly identified in astudy conducted by R Keyser (*Identification of ligands of cardiac Cx40 and their possible association with the development of the cardiac conduction disorders, progressive familial heart block type I and type II [PFHBI and PFHBII],*by its functional homology to a putative ligand of Cx40. This data validates the strategy applied in thisstudy to identify new PFHB II candidate genes.

All the recent studies on obscurin variants have involved whole exome sequencing with the unique variants being identified by comparison with large reference databases, such as Exacs and EVS, and their pathogenicity predicted using algorithms such as SIFT. This approach, based on small populations, may be biased in patient ethnicity and other factors. It is recognised that such conclusions may give a false positive association of disease with variants especially in a large protein (Walsh *et al*. 2017). Variants that cause chain termination, as found in the Rowland *et al*. (2016) and Xu *et al*. (2015) studies, are more likely to be pathogenic than missense mutations; however, none of the current studies on OBSCN variants have

any family history showing the variant segregating with the disease, which is required to confirm causality. The only study that has directly investigated the obscurin molecule in heart muscle with identified mutations was Marston *et al*.'s (2015) study of familial DCM; where obscurin haploinsufficiency was demonstrated for all the obscurin variant samples compared with familial DCM with mutations identified in other genes or in donor heart samples (Marston, 2017). This, therefore, increases the confidence that obscurin variants and familial DCM are linked in this particular group of samples from patients who had transplants for end-stage heart failure. It would be beneficial to screen PFHBII patients for obscurin variants, particularly due the gene's clinical linkage to DCM.

Conclusion

The array of putative Cx45 ligands identified in this study suggests a diversity of processes in which Cxs participate apart from cell-cell communication. The unexpected interaction of the COOH-terminal domain of Cx45 with mitochondrial proteins further shows that the role of Cxs in cellular and physiological processes is not fully understood. Although cardiac proteins were identified, it was however difficult to make a direct link between these proteins and the development of cardiac conduction disorders. Therefore, more studies need to be conducted in order to further elucidate the function of Cxs, as channel proteins and possibly regulatory proteins, in physiological processes and in the development of physiological disorders – including cardiac conduction disorders- either directly through these proteins themselves, or through their ligands. In the absence of additional data, we cannot exclude the possibility that the observed variants are simply bystander effects and that the true disease-causing mutation is elsewhere. Despite limited investigations, mutations in the obscurin gene are emerging as significant in a range of cardiomyopathies. Obscurin mutations may be causative of HCM, DCM and LVNC and other cardiomyopathies such as PFHBII, or they may work in concert with other variants in the same or other genes to initiate the pathology.

APPENDIX I

1. DNA EXTRACTION SOLUTIONS

Cell lysis buffer

Sucrose	0.32M
Triton-X-100	1%
$MgCl_2$	5mM
Tris-HCl	10mM
H_2O	1L

3M NaAc

$NaAc.3H_2O$ (Merck)	40.18g
ddH_2O	50ml

Adjust pH to 5.2 with glacial acetic acid and adjust volume to 100ml with ddH_2O

DNA extraction buffer

NaCl	0.1M
Tris-HCl	0.01M
EDTA (pH8)	0.025M
SDS	0.5%
Proteinase K	0.1mg/ml

T.B.E-BUFFER (10x stock)

Tris-HCl	0.89M
Boric Acid	0.89M
Na_2EDTA (pH8)	20Mm

2. BACTERIAL PLASMID PURIFICATION SOLUTIONS

Cell Resuspension Solution

50mM Tris-HCL, pH 7.5	2.5ml 1M Tris
10mM EDTA	1ml 0.5M EDTA

Make up to 50 ml with H2O

Cell lysis solution

0.2M NaOH	2.5ml 4M NaOH
1% SDS	5ml

Make up to 50ml with H2O

Nutralization solution

1.32M KOAc, pH 4.8	13.2ml 5M KOAc

Make up to 50ml with H2O

3. YEAST PLASMID PURIFICATION SOLUTIONS

Yeast lysis buffer

SDS	1%
Triton X-100	2%
NaCl	100mM
Tris (pH8)	10mM
EDTA (pH8)	1mM

4. ELECTROPHORESIS SOLUTIONS

10% Ammoniumpersulphate (APS)

APS	10g
ddH_2O	100ml

T.B.E-Buffer (10x stock)

Tris-HCl	0.89M
Boric Acid	0.89M
Na_2EDTA (pH8)	20mM

T.A.E Buffer

Tris-HCl	0.89M
Boric Acid	0.89M
Na_2EDTA (pH8)	20mM

SDS-Page esolving gel buffer (4x)

Tris base	109.2g
ddH_2O	330ml
10%SDS	24ml

pH to 8.8 using 1N HCL

Make up to 600ml using ddH_2O

5. LOADING DYES

Bromophenol blue

Bromophenol blue	0.2% (w/v)
Glycerol	50%
Tris (pH8)	10mM

6. MOLECULAR SIZE MARKER (LAMBDA *Pst*I)

Bacteriophage Lambda DNA (250μg)	100μl
Buffer M (Boerhinger Mannhein)	15μl
*Pst*I (Boerhinger Mannheim)	11μl
H_2O	32μl

Incubate at 37°C for 2 hours followed by heat inactivation at 65°C for 5 minutes. Load 2μl onto polyacrylamide gels.

7. PCR BUFFER

10x NH_4 PCR buffer (BIOLINE U.K.)

Ammonium sulphate	160mM
Tris-HCl (pH 8.8)	670mM
Tween-20	0.1%

8. SOLUTIONS USED FOR THE ESTABLISHMENT OF BACTERIAL COMPETENT CELLS

CAP buffer:

60 mM $CaCl_2$	2.21 g
15% glycerol	37.5ml
10mM PIPES	0.76 g

Make up to 250ml with sterile millipore H_2O. pH to 7.0. Keep in fridge.

9. BACTERIAL MEDIA

Luria-bertani (LB) media

Bacto tryptone	5g
Yeasy extract	2.5g

NaCl	5g

ddH_2O to final volume of 500ml

Autoclave at 121 for 20min and appropriate antibiotic (ampicillin, 25mg/ml; Kan 5mg/ml) to media when a temperature of >55°C is reached.

LB agar plates

Bacto tryptone	5g
Yeasy extract	2.5g
NaCl	5g
Agar	8g

ddH_2O to final volume of 500ml

Autoclave at 121°C for 20min and appropriate antibiotic (ampicillin, 25mg/ml; Kan 5mg/ml) to media when a temperature of >55°C is reached, prior to pouring plates.

10. YEAST MEDIA

YPDA media

Difco peptone	10g
Yeast extract	10g
Glucose	10g
L-adenine hemisulphate (0.2% stock)	7.5ml

Autoclave at for 121°C 15min

YPDA agar

Difco peptone	10g
Yeast extract	5g
Glucose	10g
Bacto agar	10g
L-adenine hemisulphate (0.2% stock)	7.5ml

Autoclave at 121°C for 15min and allow to cool to approximately 55°C prior to pouring plates.

SD^{-Trp} media

Glucose	12g
Yeast nitrogen base without amino acids	4g
SD^{-Trp} amino acid supplement	0.4g
0.2% adenine hemisulphate	9ml

ddH_2O to a final volume of 600ml

Autoclave at 121°C for 15min.

SD^{-Trp} plates

Glucose	12g
Yeast nitrogen base without amino acids	4g
SD^{-Trp} amino acid supplement	0.4g
Bacto agar	12g
0.2% adenine hemisulphate	9ml

ddH_2O to a final volume of 600ml

Autoclave at 121°C for 15min and allow to cool to approximately 55°C prior to pouring plates.

SD^{-Leu} media

Glucose	12g
Yeast nitrogen base without amino acids	4g
SD^{-Leu} amino acid supplement	0.4g
0.2% adenine hemisulphate	9ml

ddH_2O to a final volume of 600ml

Autoclave at 121°C for 15min.

SD^{-Leu} plates

Glucose	12g
Yeast nitrogen base without amino acids	4g
SD^{-Leu} amino acid supplement	0.4g
Bacto agar	12g
0.2% adenine hemisulphate	9ml

ddH$_2$O to a final volume of 600ml

Autoclave at 121°C for 15min and allow to cool to approximately 55°C prior to pouring plates.

SD$^{-Leu-Trp}$ media

Glucose	12g
Yeast nitrogen base without amino acids	4g
SD$^{-Leu-Trp}$ amino acid supplement	0.4g
0.2% adenine hemisulphate	9ml

ddH$_2$O to a final volume of 600ml

Autoclave at 121°C for 15min.

SD$^{-Leu-Trp}$ plates

Glucose	12g
Yeast nitrogen base without amino acids	4g
SD$^{-Leu-Trp}$ amino acid supplement	0.4g
Bacto agar	12g
0.2% adenine hemisulphate	9ml

ddH$_2$O to a final volume of 600ml

Autoclave at 121°C for 15min and allow to cool to approximately 55°C prior to pouring plates.

TDO media

Glucose	12g
Yeast nitrogen base without amino acids	4g
$SD^{-Leu-Trp-His}$ amino acid supplement	0.4g
0.2% adenine hemisulphate	9ml

ddH_2O to a final volume of 600ml

Autoclave at 121°C for 15min.

TDO plates

Glucose	12g
Yeast nitrogen base without amino acids	4g
$SD^{-Leu-Trp-His}$ amino acid supplement	0.4g
Bacto agar	12g
0.2% adenine hemisulphate	9ml

ddH_2O to a final volume of 600ml

Autoclave at 121°C for 15min and allow to cool to approximately 55°C prior to pouring plates.

QDO media

Glucose	12g
Yeast nitrogen base without amino acids	4g
$SD^{-Leu-Trp-His-Ade}$ amino acid supplement	0.4g
0.2% adenine hemisulphate	9ml

ddH_2O to a final volume of 600ml

Autoclave at 121°C for 15min.

QDO PLATES

Glucose	12g
Yeast nitrogen base without amino acids	4g

$SD^{-Leu-Trp-His-Ade}$ amino acid supplement	0.4g
Bacto agar	12g
0.2% adenine hemisulphate	9ml

ddH_2O to a final volume of 600ml

Autoclave at 121°C for 15min and allow to cool to approximately 55°C prior to pouring plates.

11. EUKARYOTIC CELL CULTURE MEDIA

Complete growth media

DMEM	90ml
Hams F12	90ml
Foetal calf serum	20ml

Serum-free media

DMEM	100ml
Hams F12	100ml

APPENDIX II

CALCULATING YEAST MATING EFFICIENCIES

Count number of colonies on all plates with 30-300 colonies after 4 days

$$\#\text{colony forming units (cfu)/ml} = \frac{\text{cfu} \times 1000\mu\text{l/ml}}{\text{volume plated (µl)} \times \text{dilution factor}}$$

1. Number of cfu/ml on SD^{-L} plates = viability of prey partner
2. Number of cfu/ml on SD^{-W} plates = viability of bait partner
3. Number of cfu/ml on SD^{-L-W} plates = viability of diploids
4. Lowest Number of cfu/ml of SD^{-L} or SD^{-W} plates indicate limiting partner

5. $$\text{Mating efficiency} = \frac{\#\text{cfu/ml of diploids} \times 100}{\#\text{cfu/ml of limiting partner}}$$

Library titre

Count number of colonies on all plates with 30-300 colonies after 4 days

$$\#\text{cfu/ml} = \frac{\#\text{colonies}}{\text{plating volume(ml)} \times \text{dilution factor}}$$

colonies clones screened= # cfu/ml x final resuspension volume

APPENDIX III

LIST OF SUPPLIERS

*Aci*I	New England Biolabs
Acrylamide	Merck
Adenie hemisulphate	Bio101
Agar	Merck
Agarose	Whitehead Scientific
$AgNO_3$	Merck
Ammonium persulphate	Merck
Ampicillin	Roche
Aptotinin	Roche
Autoradiography film	Kodak
*Bam*HI	Promega
*Ban*II	Promega
β-galactose	Southern Cross
*Bse*RI	New England Biolabs
*Bsr*I	New England Biolabs
Bis-acrylamide	Merck
Boric acid	Merck
Bromophenol blue	Merck
Calf intestinal alkaline phosphatase	Promega
Chloroform/octanol	Sigma
dATP	Boerhinger Mannheim
dCTP	Boerhinger Mannheim
*Dde*I	Promega
dGTP	Boerhinger Mannheim

DMEM	Highveld biological
dNTP mix	TaKaRa
DTT	Roche
dTTP	Boerhinger Mannheim
*Eco*RI	Promega
*EcoR*V	Promega
*Ear*I	Promega
EDTA	Boerhinger Mannheim
Ethanol	Boerhinger Mannheim
Ex Taq^{TM} polymerase	TaKaRa
Ex Taq^{TM} polymerase Mg^{2+}-containing reaction buffer	TaKaRa
FACS Lysing Solution	Beckton Dickenson
Foetal calf serum	Delta Bioproducts
Formamide	Merck
Formaldeyde	Merck
Gelbond	Merck
GFX® DNA purification kit	Amersham Pharmacia
Glucose	Kimix
Glycerol	FMC Promega
Great EScAPe^{TM} chemiluminescence detection kit	BD Biosciences
HA monoclonal antibody	Roche
*Hae*III	Promega
Ham's H12	Highveld biological
Herring sperm DNA	Promega
*Hsp*92II	Promega
Isopropanol	Merck
K-acetate	Sigma
Kanamycin	Roche

KCl	Merck
Lambda DNA	Promega
LiAc	Sigma
Matchmaker^{TM} Mammalian Assay Kit 2	BD Biosciences
Matchmaker^{TM} Two-hybrid system 3	BD Biosciences
Mineral oil	BDH Chemicals
*Mnl*I	Fermentas
$MgCl_2$	Bioline
Myc monoclonal antibody	Roche
NaAc	Merck
NaCl	BDH Chemicals
$Na_2HPO_4.7H_2O$	Merck
$Na_2HPO_4.H_2O$	Merck
NaOH	Sigma
*Nde*I	Promega
*Nla*III	New England Biolabs
*Nru*I	Promega
Oligonucleotide primers	Department of Molecular and Cell Biology, University of Cape Town (UCT), Cape Town, South Africa.
pGBKT7	BD Biosciences
PBS	Sigma
PEG4000	Merck
Penicillin/streptomycin	Highveld biological
Peptone	Difco
pG5SEAP	BD Biosciences
pGBKT7	BD Biosciences
pM	BD Biosciences
PMSF	Roche
Phenol	Merck

Phenol/choloform	Sigma
Phenol/choroform/isoamyl	Sigma
Proteinase K	Sigma
pVP16	BD Biosciences
QDO	BD Biosciences
Qiagen Kit	Stratagene
RNAse wipes	Ambion
SDS	Sigma
SD^{-Leu}	BD Biosciences
SD^{-Trp}	BD Biosciences
$SD^{-Leu-Trp}$	BD Biosciences
T4 Ligase	Promega
Taq polymerase	Bioline
TDO	BD Biosciences
TEMED	Sigma
TNT® Quick Coupled transcription/translation system	BD Biosciences
Tris	Merck
Tris-OH	Merck
Tris-HCl	Merck
Trypsin	Highveld biological
Tryptone	Fluka
Urea	BDH Chemicals
Whatman 3M paper	Whatman international
Wizard® Purefection plasmid purification kit	BD Bioscences
X-α-galactsoe	Southern Cross
Yeast extract	Difco
Yeast nitrogen base (without amino acids)	BD Biosciences

APPENDIX IV

BACTERIAL STRAIN PHENOTYPE

E.coli strain DH5α

Φ 80d *lac*ZΔ*M15* recA1, *end*A1, *Gry* A96 *thi*-1, *hsd*R17 *sup*E44, *rel*A1, *deoR* Δ(*lac*ZYA *argF*)u169

YEAST STRAIN PHENOTYPEs

Yeast strain AH109

MATa, trp1-901, leu2-3, ura3-5, his3-200, gal4Δ, gal80Δ, LYS2::$GAL1_{uas}$-$GAL1_{TATA}$-HIS3, $GAL2_{UAS}$-$GAL2_{TATA}$-ADE2, URA3::$MEL1_{UAS}$-$MEL1_{TATA}$-lacZ (James et al., 1996)

Yeast strain Y187

MATα, ura3-52, his3-200, ade2-101, trp1-901, leu2-3, 112, gal4Δ, met^-, gal80Δ, URA3::$GAL1_{UAS}$-$GAL1_{TATA}$-lacZ (Harper et al., 1993)

APPENDIX V

Reference sequence with regions used to design primers to amplify the region encoding the COOH-terminal domain of Cx45. Region highlighted in turquoise, forward primer sequence

atgcttcatttagggtttgggaccattcgagactcactaaacagtaaaaggagggaacttgaggatccgggtgcttataattatcctt
tcacttggaatacaccatctgctccccctggctataacattgctgtcaaaccagatcaaatccagtacaccgaactgtccaatgcta
agatcgcctacaagcaaaacaaggccaacacagcccaggaacagcagtatggcagccatgaggagaacctcccagctga
cctggaggctctgcagcgggagatcaggatggctcaggaacgcttggatctggcagttcaggcctacagtcaccaaaacaacc
ctcatggtccccgggagaagaaggccaaagtggggtccaaagctgggtccaacaaaagcactgccagtagcaaatcaggg
gatgggaagaactctgtctggatttaa

Alignment of the sequenced Cx45-pGBKT7 bait construct (CO2_CN4_PGKK_06a) and its reverse complimentary sequence, against the reference sequence (Cx45 COOK-term) obtained from the Genbank database (**www.ncbi.gov.org**). Sequence highlighted in red represents the unaligned region of the vector sequence; green, regions of homology *only* between the Cx45-pGBKT7 bait construct and the reference sequence; black , regions of homology between the Cx45-pGBKT7 bait construct, the reverse complimentary sequence of the construct as well and the reference sequence. Dotted regions; no homology detected.

pGBKT7 GAL4 DNA-binding domain of the pGBKT7 vector

gja7%20cyto%20tail[.....

C02_CN4_PGBK_F_06.a caagtcaagcagttgttgtatcgccagnaatttgtaatac

Reverse_Complement_ .....

Consensus

Cx45 COOH-term ref .....

C02_CN4_PGBK_F_06.a gactcactataacgcgagccgccatcatggtaggagcaga

Reverse_Complement_ .....

Consensus

Cx45 COOH-term ref .....ATGCTTCATTT

C02_CN4_PGBK_F_06.a agctgatctcagaggaggacctgcatatgATGCTTCATTT

Reverse_Complement_ .....

Consensus

Cx45 COOH-term ref AGGGTTTGGGACCATTCGAGACTCACTAAACAGTAAAAGG

C02_CN4_PGBK_F_06.a AGGGTTTGGGACCATTCGAGACTCACTAAACAGTAAAAGG

Reverse_Complement_ Consensus

Cx45 COOH-term ref AGGGAACTTGAGGATCCGGGTGCTTATAATTATCCTTTCA

C02_CN4_PGBK_F_06.a AGGGAACTTGAGGATCCGGGTGCTTATAATTATCCTTTCA

Reverse_Complement_Consensus

Cx45 COOH-term ref CTTGGAATACACCATCTGCTCCCCCTGGCTATAACATTGC

C02_CN4_PGBK_F_06.a CTTGGAATACACCATCTGCTCCCCCTGGCTATAACATTGC

Reverse_Complement_Consensus

Cx45 COOH-term ref TGTCAAACCAGATCAAATCCAGTACACCGAACTGTCCAAT

C02_CN4_PGBK_F_06.a TGTCAAACCAGATCAAATCCAGTACACCGAACTGTCCAAT

Reverse_Complement_ .....TCAAATCCAGTACACCGAACTGTCCAAT

Consensus tcaaatccagtacaccgaactgtccaat

Cx45 COOH-term ref [redacted]

C02_CN4_PGBK_F_06.a [redacted]

Reverse_Complement_ [redacted]

Consensus gctaagatcgcctacaagcaaaacaaggccaac acagcc

Cx45 COOH-term ref [redacted]

C02_CN4_PGBK_F_06.a [redacted]

Reverse_Complement_ [redacted]

Consensus cagg aacagcagtatggcagccatg aggagaacctccc

Cx45 COOH-term ref [redacted]

C02_CN4_PGBK_F_06.a [redacted]

Reverse_Complement_ [redacted]G..[redacted].[redacted]

Consensus agctgacctggaggctctgcagcggga atcagg atg

Cx45 COOH-term ref [redacted].[redacted]G[redacted]..[redacted]AG..[redacted]

C02_CN4_PGBK_F_06.a GCTCAGGnAACGCTTtGgnATCTGGCcagtTTCAGGCCTA

Reverse_Complement_ [redacted].[redacted]G[redacted]..[redacted]AG..[redacted]

Consensus gctcagg aacgctt g atctggc ttcaggccta

Cx45 COOH-term ref [redacted]TCACC..[redacted].[redacted]G

C02_CN4_PGBK_F_06.a CAGntcaCcaAAAACAACCCTCATGGnTCCCCGGGAGAAa

Reverse_Complement_ CAGTCACC..AAAACAACCCTCATGG.TCCCCGGGAGAAG

Consensus cag c aaaacaaccctcatgg tccccgggagaa

Cx45 COOH-term ref AAGGCCAAAGTGGGGTCCAAAGCTGGGTCCAACAAAGCA

C02_CN4_PGBK_F_06.a gAaa.....GGGcCCAAAGnTGGGggntcCnAAAGCn

Reverse_Complement_ AAGGCCAAAGTGGGGTCCAAAGCTGGGTCCAACAAAGCA

Consensus a ggg ccaaag tggg c aaagc

Cx45 COOH-term ref CTGCCAGTAGCAAATCAGGGGATGGGAAGAACTCTGTCTG

C02_CN4_PGBK_F_06.a tgGggntcc.....

Reverse_Complement_ CTGCCAGTAGCAAATCAGGGGATGGGAAGAcCTCcGTCTG

Consensus g

Cx45 COOH-term ref GATTTAA.....

C02_CN4_PGBK_F_06.a .....

Reverse_Complement_ GATTTAAgaattcccggggatccgtcgacctgcagcggcc

Consensus

Cx45 COOH-term ref .....

C02_CN4_PGBK_F_06.a .....

Reverse_Complement_ gcataactagcataacccctttggggcctctaaacgggtct

Consensus

Cx45 COOH-term ref .....

C02_CN4_PGBK_F_06.a .....

Reverse_Complement_ tgaggggttttttgcgcgcttgcagccaagctaattccgg

Consensus

Cx45 COOH-term ref .....

C02_CN4_PGBK_F_06.a .....

Reverse_Complement_ gcgaatttcttatgatttatgatttttattattaaataag

Consensus

Cx45 COOH-term ref .....

C02_CN4_PGBK_F_06.a .....

Reverse_Complement_ ttaaaaaaaaaaaaa

Consensus

Electropherogram sequences of preys clones in pVP16. Regions highlighted in pink, unaligned regions of the pVP16 vector; highlighted in turquoise, conserved regions of the GAL4-activation domain of the vector sequence; highlighted in red, restriction enzyme sites; regions in black, the prey specific regions of the construct.

NADH dehydrogenase subunit 4

CTGGACATGTTGGGGGACGGGGATTCCCCGGGGCCGGGATTTACCCCCCACGACTCCGCCCCCTACGGCGCTCTG
GATATGGCCGACTTCGAGTTTGAGCAGATGTTTACCGATGCCCTTGGAATTGACGAGGGGAATTCGCCCACGGGC
TTACATCCTCATTACTATTCTGCCTAGCAAACTCAAACTACGAACGCACTCACAGTCGCATCATAATCCTCTCTC
AAGGACTTCAAACTCTACTCCCACTAATAGCTTTTTGATGACTTCTAGCAAGCCTCGCTAACCTCGCCTTACCCC
CCACTATTAACCTACTGGGAGAACTCTCTGTGCTAGTAACCACGTTCTCCTGATCAAATATCACTCTCCTACTTA

CAGGACTCAACATACTAGTCACAGCCCTATACTCCCTCTACATATTTACCACAACACAATGGGGCTCACTCACCC
ACCACATTAACAACATAAAACCCTCATTCACACGAGAAAACACCCTCATGTTCATACACCTATCCCCCATTCTCC
TCCTATCCCTCAACCCCGACATCATTACCGGGTTTTCCTCTTAAACATGTCGGCCGCCTCGGCCTCTAAGGGTGG
GCATCATACGGGATCCATCGAGCTCGAGCTGCARATGAATCGTAGATACTGAAAAACCCCGCAAGTTCACTTCAA
CTGTGCATCGTGCACCATCTCAATTTCTTTCATTTATACATCGTTTTGCCTTCTTTTATGTAACTATACTCCTCT
AAGTTTCAATCTTGGCCATGTAACCTCTGATCTATAGAATTTTTTAAATGACTAGAATTATGCCATCTTTTTTTG
GACCTAAATTCTCATGAAAATATATACGAGGGCTATCAGAGCTTGACTCCTCGCAGAGGTTTGTCAGTCTCATCA
GTGTCGGCTGTCTACTGCCGAATACGAAAGATGAACGTCATCGTTGTARAWCGTGTGACTTCGTAGCGATCTAGA
TTAGATTTWTATAGTTAAAAATGTTACAGTAGKACCTAGTACGAATCTATCTGAACGCTCGTG

Thioredoxin 2

TGGGGGACGGGGATTCCCCGGGGCCGGGATTTACCCCCCACGACTCCGCCCCCTACGGCGCTCTGGATATGGCCG
ACTTCGAGTTTGAGCAGATGTTTACCGATGCCCTTGGAATTGACGAGGGGAATTCGGGGGGAGGAAGTGACGACA
GGCGTGCCCTTGACAGGCAGGGAGGGCTAGGCTGTGCATCCCTCCGCTCGCATTGCAGGGAGATGGCTCAGCGAC
TTCTTCTGAGGAGGTTCCTGGCCTCTGTCATCTCCAGGAAGCCCTCTCAGGGTCAGTGGCCACCCCTCACTTCCA
GAGCCCTGCAGACCCCACAATGCAGTCCTGGTGGCCTGACTGTAACACCCAACCCAGCCCGGACAATATACACCA
CGAGGATCTCCTTGACAACCTTTAATATCCAGGATGGACCTGACTTTCAAGACCGAGTGGTCAACAGTGAGACAC
CAGTGGTTGTGGATTTCCACGCACAGTGGTGTGGACCCTGCAAGATCCTGGGGCCGAGGTTAGAGAAGATGGTGG
CCAAGCAGCACGGGAAGGTGGTGATGGCCAAGGTGGATATTGATGACCACACAGACCCCGCCATTGAGTATGAGG
TGTCAGCGGTGCCCACTGTGCTGGCCATGAAGAATGGGGACGTGGTGGACAAGTTTGTGGGCATCAAGGATGAGG
ATCAGTTGGAGGCCTTCCTGAAGAAGCTGATTGGCTGACAAGCAGGGATGAGTCCTGGTTCCCTTGCCCGCGTGG
GACCCCAATAGAACTCAGCCCTTCCATGCCAGCCCTTCCTGCTGCCTCCCTCCTGTCTGGCTCCTGGGGCCCATG
CTTAGAGCCCAGGCTCCAGCCCTGAGTGCTTCCGAGCTGGCGGACTGCCCAGGGGCCATCAGGATGGTGGTGCTG
CTGCTGATCCGGGGACCGCTGTCTTCCCTCCCATACGCCTTTCATCCCTCCTTCTAGGGCCTATGGCAGTTCTCC
CAGGATGTGTGGCGAGAGCCTGGGCCAGCCCACAGCGTCCTAGTCAGCAGCCACACCTTGGTCCTCATCTCTGTC
CTCATCTGAACCTCGTGCTGGCTCGTCTGCACTAMCATTCTCTTCAGCTGCTGTTTGCAAGAATAGTAGAATATA
CCTGTCGGCCGCCYGG

Homo sapiens CD63-antigen

AAAAGAAGCGTAAAGTCGCCCCCCCGACCGATGTCAGCCTGGGGGACGAGCTCCACTTAGACGGCGAGGACGTGG
CGATGGCGCATGCCGACGCGCTAGACGATTTCGATCTGGACATGTTGGGGGACGGGGATTCCCCGGGGCCGGGAT
TTACCCCCCACGACTCCGCCCCCTACGGCGCTCTGGATATGGCCGACTTCGAGTTTGAGCAGATGTTTACCGATG
CCCTTGGAATTGACGAGGGGAATTCGGGGAGAGAGCCCCGGAGCCGCGGCGGGAGAGGAACGCGCAGCCAGCCTT
GGGAAGCCCAGGCCCGGCAGCCATGGCGGTGGAAGGAGGAATGAAATGTGTGAAGTTCTTGCTCTACGTCCTCCT
GCTGGCCTTTTGCGCCTGTGCAGTGGGACTGATTGCCGTGGGTGTCGGGGCACAGCTTGTCCTGAGTCAGACCAT
AATCCAGGGGGCTACCCCTGGCTCTCTGTTGCCAGTGGTCATCATCGCAGTGGGTGTCTTCCTCTTCCTGGTGGC
TTTTGTGGGCTGCTGCGGGGCCTGCAAGGAGAACTATTGTCTTATGATCACGTTTGCCATCTTTTCTGTCTCTTA
TCATGTTGGTGGGAGGTGGCCGCAGCCATTGCTGGCTATGTGTTTAGAAGATAAGGTGATGTCAGAGTTTAATAA
AMACTTCCGGGCAGCARRATKGGARGAATTACCCCGAAAAAACACCCACACCTGCCTTCCGAATTCCTGGACAGG

GATGCAAGCCAGATTTTACGTGCTGTGGGACTKGCTAACTACACAGATTTGGGAGAAAATTCCTTCAAKGTCGGG
AGGACGAGTTTCCGATTCTTGCCTGCCAATTAATT

Myomegalin

AGGACGTGGCGATGGCGCATGCCGACGCGCTAGACGATTTCGATCTGGACATGTTGGGGGACGGGGATTCCCCGG
GGCCGGGATTTACCCCCCACGACTCCGCCCCCTACGGCGCTCTGGATATGGCCGACTTCGAGTTTGAGCAGATGT
TTACCGATGCCCTTGGAATTGACGAGGGGGATCCGGGGACACATMCCMARAGACACTGAGAGAGACAGACAGACA
GTAAACAGAGGAGCACTAACCACAAACGGTTTACAAATGACCTCTGWGCTCATTCACCTGTCTGTTCCCCACCTT
GCCTTTTATARCAACTATAGCAACAGCCATGARAGTCATTGTGGAAAGAAATAAAATAAAATTAAAAAYTCCTGG
AAGCTTGTAAAGAATGTGAGCAAAGGGGARGAAGTTGYRAAWAAAATGAWCWA

SCF apoptosis response protein 1

TAAAGTCGCCCCCCCGACCGATGTCAGCCTGGGGGACGAGCTCCACTTAGACGGCGAGGACGTGGCGATGGCGCA
TGCCGACGCGCTAGACGATTTCGATCTGGACATGTTGGGGGACGGGGATTCCCCGGGGCCGGGATTTACCCCCCA
CGACTCCGCCCCCTACGGCGCTCTGGATATGGCCGACTTCGAGTTTGAGCAGATGTTTACCGATGCCCTTGGAAT
TGACGAGGGGAATTCCGGGGAGGGAAGGGGAAAGAGGTCACCAAGGGMAGAGGTGTCCAGGCCGGAGCCAGGGGC
CCCACTGTTGGGATGCTGGCTGCAGTGGGGCGCCCCAAGCCCAGGTCCCCTCTGTCTTCTCTTTCGACTTTGCAG
CTGTACTTGTTTTGCTCCTCTACCCGCAGGAGCTGACATGGACCCAAATCCTCGGGCCGCCCTGGAGCGCCAGCA
GCTCCGCCTTCGGGAGCGGCAAAAATTCTTCGAGGACATTTTACAGCCAGAGACAGAGTTTGTCTTTCCTCTGTC
CCATCTGCATCTCGAGTCGCAGAGACCCCCCATAGGTAGTATCTCATCCATGGAAGTGAATGTGGACACACTGGA
GCAAGTAGAACTTATTGACCTTGGGGACCCGGATGCAGCAGATGTGTTCTTGCCTTGCGAAGATCCTCCACCAAC
CCCCCAGTCGTCTGGGGTGGACAACCATTTGGAGGAGCTGAGCCTGCCGGTGCCTACATCAGACAGGACCACATC
TAGGACCTCCTCCTCCWCCTCCTCCRACTCCTCCACCAACCTGCATAGCCCAAATCCAAGTGATGATGGAGCAGA
TACGCCCTTGGCACAGTCGGATGAAGAGGAGGAAAGGGGTGATGGAGGGGCAGAGCCTGGAGCCTGCAGCTAGCA
GTGGGCCCCTGCCTACAGACTGACCACGCTGGCTATTCTCCACATGAGACCACAGGCCCAGCCAGAGCCTGTCGG
GAGAAGACCAGACTCTTTACTTGCAGTAGGCACCAGAGGTGGGAAGGATGGTGGGATTGTGTACCTTTCTAAGAA
TTAACCCTCTCCTGCTTTACTGCTAATTTTTTCCTGCTGCAACCTCCCAMCAGTTTTGGCTTACTCTGARATATG
ATTGCAATGAGAGAGARAGATGAGGTTGGACAAGATGCCACTGCTTTTCTAGCMCTCTTCCTCCCTAAACAATCC
GTAGTCTTTCTAATACAGTCTCTCAGAMCAGKGTCTCTGAATGATGTGAACTCATTACTCATCAAGTAAGAGTAG
SW

Obscurin

CCCTAAAAAGAAGCGTAAAGTCGCCCCCCCGACCGATGTCAGCCTGGGGGACGAGCTCCACTTAGACGGCGAGGA
CGTGGCGATGGCGCATGCCGACGCGCTAGACGATTTCGATCTGGACATGTTGGGGGACGGGGATTCCCCGGGGCC
GGGATTTACCCCCCACGACTCCGCCCCCTACGGCGCTCTGGATATGGCCGACTTCGAGTTTGAGCAGATGTTTAC
CGATGCCCTTGGAATTGACGAGGGGAATTCGGGGCAGCTGGCCCTCATCAGTGGTGGACTCTGTTCCCTCCTGCT

CCCGGCTGGACAGGTAGCCTTGGGCACTGAAGTAGGATGAGGACTCCGTGGCATCTGCTGCAGTGTCATAGTCTG
TGCTTGTCAAGTCCACACGGAGCTCAGCCTTGGTGGAGGAGACACCCATGCTGTTCTCGGCCAGGCAGCGGTAGA
CGCCCATGTCTGCTGGCACCACGGCTGTGATGATGAGCTGATGGCCACCCTGTTGGTCTTCATTAATCATGTAGT
GATCATCCTCCTCCAAAAAACCTTGTCGGCCGCCTCGGCCTCTANAGGGTGGGCATCGATACGGGATCCATCGAG
CTCGAGCTGCANATGAATCGTAAATACTGAAAAACCCCGCAAGTTCACTTCAACTGTGCATCGTGCACCATCTCA
ATTTCTTTCATTTATACATCGTTTTGCCTTCTTTTATGTAACTATACTCCTCTAAGTTTCAATCTTGGCCATGTA
ACCTCTGATCTATANAATTTTTTAAATGACTANAATTAATGCCCATCTTTTTTTTTGGACCTAAATTCTTCATGA
AAATATATTACGAGGGCTTATNCAAAACTTTGGACNTCTTCCCCNNAAGTTTGGTCAAGTCCCCANTCANGGTTG
TCGGCTTGTCTACNTNGCCNAAAA

Cytochrome C oxidase subunit 1

GCCTCTGAGCTATTCCAGAAGTAGTGAAGAGGCTTTTTTGGAGGAGATCTAAGCTAGCGCCGCCACCATGGGCCC
TAAAAAGAAGCGTAAAGTCGCCCCCCCGACCGATGTCAGCCTGGGGGACGAGCTCCACTTAGACGGCGAGGACGT
GGCGATGGCGCATGCCGACGCGCTAGACGATTTCGATCTGGACATGTTGGGGGACGGGGATTCCCCGGGGCCGGG
ATTTACCCCCCACGACTCCGCCCCCTACGGCGCTCTGGATATGGCCGACTTCGAGTTTGAGCAGATGTTTACCGA
TGCCCTTGGAATTGACGAGGGGAATTCGGGGACCCCATTCTATACCAACACCTATTCTGATTTTTCGGTCACCCT
GAAGTTTATATTCTTATCCTACCAGGCTTCGGAATAATCTCCCATATTGTAACTTACTACTCCGGAAAAAAAGAA
CCATTTGGATACATAGGTATGGTCTGAGCTATGATATCAATTGGCTTCCTAGGGTTTATCGTGTGAGCACACCAT
ATATTTACAGTAGGAATAGACGTAGACACACGAGCATATTTCACCTCCGCTACCATAATCATCGCTATCCCCACC
GGCGTCAAAGTATTTAGCTGACTCGCCACACTCCACGGAAGCAATATGAAATGATCTGCTGCAGTGCTCTGGGCC
CTAGGATTCATCTTTCTTTTCACCGTAGGTGGCCTGACTGGCATTGTATTAGCAAACTCATCACTAGACATCGTA
CTACACGACACGTACTACGTTGTAGCTCACTTCCACTATGTCCTATCAATAGGAGCTGTATTTGCCATCATAGGA
GGCTTCATTCACTGATTTCCCCTATTCTCAGACTACACCCTAGACCAAACCTACGCCAAAATCCATTTCACTATC
ATATTCATCGGCGTAAATCTAACTTTCTTCCCACAACACTTTCTCGGCCTATCCGGAATGCCCCGACGTTACTCG
GACTACCCCGATGCATACACCACATGAAACATCCTATCATCTGTAGGCTCATTCATTTCTCTAACAGCAGTAATA
TTAATAATTTTCATGATTTGAGAAGCCTTCGCTTCGAAGCGAAAGTCCTAATAGTAGAAGAACCCTCCATAAACC
TGGAGTGACTATATGGATGCCCCCCCACCCTACCACACATTCGAGACCCGTATACATAAAATCTAGACAAAAAAA
GAGATCGACCCCCAAGCTGGTTCAGCACCATGCTCATGACTTTCAAAAAAACAGAAAAAACTGTTCGCGCCTCGC
YCTAAGTGCATCGAWCCGGATCCATCGRGCYTCGAGACTSA

Electropherogram sequence of Cx45-bait fragment cloned in pM. Regions highlighted in pink, unaligned region of the pM vector; highlighted in turquoise, conserved regions of the GAL4-DNA binding domain of the vector sequence; highlighted in red, restriction enzyme site; region in black, the Cx45-bait specific region of the construct.

Cx45-pM bait construct for M2H

TGTTAACAGGATTATTTGTACAAGATAATGTGAATAAAGATGCCGTCACAGATAGATTGGCTTCAGTGGAGACTG
ATATGCCTCTAACATTGAGACAGCATAGAATAAGTGCGACATCATCATCGGAAGAGAGTAGTAACAAAGGTCAAA
GACAGTTGACTGTATCGCCGGAATTCATGCTTCATTTAGGGTTTGGGACCATTCGAGACTCACTAAACAGTAAAA
GGAGGGAACTTGAGGATCCGGGTGCTTATAATTATCCTTTCACTTGGAATACACCATCTGCTCCCCCTGGCTATA
ACATTGCTGTCAAACCAGATCAAATCCAGTACACCGAACTGTCCAATGCTAAGATCGCCTACAAGCAAAACAAGG
CCAACACAGCCCAGGnAACAGCAGTATGGCAGCCATGAGGAGAACCTCCCAGCTGACCTGGAGGCTCTGCAGCGG
GAAGATCAGGATGGCTCAGGAACGCTTTGGATCTGGCCAGTTTCAGGCCTACAGTCCCCAAAAACAACCCTCATG
GTCCCCGGGAGAAAAAGGCCAAAGTGGGGTCCAAAGCTGGGTCCAACAAAAGCACTGCCAGTAGCAAATCAGGGG
ATGGGAAGAACTCTGTCTGG

REFERENCES

Adzhubei, I. A. *et al*. A method and server for predicting damaging missense mutations. *Nat. Methods* 7, 248–249, 2010.

Ai Z, Fischer A, Spray DC, Brown AM, and Fishman GI. Wnt-1 regulation of connexin43 in cardiac myocytes. *J Clin Invest* 105:161–171, 2000.

Alcolea S, Jarry-Guichard T, de Bakker J, Gonzalez D, Lamers W, Coppen S, Barrio L, Jongsma H, Gros D, and van Rijen H. Replacement of connexin40 by connexin45 in the mouse: impact on cardiac electrical conduction. *Circ Res* 94:100-109, 2004.

Alcolea S, Theveniau-Ruissy M, Jarry-Guichard T, Marics I, Tzouanacou E, Chauvin JP, Briand JP, Moorman AF, Lamers WH, and Gros DB. Downregulation of connexin 45 gene products during mouse heart development. *Circ Res* 84:1365-79, 1999.

Alexander DB, and Goldberg GS. Transfer of biologically important molecules between cells through gap junction channels. *Curr Med Chem* 10:2045-2058, 2003.

Anderson CL, Zundel MA, and Werner R. Variable promoter usage and alternative splicing in five mouse connexin genes. *Genomics* 85:238-244, 2005.

Anumonwo JM, Taffet S, and Gu H. The carboxyl terminal domain regulates the unitary conductance and voltage dependence of connexin40 gap junction channels. *Circ Res* 88: 666–673, 2001.

Arieff Z. The search for the PFHBI gene: Refining the target area and identification and analysis of candidate gene transcripts. *PhD thesis – University of Stellenbosch*, *Department of Biomedical Sciences*, 2004.

Arizmendi JM, Runswick MJ, Skehel JM, Walker JE. NADH: ubiquinone oxidoreductase from bovine heart mitochondria. A fourth nuclear encoded subunit with a homologue encoded in chloroplast genomes. *FEBS Lett* 301:237-42, 1992.

Basson CT, Bachinsky DR, Lin RC, Levi T, Elkins JA, Soults J, Grayzel D, Kroumpouzou E, Traill TA, Leblanc-Straceski J, Renault B, Kucherlapati R, Seidman JG, and Seidman CE. Mutations in human cause limb and cardiac malformation in Holt-Oram syndrome. *Nature Genet* 15: 30-35, 1997.

Basson CT, Cowley GS, Solomon SD, Weissman B, Poznanski AK, Traill TA, Seidman, JG, and Seidman CE. The clinical and genetic spectrum of the Holt-Oram syndrome (heart-hand syndrome). *New Eng J Med* 330: 885-891, 1994.

Basson CT, Huang T, Lin RC, Bachinsky DR, Weremowicz S, Vaglio A, Bruzzone R, Quadrelli R, Lerone M, Romeo G, Silengo M, Pereira A, *et al*. Different TBX5 interactions in heart and limb defined by Holt-Oram syndrome mutations. *Proc Nat Acad Sci* 96: 2919-2924, 1999.

Bastide B, Neyses L, Ganten D, Paul M, Willecke K, and Traub O. Gap junction protein connexin40 is preferentially expressed in vascular endothelium and conductive bundles of rat myocardium and is increased under hypertensive conditions. *Circ Res* 73:1138-1149, 1993.

Bennett MV, Contreras JE, Bukauskas FF, and Saez JC. New roles for astrocytes: gap junction hemichannels have something to communicate. *Trends Neurosci* 11:610-617, 2003.

Bennett MV, Zheng X, and Sogin ML. The connexins and their family tree. *Soc Gen Physiol Ser* 49:223-233, 1994.

Brink AJ, and Torrington M. Progressive familial heart block-two types. *S Afr Med J* 52:53-59, 1977.

Brink PA, Ferreira A, Moolman JC, Weymar HW, van der Merwe PL, and Corfield VA. Gene for progressive familial heart block type I maps to chromosome 19q13. *Circulation* 91:1633-1640, 1995.

Brink PA. A molecular genetic approach to the aetiology of cardiovascular disease in South Africa with reference to progessive familial heart block. *PhD thesis. University of Stellenbosch, Department of Biomedical Sciences*, 1997.

Brink PR, and Dewey MM. Evidence for fixed charge in the nexus. *Nature* 285:101-102, 1980.

Brook JD, Zemelman BV, Hadingham K, Siciliano MJ, Crow S, Harley HG, Rundle SA, Buxton J, Johnson K, Almond JW. Radiation-reduced hybrids for the myotonic dystrophy locus. *Genomics* 13:243-250, 1992.

Bruneau BG, Nemer G, Schmitt JP, Charron F, Robitaille L, Caron S, Conner DA, Gessler M, Nemer M, Seidman CE, and Seidman JG. A murine model of Holt-Oram syndrome defines roles of the T-box transcription factor Tbx5 in cardiogenesis and disease. *Cell* 106:709-721, 2001.

Bruneau BG. Transcriptional regulation of vertebrate cardiac morphogenesis. *Circ Res* 90:509-519, 2002.

Bruzzone K. Learning the language of cell-cell communication through connexin channels. *Genome Biol* 2:11-16, 2001.

Bukauskas FF, and Peracchia C. Two distinct gating mechanisms in gap junction channels: CO2-sensitive and voltage-sensitive. *Biophys J* 72:2137-2142, 1997.

Bukauskas FF, and Verselis VK. Gap junction channel gating. *Biochim Biophys Acta* 1662:42-60, 2004.

Bukauskas FF, Bukauskiene A, Bennett MV, and Verselis VK. Gating properties of gap junction channels assembled from connexin43 and connexin43 fused with green fluorescent protein. *Biophys J* 81:137–152, 2001.

Bukauskas FF, Bukauskiene A, Verselis VK, and Bennett MVL. Coupling asymmetry of heterotypic connexin 45/connexin 43-EGFP gap junctions: properties of fast and slow gating mechanisms. *Proc Natl Acad Sci* 99:7113–7118, 2002.

Bukauskas FF, Elfgang C, Willecke K, and Weingart R. Biophysical properties of gap junction channels formed by mouse connexin40 in induced pairs of transfected human HeLa cells. *Biophys J* 68:2289-98, 1995.

Cancelas JA, Koevoet WL, de Koning AE, Mayen AE, Rombouts EJ, Ploemacher RE. Connexin-43 gap junctions are involved in multiconnexin-expressing stromal support of hemopoietic progenitors and stem cells. *Blood* 96:498-505, 2000.

Causier B, Davies B. Analysing protein-protein interactions with the yeast two-hybrid system. *Plant Mol Biol* 50:855-70, 2002.

Chien CT, Bartel PL, Sternglanz R, and Fields S. The two-hybrid system: a method to identify and clone genes for proteins that interact with a protein of interest. *Proc Natl Acad Sci USA* 88:9578-9582, 1991.

Cho DH, and Tapscott SJ. Myotonic dystrophy: Emerging mechanisms for DM1 and DM2. *Biochim Biophys Acta,* 146:201-211, 2006.

Ciray HN, Persson BE, Backstrom T, Roomans GM, and Ulmsten U. Direct intracellular injections for studying human myometrial gap junctions prior to labor. *Acta Obstet Gynecol Scand* 73:97-102, 1994.

Common JE, Di WL, Davies D, Galvin H, Leigh IM, O'Toole EA, and Kelsell DP. Cellular mechanisms of mutant connexins in skin disease and hearing loss. *Cell Commun Adhes* 10:347-51, 2003.

Coppen SR, Kodama I, Boyett MR, Dobrzynski H, Takagishi Y, Honjo H, Yeh HI, and Severs NJ. Connexin45, a major connexin of the rabbit sinoatrial node, is co-expressed with connexin43 in a restricted zone at the nodal-crista terminalis border. *J Histochem Cytochem* 47:907-918, 1999.

Cottrell GT, Lin R, Warn-Cramer BJ, Lau AF, and Burt JM. Mechanism of v-Src- and mitogen-activated protein kinase-induced reduction of gap junction communication. *Am J Physiol Cell Physiol* 284:511-520, 2003.

Damdimopoulos AE, Miranda-Vizuete A, Pelto-Huikko M, Gustafsson JA, Spyrou G. Human mitochondrial thioredoxin. Involvement in mitochondrial membrane potential and cell death. *J Biol Chem* 277:33249-57, 2002.

Davies, P. Obituary: S. Oram, MD, FRCP. *Brit Med J* 304: 500, 1992.

Davis LM, Kanter HL, Beyer EC, and Saffitz JE. Distinct gap junction protein phenotypes in cardiac tissues with disparate conduction properties. *J Am Coll Cardiol* 24:1124–1132, 1994.

Day JW, Ricker K, Jacobsen JF, Rasmussen LJ, Dick KA, Kress W, Schneider C, Koch MC, Beilman GJ, Harrison AR, Dalton JC, Ranum LP. Myotonic dystrophy type 2: molecular, diagnostic and clinical spectrum. *Neurology* 60:657-664, 2003.

de la Pompa JL, Timmerman LA, Takimoto H, Yoshida H, Elia AJ, Samper E, Potter J, Wakeham A, Marengere L, Langille BL, Crabtree GR, and Mak TW. Role of the NF-ATc transcription factor in morphogenesis of cardiac valves and septum. *Nature* 392:182-186, 1998.

Délèze J. Calcium ions and the healing-over in heart fibers. *Electrophysiology of the Heart*, Pergamon, Elmsford, New York 147–148, 1965.

Délèze J. The recovery of resting potential and input resistance in sheep heart injured by knife or laser. *J Physiol* 208:547–562, 1970.

Delmar M. Connexin diversity: discriminating the message. *Circ Res* 91:85-86, 2002.

Denker BM, and Nigam SK. Molecular structure and assembly of the tight junction. *Am J Physiol Renal Physiol* 274:1–9, 1998.

Dhein S. Cardiac ischemia and uncoupling: gap junctions in ischemia and infarction. *Adv Cardiol* 42:198-212, 2006.

Duffy HS, Delmar M, and Spray DC. Formation of the gap junction nexus: binding partners for connexins. *J Physiol* 96:243-249, 2002.

Duffy HS, Delmar M, and Spray DC. Formation of the gap junction nexus: binding partners for connexins. *J Physiol Paris* 96:243-249, 2002.

Duffy HS, Sorgen PL, Girvin ME, O'Donnell P, Coombs W, Taffet SM, Delmar M, and Spray DC. pH-dependent intramolecular binding and structure involving Cx43 cytoplasmic domains. *J Biol Chem* 277:36706-36714, 2002.

Duncan JC, and Fletcher WH. alpha 1 Connexin (connexin43) gap junctions and activities of cAMP-dependent protein kinase and protein kinase C in developing mouse heart. *Dev Dyn* 223:96-107, 2002.

Durfee T, Becherer K, Chen PL, Yeh SH, Yang Y, Kilburn AE, Lee WH, Elledge SJ. The retinoblastoma protein associates with the protein phosphatase type 1 catalytic subunit. *Genes Dev* 7:555-569, 1993.

Elenes S, Martinez AD, Delmar M, Beyer EC, and Moreno AP. Heterotypic docking of Cx43 and Cx45 connexons blocks fast voltage gating of Cx43. *Biophys J* 81:1406–1418, 2001.

Elenes S, Rubart M and Moreno AP. Junctional communication between isolated pairs of canine atrial cells is mediated by homogeneous and heterogeneous gap junction channels. *J Cardiovasc Electrophys* 10: 990–1004, 1999.

Engelmann TW. Vergleichende Untersuchungen zur Lehre von der Muskel und Nervenelektricität. *Arch Ges Physiol* 15**:**116–148, 1877.

Evans WH, and Martin PE. Gap junctions: structure and function. *Mol Membr Biol* 19:121-136, 2002.

Fernandez P, Corfield VA, and Brink PA. Progressive familial heart block type II (PFHBII): a clinical profile from 1977 to 2003. *Cardiovasc J S Afr* 15:129-132, 2004.

Fernandez P, Moolman-Smook J, Brink P, and Corfield V. A gene locus for progressive familial heart block type II (PFHBII) maps to chromosome 1q32.2-q32.3. *Hum Genet* 118:133-137, 2005.

Fernandez P. A candidate and novel gene search to identify the PFHBII-causitive gene. *PhD thesis. University of Stellenbosch, Department of Biomedical Sciences*, 2004.

Fields S, and Song O. A novel genetic system to detect protein-protein interactions. *Nature* 340:245-246, 1989.

Flenniken AM, Osborne LR, Anderson N, Ciliberti N, Fleming C, Gittens JE, *et al*. A Gja1 missense mutation in a mouse model of oculodentodigital dysplasia. *Development* 132:4375-4386, 2005.

Frenzel EM, and Johnson RG. Gap junction formation between cultured embryonic lens cells is inhibited by antibody to N-cadherin. *Dev Biol* 179:1–16, 1996.

Fukuzawa A, Idowu S, Gautel M . Complete human gene structure of obscurin: implications for isoform generation by differential splicing. *J Musc Res Cell Motil* 26(6–8):427–434, 2005.

Furshpan EJ, and Potter DD. Transmission at the giant motor synapses of the crayfish. *J Physiol* 145:289-325, 1959.

Fusco C, Reymond A, and Zervos AS. In vivo construction of cDNA libraries for use in the yeast two-hybrid system. Yeast. *Methods* 15:715-720, 1999.

Gatchel JR, and Zoghbi HY. Diseases of unstable repeat expansion: mechanisms and common principles. *Nat Rev Genet* 6:743-755, 2005.

Gaussin V. Offbeat mice. *Mol Cell Evol Biol* 280:1022-1026, 2004.

Ghosh TK, Packham EA, Bonser AJ, Robinson TE, Cross SJ, and Brook JD. Characterization of the TBX5 binding site and analysis of mutations that cause Holt-Oram syndrome. *Hum Mol Genet* 10:1983-1994, 2001.

Giepmans BN, Verlaan I, Hengeveld T, Janssen H, and Calafat J. Gap junction protein connexin-43 interacts directly with microtubules. *Curr Biol* 11:1364–368, 2001.

Girsch SJ, and Peracchia C. Calmodulin interacts with a C-terminus peptide from the lens membrane protein MIP26. *Curr Eye Res* 10:839-849, 1991.

Goodenough DA, Goliger JA, and Paul DL. Connexins, connexons, and intercellular communication. *Annu Rev Biochem* 65:475-502, 1996.

Govindarajan R, Zhao S, Song XH, Guo RJ, and Wheelock M. Impaired trafficking of connexins in androgen-independent human prostate cancer cell lines and its mitigation by alpha-catenin. *J Biol Chem.* 277:50087–50097, 2002.

Gros D, Jarry-Guichard T, Ten Velde I, de Maziere A, van Kempen MJ, Davoust J, Briand JP, Moorman AF, and Jongsma HJ. Restricted distribution of connexin40, a gap junctional protein, in mammalian heart. *Circ Res* 74:839-851, 1994.

Guo Y, Martinez-Williams C, and Rannels DE. Gap junction-microtubule associations in rat alveolar epithelial cells. *Am J Physiol* 285:1213–1221, 2003.

Gutstein DE, Morley GE, Tamaddon H, Vaidya D, Schneider MD, Chen J, Chein KR, Stuhlmann H, and Fishman GI. Conduction slowing and sudden arrhythmic death in mice with cardiac-restricted inactivation of connexin43. *Circ Res* 88:333 - 339, 2001.

Hama K. Some observations on the fine structure of the giant nerve fibers of the earthworm, Eisenia foetida. *J Biophys Biochem Cytol* 6:61-66, 1959.

Harper PS. Congenital myotonic dystrophy in Britain. II. Genetic basis. *Arch Dis Child* 50:514-521, 1975.

Harris LC, and Osborne WP. Congenital absence or hypoplasia of the radius with ventricular septal defect: ventriculo-radial dysplasia. *J Pediat* 68: 265-272, 1966.

He DS, and Burt JM. Mechanism and selectivity of the effects of halothane on gap junction channel function. *Circ Res* 86:104–109, 2000.

Hertig CM, Eppenberger-Eberhardt M, Koch S, and Eppenberger HM. N-cadherin in adult rat cardiomyocytes in culture. Functional role of N-cadherin and impairment of cellcell contact by a truncated N-cadherin mutant. *J Cell Sci* 109:1–10, 1996.

Herve JC, and Sarrouilhe D. Modulation of junctional communication by phosphorylation: protein phosphatases, the missing link in the chain. *Biol Cell* 94:423-432, 2002.

Herve JC, Bourmeyster N, and Sarrouilhe D. Diversity in protein-protein interactions of connexins: emerging roles. *Biochim Biophys Acta* 1662:22-41, 2004.

Hiroi Y, Kudoh S, Monzen K, Ikeda Y, Yazaki Y, Nagai R, and Komuro I. Tbx5 associates with Nkx2-5 and synergistically promotes cardiomyocyte differentiation. *Nat Genet* 28:276-280, 2001.

Holder JW, Elmore E, and Barrett JC. Gap junction function and cancer. *Cancer Res* 53:3475-3485, 1993.

Holt M, and Oram S. Familial heart disease with skeletal malformations. *Brit Heart J* 22: 236-242, 1960.

Hu LYR and Kontrogianni-Konstantopoulos A. The kinase domains of obscurin interact with intercellular adhesion proteins. *FASEB J* 27:2001–2012, 2013.

Huang Q, Zhou HJ, Zhang H, Huang Y, Hinojosa-Kirschenbaum F, Fan P, Yao L, Belardinelli L, Tellides G, Giordano FJ, Budas GR, Min W. Thioredoxin-2 inhibits mitochondrial reactive oxygen species generation and apoptosis stress kinase-1 activity to maintain cardiac function.

Circulation. 131:1082–97, 2015.

Itoh M, Nagafuchi A, Yonemura S, Kitani- Yasuda T, and Tsukita S. The 220-kD protein colocalizing with cadherins in nonepithelial cells is identical to ZO-1, a tight junction-associated protein in epithelial cells:cDNAcloning and immunoelectron microscopy. *J Cell Biol* 121:491–502, 1993.

Juliano RL. Signal transduction by cell adhesion receptors and the cytoskeleton: functions of integrins, cadherins, selectins, and immunoglobulin-superfamily members. *Annu Rev Pharmacol Toxicol* 42:283-323, 2002.

Kadenbach B, Stroh A, Becker A, Eckerskorn C, Lottspeich L. Tissue- and species-specific expression of cytochrome c oxidase isozymes in vertebrates. *Biochim Biophys Acta* 1015:368-372, 1990.

Kelmanson IV, Shagin DA, Usman N, Matz MV, Lukyanov SA, and Panchin YV. Altering electrical connections in the nervous system of the pteropod mollusc Clione limacina by neuronal injections of gap junction mRNA. *Eur J Neurosci* 16:2475-2476, 2002.

Keyser R. Identifying ligands of the C-terminal domain of cardiac expressed connexin 40 and assessing its involvement in cardiac conduction disease. *MSc thesis. University of Stellenbosch, Department of Biomedical Sciences*, 2007.

Kirchhoff S, Nelles E, Hagendorff A, Kruger O, Traub O, and Willecke K. Reduced cardiac conduction velocity and predisposition to arrhythmias in connexin40-deficient mice. *Curr Biol* 8:299-302, 1998.

Kontrogianni-Konstantopoulos A, Catino DH, Strong JC, Sutter S, Borisov AB, Pumplin DW, Russell MW, Bloch RJ. Obscurin modulates the assembly and organization of sarcomeres and the sarcoplasmic reticulum. *FASEB J* 20:2102-2111, 2006.

Kostin S, Hein S, Bauer EP, and Schaper J. Spatiotemporal development and distribution of intercellular junctions in adult rat cardiomyocytes in culture. *Circ Res* 85:154–167, 1999.

Kruger O, Plum A, Kim JS, Winterhager E, Maxeiner S, Hallas G, Kirchhoff S, Traub O, Lamers WH, and Willecke K. Defective vascular development in connexin 45-deficient mice. *Development* 127:4179-4193, 2000.

Kumai M, Nishii K, Nakamura K, Takeda N, Suzuki M, and Shibata Y. Loss of connexin45 causes a cushion defect in early cardiogenesis. *Development* 127:3501-3512, 2000.

Laing JG, Manley-Markowski RN, Koval M, Civitelli R, and Steinberg TH. Connexin45 interacts with zonula occludens-1 in osteoblastic cells. *Cell Commun Adhes* 8:209-212, 2001.

Lampe PD, and Lau AF. Regulation of gap junctions by phosphorylation of connexins. *Arch Biochem Biophys* 384:205–215, 2000.

Lange S, OuyangK,Meyer G, Cui L, Cheng H, Lieber RL, Chen J. Obscurin determines the architecture of the longitudinal sarcoplasmic reticulum. *J Cell Sci* 122:2640–2650, 2009.

Latour P, Levy N, Paret M, Chapon F, Chazot G, Clavelou P, Couratier P, Dumas R, Ollagnon E, Pouget J, Setiey A, Vallat JM, Boucherat M, Fontes M, and Vandenberghe A. Mutations in the X-linked form of Charcot-Marie-Tooth disease in the French population. *Neurogenetics* 1:117-23, 1997.

Lee S, Kim SM and Lee RT. Thioredoxin and thioredoxin target proteins: from molecular mechanisms to functional significance. *Antioxid Redox Signal*. 18:1165–207, 2013.

Lehnart SE, Wehrens XH, Reiken S, Warrier S, Belevych AE, Harvey RD, Richter W, Jin SL, Conti M, Marks AR. Phosphodiesterase 4D deficiency in the ryanodine-receptor complex promotes heart failure and arrhythmias. *Cell* 123:25-35, 2005.

Leite MF, Hirata K, Pusl T, Burgstahler AD, Okazaki K, Ortega JM, Goes AM, Prado MA, Spray DC, and Nathanson MH. Molecular basis for pacemaker cells in epithelia. *J Biol Chem* 277:16313–16323, 2002.

Lewis KB, Bruce RA, Baum D, and Motulsky AG. The upper limb-cardiovascular syndrome. An autosomal dominant genetic effect on embryogenesis. *JAMA.* 193: 1080-1086, 1965.

Li QY, Newbury-Ecob RA, Terrett JA, Wilson DI, Curtis ARJ, Yi CH, *et al*. Holt-Oram syndrome is caused by mutations in TBX5, a member of the Brachyury (T) gene family. *Nature Genet* 15: 21-29, 1997.

Liquori CL, Ricker K, Moseley ML, Jacobsen JF, Kress W, Naylor SL, Day JW, and Ranum LP. Myotonic dystrophy type 2 caused by a CCTG expansion in intron 1 of ZNF9. *Science* 293:864-867, 2001.

Lo CW, Waldo KL, and Kirby ML. Gap junction communication and the modulation of cardiac neural crest cells. *Trends Cardiovasc. Med* 9:63-69, 1999.

Loddenkemper T, Grote K, Evers S, Oelerich M, and Stogbauer F. Neurological manifestations of the oculodentodigital dysplasia syndrome. *J Neurol* 249:584-595, 2002.

Lurtz MM, and Louis CF. Effect of a sustained increase in intracellular calcium concentration on connexin43 gap junction permeability. *Biophys J* 84:525, 2003.

Ma J, and Ptashne M. Converting a eukaryotic transcriptional inhibitor into an activator. *Cell* 55:443-446, 1988.

Manring *et al*. Obscure functions: the location–function relationship of obscurins. *Biophys Rev* 9:245–258, 2017.

Martin PE,and Evans WH. Incorporation of connexins into plasma membranes and gap junctions. *Cardiovasc Res* 62:378-387, 2004.

Marston S *et al*. OBSCN mutations associated with dilated cardiomyopathy and Haploinsufficiency. *PLoS ONE* 10, 2015.

McKusick, VA, Abbey H, Bowen P, Boyer SH, Cohen BH, Danks DM, Emery AEH, Finn R, Ferguson-Smith MA, Goodman RM, Handmaker SD, and Harris WS. Medical genetics 1960. *J Chronic Dis* 15: 1-198, 1961.

McPherson CA, and Rosenfeld LE. Heart rhythm disorders (Chapter 16). *Yale university school of medicine heart book* (http://www.med.yale.edu/library/heartbk/16.pdf) 195 – 204, 2006.

Metzelaar MJ, Korteweg J, Sixma JJ, Nieuwenhuis HK. Comparison of platelet membrane markers for the detection of platelet activation in vitro and during platelet storage and cardiopulmonary bypass surgery. *J Lab Clin Med* 121:579-587, 1993.

Metzelaar MJ, Wijngaard PL, Peters PJ, Sixma JJ, Nieuwenhuis HK, Clevers HC. CD63 antigen. A novel lysosomal membrane glycoprotein, cloned by a screening procedure for intracellular antigens in eukaryotic cells. *J Biol Chem* 266:3239-3245, 1991.

Fukai K, Oh J, Frenk E, Almodovar C, Spritz RA. Linkage disequilibrium mapping of the gene for Hermansky-Pudlak syndrome to chromosome 10q23.1-q23.3. *Hum Mol Genet* 4:1665-1669, 1995.

Meyer RA, Laird DW, Revel JP, and Johnson RG. Inhibition of gap junction and adherens junction assembly by connexin and A-CAM antibodies. *J. Cell Biol.* 119:179–189, 1992.

Mimaki M, **Ikota A**, **Sato A**, **Komaki H**, **Akanuma J**, **Nonaka I**, **Goto Y**. A double mutation (G11778A and G12192A) in mitochondrial DNA associated with Leber's hereditary optic neuropathy and cardiomyopathy. *J Hum Genet* 48:47-50, 2003.

Moreno AP, Chanson M, Anumonwo J. Role of the carboxyl terminal of connexin43 in transjunctional fast voltage gating. *Circ Res* 90:450–457, 2002.

Moreno AP, Laing JG, Beyer EC, and Spray DC. Properties of gap junction channels formed of connexin 45 endogenously expressed in human hepatoma (SKHep1) cells. *Am J Physiol* 268:356–365, 1995.

Moreno AP, Rook MB, Fishman GI, and Spray DC. Gap junction channels: distinct voltage-sensitive and -insensitive conductance states. *Biophys J* 67:113–119, 1994.

Moreno AP. Biophysical properties of homomeric and heteromultimeric channels formed by cardiac connexins. *Cardiovasc Res* 62:276-286, 2004.

Moreno AP. Connexin phosphorylation as a regulatory event linked to channel gating. *Biochim Biophys Acta* 1711:164-171, 2005.

Mussini I, Biral D, Marin O, Furlan S, and Salvatori S. Myotonic dystrophy protein kinase expressed in rat cardiac muscle is associated with sarcoplasmic reticulum and gap junctions. *J Histochem Cytochem* 47:383-392, 1999.

Nagafuchi A. Molecular architecture of adherens junctions. *Curr Opin Cell Biol* 13: 600–603, 2001.

Nishibori M, Cham B, McNicol A, Shalev A, Jain N, Gerrard JM. The protein CD63 is in platelet dense granules, is deficient in a patient with Hermansky-Pudlak syndrome, and appears identical to granulophysin. *J Clin Invest* 91:1775-1782, 1993.

Nishii K, Kumai M, Egashira K, Miwa T, Hashizume K, Miyano Y, and Shibata Y. Mice lacking connexin45 conditionally in cardiac myocytes display embryonic lethality similar to that of germline knockout mice without endocardial cushion defect. *Cell Commun Adhes* 10:365-369, 2003.

Otomo J, Kure S, Shiba T, Karibe A, Shinozaki T, Yagi T, Naganuma H, Tezuka F, Miura M, Ito M, Watanabe J, Matsubara Y, Shirato K. Electrophysiological and histopathological characteristics of progressive atrioventricular block accompanied by familial dilated cardiomyopathy caused by a novel mutation of lamin A/C gene. *J Cardiovasc Electrophysiol* 16:137-145, 2005.

Oyamada M, Oyamada Y, and Takamatsu T. Regulation of connexin expression. *Biochim Biophys Acta* 1719:6-23, 2005.

Paul DL, Yu K, Bruzzone R, Gimlich RL, and Goodenough DA. Expression of a dominant negative inhibitor of intercellular communication in the early *Xenopus* embryo causes delamination and extrusion of cells. *Development* 121:371–381, 1995.

Paznekas WA, Boyadjiev SA, Shapiro RE, Daniels O, Wollnik B, Keegan CE, *et al*. Connexin 43 (GJA1) mutations cause the pleiotropic phenotype of oculodentodigital dysplasia. *Am J Hum Genet* 72:408-418, 2003.

Peracchia C, Chen JT, and Peracchia LL. CO_2 sensitivity of voltage gating and gating polarity of gap junction channels–connexin40 and its COOH-terminus truncated mutant. *J Membr Biol* 200: 105–113, 2004.

Peracchia C, Wang X, Li L, and Peracchia LL. Inhibition of calmodulin expression prevents low-pH-induced gap junction uncoupling in Xenopus oocytes. *Pflugers Arch* 431:379-387, 1996.

Peracchia C. Chemical gating of gap junction channels. Roles of calcium, pH and calmodulin. *Biochim Biophys Acta* 1662: 61–80, 2004.

Peracchia C. Structural correlates of gap junction permeation. *Int Rev Cytol* 66:81–146, 1980.

Pike LJ. Lipid rafts: heterogeneity on the high seas. *Biochem. J.* 378:281–292, 2004.

Ploemacher RE, Mayen AE, De Koning AE, Krenacs T, Rosendaal M. Hematopoiesis: Gap Junction Intercellular Communication is Likely to be Involved in Regulation of Stroma-dependent Proliferation of Hemopoietic Stem Cells. *Hematology* 5:133-147, 2000.

Ragan CI, Galante YM, Hatefi Y. Purification of three iron-sulfur proteins from the iron-protein fragment of mitochondrial NADH-ubiquinone oxidoreductase. *Biochemistry* 21:2518-2524, 1982.

Ranger AM, Oukka M, Rengarajan J, and Glimcher LH. Inhibitory function of two NFAT family members in lymphoid homeostasis and Th2 development. *Immunity* 9:627-635, 1998.

Reaume AG, de Sousa PA, Kulkarni S, Langille BL, Zhu D, Davies TC, *et al.* Cardiac malformation in neonatal mice lacking connexin43. *Science* 267:1831 -1834, 1995.

Ricker K, Koch MC, Lehmann-Horn F, Pongratz D, Speich N, Reiners K, Schneider C, Moxley RT 3rd. Proximal myotonic myopathy. Clinical features of a multisystem disorder similar to myotonic dystrophy. *Arch Neurol* 52:25-31, 1995.

Roscoe WA, Barr KJ, Mhawi AA, Pomerantz DK, and Kidder GM. Failure of spermatogenesis in mice lacking connexin43. *Biol.] Reprod* 65:829-838, 2001.

Rose B, and Loewenstein WR. Permeability of a cell junction and the local cytoplasmic free ionized calcium concentration: a study with aequorin. *J Membr Biol* 28:87–119, 1976.

Rose B, and Loewenstein WR. Permeability of cell junction depends on local cytoplasmic calcium activity. *Nature* 254:250–252, 1975.

Rousseau DL, Ching Y, Wang J. Proton translocation in cytochrome c oxidase: redox linkage through proximal ligand exchange on cytochrome a3. *J Bioenerg Biomembr* 25:165-176, 1993.

Saez JC, Berthoud VM, Branes MC, Martinez AD, and Beyer EC. Plasma membrane channels formed by connexins: their regulation and functions. *Physiol Rev* 83:1359-1400, 2003.

Saez JC, Nairn AC, Czernik AJ, Spray DC, Hertzberg EL, Greengard P, and Bennett MV. Phosphorylation of connexin 32, a hepatocyte gap-junction protein, by cAMP-dependent protein kinase, protein kinase C and Ca^{2+}/calmodulin-dependent protein kinase II. *Eur J Biochem* 192:263-273, 1990.

Salvatori S, Biral D, Furlan S, and Marin O. Evidence for localization of the myotonic dystrophy protein kinase to the terminal cisternae of the sarcoplasmic reticulum. *J Muscle Res Cell Motil* 18:429-440, 1997.

Schubert AL, Schubert W, Spray DC, and Lisanti MP. Connexin family members target to lipid raft domains and interact with caveolin-1. *Biochemistry* 41:5754–5764, 2002.

Schultz J, Ferguson B and Sprague FG. Signal transduction and growth control in yeast. *Curr Opin Genet Dev* 6:31-37, 1995.

Severs NJ, Coppen SR, Dupont E, Yeh HI, Ko YS, and Matsushita T. Gap junction alterations in human cardiac disease. *Cardiovasc Res* 62:368-377, 2004.

Severs NJ, Dupont E, Coppen SR, Halliday D, Inett E, Baylis D,and Rothery S. Remodelling of gap junctions and connexin expression in heart disease. *Biochim Biophys Acta* 1662:138-148, 2004.

Severs NJ, Rothery S, Dupont E, Coppen SR, Yeh HI, Ko YS, Matsushita T, Kaba R, and Halliday D. Immunocytochemical analysis of connexin expression in the healthy and diseased cardiovascular system. *Microsc Res Tech* 52:301-322, 2001.

Severs NJ. The cardiac muscle cell. *Bioessays* 22:188-199, 2000.

Shoffner JM, Wallace DC. Mitochondrial genetics: principles and practice. *Am J Hum Genet* 51:1179-1186, 1992.

Shoffner JM, Wallace DC. Oxidative phosphorylation diseases and mitochondrial DNA mutations: diagnosis and treatment. *Annu Rev Nutr* 14:535-568, 1994.

Simon AM, Goodenough DA, and Paul DL. Mice lacking connexin40 have cardiac conduction abnormalities characteristic of atrioventricular block and bundle branch block. *Curr Biol* 8:295-298, 1998.

Simon AM, McWhorter AR, Dones JA, Jackson CL, and Chen H. Heart and head defects in mice lacking pairs of connexins. *Dev Biol* 265:369-383, 2004.

Simpson I, Rose B, and Loewenstein WR. Size limit of molecules permeating the junctional membrane channels. *Science* 1: 294-296, 1977.

Singal R, **Tu ZJ**, **Vanwert JM**, **Ginder GD**, and **Kiang DT**. Modulation of the connexin26 tumor suppressor gene expression through methylation in human mammary epithelial cell lines. *Anticancer Res* 20:59-64, 2000.

Skerrett M, Kasperek E, Cao FL, Shin JH, Aronowitz J, Ahmed S, and Nicholson BJ. Application of SCAM (substituted cysteine accessibility method) to gap junction intercellular channels. *Cell Commun Adhes* 8:179-185, 2001.

Sobhanifar S. The yeast two-hybrid assay: an exercise in experimental eloquence. *The Science creative quarterly* 2:246, 2006.

Soejima H, **Kawamoto S**, **Akai J**, **Miyoshi O**, **Arai Y**, **Morohka T**, **Matsuo S**, **Niikawa N**, **Kimura A**, **Okubo K**, **Mukai T**. Two novel heart-specific genes, Isolation of novel heart-specific genes using the BodyMap database. *Genomics* 74:115-120, 2001.

Sohl G, and Willecke K. An update on connexin genes and their nomenclature in mouse and man. *Cell Commun Adhes* 10:173-180, 2003.

Sohl G, and Willecke K. Gap junctions and the connexin protein family. *Cardiovasc Res* 62:228-232, 2004.

Spray DC. Gap junction channels: yes, there are substates, but what does that mean? *Biophys J* 67:491-492, 1994.

Schwarz, J. M., Rödelsperger, C., Schuelke, M. & Seelow, D. MutationTaster evaluates disease-causing potential of sequence alterations. *Nat. Methods* 7**,** 575–576, 2010.

Schwarz, J. M., Cooper, D. N., Schuelke, M. & Seelow, D. MutationTaster2: mutation prediction for the deep-sequencing age. *Nat. Methods* 11, 361–362, 2014.

B. Sun, Z.H. Chen, L. Ling, Y.F. Li, L.Z. Liu, F. Yang, X.S. Huang, Mutation analysis of gap junction protein beta 1 and genotype-phenotype correlation in X-linked Charcot- Marie-Tooth disease in Chinese patients, *Chin. Med. J*. 129 1011–1016, 2016.

Teunissen BE, and Bierhuizen MF. Transcriptional control of myocardial connexins. *Cardiovasc Res* 62:246-255, 2004.

Theiss C, and Meller K. Microinjected antiactin antibodies decrease gap junctional intercellular commmunication in cultured astrocytes. *Exp Cell Res* 281:197–204, 2002.

Thomas MA, Huang S, Cokoja A, Riccio O, Staub O, Suter S, and Chanson M. Interaction of connexins with protein partners in the control of channel turnover and gating. *Biol Cell* 94:445-456, 2002.

Thornton CA, Wymer JP, Simmons Z, McClain C, Moxley RT 3rd. Expansion of the myotonic dystrophy CTG repeat reduces expression of the flanking DMAHP gene. *Nat Genet* 16:407-409, 1997.

Torok K, Stauffer K, and Evans WH. Connexin 32 of gap junctions contains two cytoplasmic calmodulin-binding domains. *Biochem J* 326:479-83, 1997.

Toyofuku T, Yabuki M, Otsu K, Kuzuya T, Hori M, and Tada M. Direct association of the gap junction protein connexin-43 with ZO-1 in cardiac myocytes. *J Biol Chem* 273:12725–12731, 1998.

Uys G, Ramburan A, Loos B, Kinnear CJ, Korkie LJ, Mouton J, Riedemann J and Moolman-Smook JC. Myomegalin is a novel A-kinase anchoring protein involved in the phosphorylation of cardiac myosin binding protein C. *BMC Cell Biology*, 12:18, 2011.

Valiunas V. Biophysical properties of connexin-45 gap junction hemichannels studied in vertebrate cells. *J Gen Physiol* 119:147-164, 2002.

Valiunas V, Beyer EC, and Brink PR. Cardiac gap junction channels show quantitative differences in selectivity. *Circ Res* 91:104-111, 2002.

Valiunas V, Weingart R, and Brink PR. Formation of heterotypic gap junction channels by connexins 40 and 43. *Circ Res* 86:42–49, 2000.

Van Criekinge W, Beyaert R. Yeast Two-Hybrid: State of the Art. *Biol Proced Online*. 4;2:1-38, 1999.

van der Merwe PL, Rose AG, van der Walt JJ, Weymar HW, Hunter JC, and Weich HF. Progressive familial heart block type I. Clinical and pathological observations. *S Afr Med J* 80:34-38, 1991.

van der Merwe PL, Weymar HW, Torrington M, Brink AJ. Progressive familial heart block (type I). A follow-up study after 10 years. *S Afr Med J* 73:275-276, 1988.

van der Ven PF, Jansen G, van Kuppevelt TH, Perryman MB, Lupa M, Dunne PW, ter Laak HJ, Jap PH, Veerkamp JH, and Epstein HF. Myotonic dystrophy kinase is a component of neuromuscular junctions. *Hum Mol Genet* 2:1889-1894, 1993.

van Veen AA, van Rijen HV, and Opthof T. Cardiac gap junction channels: modulation of expression and channel properties. *Cardiovasc Res* 51:217-229, 2001.

Veenstra RD, Wang HZ, and Beblo DA. Selectivity of connexin-specific gap junctions does not correlate with channel conductance. *Circ Res* 77:1156–1165, 1995.

Veenstra RD. Size and selectivity of gap junction channels formed from different connexins. *J Bioenerg Biomembr* 28:327–337, 1996.

Veenstra RD. Voltage-dependent gating of gap junctional conductance in embryonic chick heart. *Ann N Y Acad Sci* 588:93-105, 1990.

Vinken M, Vanhaecke T, Papeleu P, Snykers S, Henkens T, and Rogiers V. Connexins and their channels in cell growth and cell death. *Cell Signal* 18:592-600, 2006.

Wahl JK, Kim YJ, Cullen JM, Johnson KR, and Wheelock MJ. N-cadherin-catenin complexes form prior to cleavage of the proregion and transport to the plasma membrane. *J Biol Chem* 278:17269-17276, 2003.

Wallace DC, Lott MT, Shoffner JM, Ballinger S. Mitochondrial DNA mutations in epilepsy and neurological disease. *Epilepsia*. 1:43-50, 1994.

Wang XG, and Peracchia C. Chemical gating of heteromeric and heterotypic gap junction channels. *J Membr Biol* 162:169-176, 1998.

WangY, and Rose B. Clustering of Cx43 cell-to-cell channels into gap junction plaques: regulation by cAMP and microfilaments. *J Cell Sci* 108:3501–3508, 1995.

Warn-Cramer BJ, Cottrell GT, Burt JM, and Lau AF. Regulation of connexin-43 gap junctional intercellular communication by mitogen-activated protein kinase. *J Biol Chem* 273:9188-9196, 1998.

Wei J-C, Xu X, and Lo CW. Connexins and cell signaling in development and disease. *Annu Rev Cell Dev Biol* 20:811–838, 2004.

Weidmann S. Cardiac muscle: the functional significance of the intercalated disks.*Ann N Y Acad Sci* 137:540-542, 1966.

Weidmann S. The diffusion of radiopotassium across intercalated disks of mammalian cardiac muscle. *J Physiol* 187:323-342, 1966.

Wheelock MJ, and Johnson KR. Cadherin-mediated cellular signaling. *Curr Opin Cell Biol* 15:509–514, 2003.

Whitney G, Throckmorton D, Isales C, Takuwa Y, Yeh J, Rasmussen H, Brophy C. Kinase activation and smooth muscle contraction in the presence and absence of calcium. *J Vasc Surg* 22:37-44, 1995.

Wisloff U, Najjar SM, Ellingsen O, Haram PM, Swoap S, Al-Share Q, Fernstrom M, Rezaei K, Lee SJ, Koch LG, Britton SL. Cardiovascular risk factors emerge after artificial selection for low aerobic capacity. *Science* 307:418-420, 2005.

Wu JC, Tsai RY, and Chung TH. Role of catenins in the development of gap junctions in rat cardiomyocytes. *J Cell Biochem* 88:823–835, 2003.

Ya J, Erdtsieck-Ernste EB, de Boer PA, van Kempen MJ, Jongsma H, Gros D, Moorman AF, and Lamers WH. Heart defects in connexin43-deficient mice. *Circ Res* 82:360-366, 1998.

Yamada KA, Kanter EM, Green KG, and Saffitz JE. Transmural distribution of connexins in rodent hearts. *J Cardiovasc Electrophysiol* 15:710-715, 2004.

Yano T, Ito F, Yamasaki H, Hagiwara K, Ozasa H, Nakazawa H, and Toma H. Epigenetic inactivation of connexin 32 in renal cell carcinoma from hemodialytic patients. *Kidney Int* 65:1519, 2004.

Yao JA, Gutstein DE, Liu F, Fishman GI, and Wit AL. Cell coupling between ventricular myocyte pairs from connexin43-deficient murine hearts. *Circ Res* 93:736-743, 2003.

Yule DI, Stuenkel E, and Williams JA. Intercellular calcium waves in rat-pancreatic acini: mechanism of transmission. *Am J Physiol* 271:1285–1294, 1996.

Zuppinger C, Schaub MC, Eppenberger HM. Dynamics of early contact formation in cultured adult rat cardiomyocytes studied by N-cadherin fused to green fluorescent protein. *J Mol Cell Cardiol* 32:539–555, 2000.